Ministry of Higher Education and Scientific Research

وزارة التعليم العالي والبحث العلمي

Badji Mokhtar Annaba University
Université Badji Mokhtar – Annaba
Faculty of Technology
Electromechanical Department

جامعة باجي مختار – عنابـــــــــــة
كلية التكنولوجيا
قســـــــم الالكتروميكانيك

Thesis

Presented to obtain the diploma of

Doctorate

Specialty: Mechatronics

Field: Electromechanics

By:

REHAIL Ayoub

Theme:

Optimization and Performance Analysis of a Multi-Source and Multi-Load Energy System

Thesis defended on November 10, 2026 ahead the jury composed of:

N°	Full name	Degree	Institution	Quality
01	RACHEDI Mohamed Faouzi	Prof.	Badji Mokhtar -Annaba University	President
02	CHEGHIB Hocine	Prof.	Badji Mokhtar -Annaba University	Supervisor
03	BOUCHAHED Adel	MCA.	University of Constantine 1	Examiner
04	DJELLAD Abdelhak	MCA.	National Higher School of Technology and Engineering – Annaba	Examiner
05	OUADA Mehdi	MCA.	Badji Mokhtar -Annaba University	Examiner

Acknowledgement

This thesis is the result of work carried out at the Laboratory of Electromechanical Systems, Department of Electromechanics Engineering at Badji Mokhtar -Annaba University.

First of all, I would like to thank my supervisor, Prof. CHEGHIB Hocine, for accepting the responsibility of supervising me during the final stage of this thesis his support, guidance and willingness to continue this work were essential for the successful completion of this research. He receives here the expression of my deep respect and with all my gratitude.

Also, I would like to express my sincere gratitude to Prof. MEGHNI Billel for his valuable guidance, continuous support, and helpful advice throughout the realization of this thesis. His expertise and encouragement were essential to the completion of this work.

I would like to thank the president of the jury Prof. RACHEDI Mohammed Faouzi professor at the University of Badji Mokhtar Annaba who kindly did me the honor of presiding over this jury. He finds here the expression of my deepest gratitude and respectful thanks. I would also like to express my deepest thanks to the members of the jury for having done me the honor of judging this work as examiners.

I warmly thank all the members of my family and friends for their encouragement, affection, and moral support.

Finally, I address my gratitude to all the teachers, who in some way contributed to this success even if they certainly do not remember me. May they find here the expression of my deep gratitude!

Dedication

Not all words can express gratitude, I promise to perpetuate your memory, as long as I'm in life. No dedication can express my respect, my eternal love and my consideration for the sacrifices you have made for my instruction and my well-being.

To My father I thank you for all the support and love you have shown me since my birth and I hope that you're blessing always accompanies me. May this modest work be the fulfillment of your many wishes, the fruit of your countless sacrifices, though I can never do enough for you.

May God, the Highest, grant your health and happiness and so that I will never disappoint you.

To my sister I thank you for your help, encouragement, moral support and love. May God bless you in your life.

I dedicate this success to my brothers, the most formidable and exceptional in the world, whose unconditional support and brotherly love have been an inexhaustible source of strength and inspiration.

Abstract

Hybrid renewable energy systems represent a promising solution for reliable and sustainable electricity generation, especially in isolated or rural areas. The durability and efficiency of such systems depend strongly on effective energy management strategies and the dynamic coordination between generation units and storage devices.

This work is a contribution to the optimization and performance analysis of a hybrid multi-source and multi-load system composed of photovoltaic panels, a fuel cell and hybrid storage elements (battery and supercapacitor). The study is carried out through detailed modeling and simulation under MATLAB/Simulink.

The research is divided into two main parts. In the first part, classical management strategies are implemented to evaluate their capabilities and limitations under different operating scenarios. In the second part, intelligent approaches are proposed: a fuzzy-rule–based management strategy for system-wide energy coordination and an LSTM-based controller integrated into the photovoltaic subsystem for adaptive and accurate maximum power point tracking.

The results demonstrate that the hybrid system operates near its maximum potential under varying conditions, while ensuring supply–demand balance, prolonging storage lifetime, and improving overall stability. This confirms the effectiveness of combining classical and intelligent methods for hybrid renewable energy systems.

Keywords: Hybrid energy system; Photovoltaic; Fuel cell; Battery; Supercapacitor; Fuzzy logic; Energy management; MPPT; LSTM.

ملخص

تمثل أنظمة الطاقة المتجددة الهجينة حلا واعدا لتوليد الكهرباء بشكل موثوق ومستدام ، خاصة في المناطق المعزولة أو الريفية. تعتمد متانة وكفاءة هذه الأنظمة بشدة على استراتيجيات إدارة الطاقة الفعالة والتنسيق الديناميكي بين وحدات التوليد وأجهزة التخزين.

هذا العمل هو مساهمة في تحسين وتحليل الأداء لنظام هجين متعدد المصادر ومتعدد الأحمال يتكون من الألواح الكهروضوئية وخلية الوقود وعناصر التخزين الهجينة (البطارية والمكثف الفائق). يتم إجراء الدراسة من خلال النمذجة والمحاكاة التفصيلية تحت ماتلاب/سيملينك.

ينقسم البحث إلى قسمين رئيسيين. في الجزء الأول ، يتم تنفيذ استراتيجيات الإدارة الكلاسيكية لتقييم قدراتها وقيودها في ظل سيناريوهات التشغيل المختلفة. في الجزء الثاني ، يتم اقتراح مناهج ذكية: استراتيجية إدارة قائمة على قواعد غامضة لتنسيق الطاقة على مستوى النظام ، ووحدة تحكم قائمة على لستم مدمجة في النظام الفرعي الكهروضوئي لتتبع أقصى نقطة طاقة تكيفية ودقيقة .

تظهر النتائج أن النظام الهجين يعمل بالقرب من أقصى إمكاناته في ظل ظروف مختلفة ، مع ضمان توازن العرض والطلب ، وإطالة عمر التخزين ، وتحسين الاستقرار العام. هذا يؤكد فعالية الجمع بين الأساليب الكلاسيكية والذكية لأنظمة الطاقة المتجددة الهجينة.

الكلمات المفتاحية: نظام الطاقة الهجين ؛ كهروضوئية ؛ خلية الوقود ؛ البطارية ؛ مكثف فائق ؛ المنطق الضبابي ؛ إدارة الطاقة ؛ تتبع نقطة القدرة القصوى ؛ شبكة الذاكرة القصيرة المدى المطوَّلة .

Résumé

Les systèmes énergétiques hybrides renouvelables représentent une solution prometteuse pour une production d'électricité fiable et durable, en particulier dans les zones isolées ou rurales. La durabilité et l'efficacité de tels systèmes dépendent fortement de stratégies de gestion de l'énergie efficaces et de la coordination dynamique entre les unités de production et les dispositifs de stockage.

Ce travail constitue une contribution à l'optimisation et à l'analyse des performances d'un système hybride multi-sources et multi-charges composé de panneaux photovoltaïques, d'une pile à combustible ainsi que d'éléments de stockage hybrides (batterie et supercondensateur). L'étude a été menée à travers une modélisation détaillée et des simulations sous MATLAB/Simulink.

La recherche est divisée en deux principales parties. Dans la première, des stratégies classiques de gestion ont été implémentées afin d'évaluer leurs capacités et leurs limites dans différents scénarios de fonctionnement. Dans la seconde, des approches intelligentes sont proposées : une stratégie de gestion basée sur des règles floues pour la coordination énergétique du système, et un contrôleur basé sur les réseaux de neurones LSTM intégré au sous-système photovoltaïque pour un suivi adaptatif et précis du point de puissance maximale.

Les résultats démontrent que le système hybride fonctionne proche de son potentiel maximal dans des conditions variables, tout en assurant l'équilibre entre production et consommation, en prolongeant la durée de vie du stockage et en améliorant la stabilité globale. Cela confirme l'efficacité de la combinaison entre méthodes classiques et intelligentes pour les systèmes hybrides d'énergie renouvelable.

Mots-clés : Système hybride d'énergie ; Photovoltaïque ; Pile à combustible ; Batterie ; Supercondensateur ; Logique floue ; Gestion de l'énergie ; MPPT ; LSTM.

Table of contents

Acknowledgement I
Dedication II
Abstract III
ملخص IV
Résumé V
List of figures VI
List of tables VIII
List of Abbreviations and Acronyms IX
General introduction 1
I.1. Introduction to hybrid energy 3
I.2. Main components of hybrid systems 5
I.2.1. Renewable energy generators 5
I.2.1.1. PV generator 5
I.2.1.2. Wind generator 7
I.2.1.3. Fuel cell 8
I.2.2. Conventional energy generators (diesel, gas, etc.) 8
I.2.2.1. Diesel generator 8
I.2.2.2. Gas generator 9
I.2.3. Energy storage (batteries, supercapacitors) 9
I.2.3.1. Batteries 9
I.2.3.2 Supercapacitor 10
I.3. Common hybrid technologies and architecture 11
I.3.1. Grid-connected systems 11
I.3.2. Autonomous systems for rural and remote applications 12
I.3.3. Hybrid micro-grids 13
I.4. Advantages and challenges of hybrid systems 14
I.4.1. Energy efficiency and emissions reduction 14
I.4.2. Challenges of hybrid systems 15
I.4.2.1. Technical Challenges 15
I.4.2.2. Cost 15
I.4.2.3. Environmental Challenge 16
I.4.2.4. Regulatory & Policy Challenges 16
I.5. Case studies and real-life applications 17
I.5.1. Notable projects around the world 17
I.5.2. Feedback and lessons learned 19

I.6. Current trends and innovations 19
I.6.1. New technologies and materials 19
I.6.2. Future prospects and emerging areas of research 20
I.7. Energy Transition and the potential of Hybrid Energy in Algeria 20
I.7.1. Adoption of Hybrid Energy in Algeria 21
I.7.2. Integration of Hybrid Energy Systems in Algeria 22
1.7.3. Institutional Framework for Renewable Energy Development in Algeria 22
I.7.4. The legal and legislative framework for renewable energy in Algeria 24
I.8. Regulations, policies and incentives 25
I.8.1. Government and international initiatives 25
I.8.2. Standards and protocols for hybrid integration 25
I.9. Conclusion 26
II.1. Introduction 26
II.2. Definition of multi-source system modelling 26
II.3. Study, analysis and choice of the final system architecture 26
II.3.1. AC coupling 26
II.3.2. Mixed DC/AC coupling 27
II.3.3. DC coupling 28
II.4. Development of energy source models 28
II.4.1. Photovoltaic System Modelling 28
II.4.1.1. I-V characteristic curve 30
II.4.1.2. P-V characteristic 30
II.4.1.3. Irradiance Influence on *P-V* and *I-V* curves 31
II.4.1.4. Temperature Influence on *P-V* and *I-V* characteristics 31
II.4.2. Fuel cell modelling 32
II.4.2.1 Activation losses 33
II.4.2.2. Ohmic losses 34
II.4.2.3. Concentration losses 34
II.4.3. Storage system modelling 34
II.4.3.1. Battery modelling 35
II.4.3.2. Modeling of supercapacitor 37
II.4.3.2 Supercapacitor state of charge (SOC) 37
II.4.4. Modelling the various power converters 38
II.4.4.1. Modeling of the boost converter 38
II.4.4.3. Modelling the inverter 40
II.4.4.4. Modelling the DC bus 41
II.5. Evaluation the components of the hybrid system 42
II.6. Conclusion 42

III.1. Introduction 46
III.2. Maximum power point tracking 46
III.3. Control of photovoltaic power generation systems 47
III.3.1. State of the art on different MPPT techniques (Seeking Loop) 47
III.3.1.1. Conventional techniques 48
III.3.1.2. Enhanced conventional MPPT techniques 49
III.3.1.3. Advanced techniques 50
III.3.1.4. Techniques based on non-linear control 53
III.3.2. Maintaining Operation at Maximum Power Point (Tracking Loop) 54
III.4. Challenges in MPPT and Control Strategies 55
III.5. Proposed LSTM-Based Control Approach 55
III.5.1. Long Short-Term Memory 55
III.6. Development of LSTM based controller 57
III.7. Performance evaluation of LSTM controller 59
III.8. Training of the LSTM network-based controller 60
III.9. Dynamic performance evaluation of the LSTM based controller 61
III.9.1. Step change in reference voltage Evaluation of LSTM in different operating regions 61
III.9.1. LSTM controller stair reference voltage evaluation 63
III.10. Partial shading evaluation of LSTM 63
III.12. Conclusion 65
IV.1. Introduction 68
IV.2. Hybrid system optimization criteria 68
IV.2.1. Cost of energy 68
IV.2.2. Life Cycle Cost (LCC) 69
IV.2.3. Loss of Load Probability (LOLP) 69
IV.3. Proposed sizing procedure for a hybrid system 70
IV.3.1. Load profile 71
IV.3.2. Radiation, temperature 71
IV.3.3. Energy produced by the hybrid system 71
IV.3.4. The state of charge of battery and supercapacitor 72
IV.4. Overviews of optimal electrical energy management control strategies adapted to the hybrid system 72
IV.4.1. Management strategy based on Predictive Control (MPC) 73
IV.4.2. Management strategy based on sliding mode control (SMC) 73
IV.4.3. Management strategy based on artificial neural network (ANN) 74
IV.4.4. Management strategy based on fuzzy logic control (FLC) 75
IV.5. Analysis of classical energy management in the proposed hybrid system 77
IV.6. Development of fuzzy logic-based optimization strategy for electric power management of the proposed hybrid system 78

IV.6.1. Identification of input and output variables with membership functions for the proposed CLF management unit 80
IV.6.2. Definition of fuzzy rules for decision making 84
IV.6.3. Performance Evaluation under Diverse Operating Scenarios 87
IV.6.3.1. Energy Surplus Management (Scenarios 5 and 6) 87
IV.6.3.2. System Equilibrium and Preservation (Scenario 1) 87
IV.6.3.3. Power Deficit Mitigation (Scenarios 2, 3, and 4) 88
IV.6.3.4. Boundary Protection and Maximum Stress Response (Scenarios 7 and 8) 88
IV.6.4. Adaptation of the proposed control algorithm under variable operating conditions 89
IV.7. Implementation optimization algorithm of the in a MATLAB 90
General Conclusion 101
Appendices 103
References 105

List of figures

Chapter I: State of the art of the hybrid energy production system

Figure I.1. Electricity generation by energy source 2015-2024 [6]. 5
Figure I.2. PV global capacity and annual additions ,2015-2024 [6]..... 6
Figure I.3. Principle of photovoltaic cell operation [8]. 6
Figure I.4.Wind power global capacity and annual additions ,2015-2024 [6]. 7
Figure I.5. Wind turbine [10]. 7
Figure I.6. Schematic diagram of a fuel cell [11]. 8
Figure I.7. Diesel generator [13]. 9
Figure I.8. Electrochemical battery [17]. 10
Figure I.9. Schematic illustration of a supercapacitor [20]. 11
Figure I.10. Classified of common hybrid technologies and architectures. 11
Figure I.11. Basic components of a grid connected system. 12
Figure I.12. Stand-alone hybrid energy system [23]. 13
Figure I.13. Schematic diagram of a hybrid micro-grid [25]. 14
Figure I.14. Expected penetration rate of renewable energies in national production [50]. 21

Chapter II: Modelling of multi-source system: different production systems

Figure II.1. The structure of the hybrid system with bus AC. 27
Figure II.2. The structure of the hybrid system with mix bus AC and bus DC. 27
Figure II.3. The structure of the hybrid system with DC bus. 28
Figure II.4. Equivalent electrical diagram of a PV cell. 29
Figure II.5. Typical I-V characteristic of a solar module. 30
Figure II.6. Typical P-V characteristic of a solar module. 30
Figure II.7. Effect of variable irradiance on the P-V and I-V characteristic curve. 31
Figure II.8. Effect of variable temperature on the P-V and I-V characteristic curve. 32
Figure II.9. Schematic diagram of a fuel cell. 32
Figure II.10. Polarization and power density curves of a PEMFC at 70 °C. 33
Figure II.11. Proposed hybrid energy storage system. 35
Figure II.12. Equivalent battery circuit. 35
Figure II.13. Battery discharge characteristics under nominal and variable load currents. 37
Figure II.14. Schematic diagram of a boost converter. 38
Figure II.15. Equivalent circuit of a converter in the closed state. 38
Figure II.16. Equivalent circuit of a converter in the opened state. 39
Figure II.17. Electrical diagram of the bidirectional DC/DC chopper. 40
Figure II.18. Voltage converter operating in inverter mode. 40
Figure II.19. Electrical diagram of the DC bus. 41
Figure II.20. The structure of the hybrid energy system studied. 42

Chapter III: Design of an optimal control for a PV generator

Figure III.1. Classification of MPPT techniques. 47

Figure III.2. The architecture of an LSTM cell. 57
Figure III.3. LSTM training using optimal PI* input/output data. 58
Figure III.4. Different regions of the P-V curve and derived optimal controllers for each region. 58
Figure III.5. Steps of the proposed LSTM controller training procedure. 59
Figure III.6. Training progress of the proposed LSTM network using all regions data. 61
Figure III. 7. PV power response in current region. 62
Figure III.8. PV power response in power region. 62
Figure III.9. PV voltage response in voltage region. 62
Figure III.10. PV system evaluation using the LSTM controller stair shaped reference voltage. 63
Figure III.11. PV voltage response using PI and LSTM controllers under PS. 63
Figure III.12. PV power response using PI and LSTM controllers under PS. 64

Chapter IV: Optimization and Management of energy flows of a multi-load Hybrid System

Figure IV.1. Illustration of the principle of control in sliding mode. 74
Figure IV.2. Operation of a fuzzy logic system. 75
Figure IV.3. Classical Supervisory Energy Management Algorithm. 78
Figure IV.4. Proposed Supervisory Energy Management Algorithm. 79
Figure IV.5. Membership function of net current. 80
Figure IV.6. Membership function of battery state of charge. 81
Figure IV.7. Membership function of supercapacitor state of charge. 81
Figure IV.8. Membership function of solar irradiance. 82
Figure IV.9. Membership function of ambient temperature. 82
Figure IV.10. Membership function of battery current reference. 83
Figure IV.11. Membership function of supercapacitor current reference. 83
Figure IV.12. Membership function of grid enable signal. 83
Figure IV.13. Membership function of dump load activation. 84
Figure IV.14. Membership function of PV source activation. 84
Figure IV.15. Energy management and control unit based on fuzzy logic. 85
Figure IV.16. diagram of the dual-layer intelligent architecture. 90
Figure IV.17. Evolution of the temperature. 90
Figure IV.18. Evolution of the irradiation. 91
Figure IV.19. Change in power demand. 91
Figure IV.20. Evolution of PV power. 91
Figure IV.21. Evolution of the power of the fuel cell. 92
Figure IV.22. Evolution state of charge of battery. 93
Figure IV.23. Evolution the state of charge supercapacitor. 93
Figure IV.24. Evolution of the battery power. 94
Figure IV.25. Evolution of the supercapacitor power. 94
Figure IV.26. Evolution of the DC bus voltage. 95
Figure IV.27. Evolution the power of dump load. 96
Figure IV.28. Evolution of active power. 97
Figure IV.29. Evaluation the reactive power. 97

List of tables

Table I.1. National Renewable Energy and Energy Efficiency Program 2015-2030 [52]..... 22
Table I.2. Table hybrid solar energy projects in Algeria [50]..... 22

Table II.1. Comparative Characteristics of Batteries and Supercapacitors..... 35

Table III.1. Collected training data description..... 60
Table III.2. Step change evaluation comparison results..... 62
Table III.3. Comparative analysis against conventional and advanced MPPT methods..... 64

Table IV.1. Comparative Analysis of Energy Management Techniques..... 76
Table IV.2. Fuzzy input rules for the energy management unit..... 86
Table IV.3. Fuzzy output rules for the energy management unit..... 86
Table IV.4. Performance Evaluation under Diverse Operational Scenarios..... 99

List of Abbreviations and Acronyms

AC	Alternating Current
ACO	Ant Colony Optimization
ANN	Artificial Neural Network
B.Ch	Big Charged
B.Dich	Big Discharged
BESS	Battery Energy Storage System
CNN	Convolutional Neural Network
COE	Cost of Energy
DC	Direct Current
DOE	Department of Energy (U.S.)
EMS	Energy Management System
FC	Fuel Cell
FLC	Fuzzy logic control
G	Solar Irradiance
GA	Genetic Algorithm
GWO	Grey Wolf Optimizer
HES	Hybrid Energy Systems
HESS	Hybrid Energy Storage System
HRES	Hybrid Renewable Energy Systems
HT	Hidden State at Time t
INC	Incremental Conductance
K	Bolztmann constant
K-dump	Dump Load Activation
$\mathbf{K_{pv}}$	PV Source Activation
LCC	Life Cycle Cost
LOLP	Loss of Load Probability
LPSP	probability of power loss
LSTM	Long Short-Term Memory
M.Ch	Moderately Charged
M.Dich	Moderately Discharged
MPC	Model Predictive Control
MPP	Maximum Power Point
MPPT	Maximum Power Point Tracking
NB	Negative Big
NM	Negative Medium
NPV	Net Present Value
NS	Negative Small
OC	Open Circuit

OCV	Open Circuit Voltage
P&O	Perturb and Observe
PB	Positive Big
PI	Proportional–Integral Controller
PM	Positive Medium
PMSG	Permanent Magnet Synchronous Generator
PS	Positive Small
PSO	Particle Swarm Optimization
PV	Photovoltaic
PWM	Pulse Width Modulation
RE	Renewable Energy
RNN	Recurrent Neural Network
S.Ch	Small Charged
S.Dich	Small Discharged
SC	Supercapacitor
SCC	Short Circuit Current
SMC	sliding Mode Control
SOC	State of Charge
SOC-bat	Battery State of Charge
SOC-sc	Supercapacitor State of Charge
T	Temperature
V-I/P-V	Voltage-Current / Power-Voltage
WECS	wind energy conversion systems
WOA	Whale Optimization Algorithm
WT	Wind Turbine
$\mathbf{X_t}$	Input at Time t
Z	Zero

General introduction

General introduction

The growing worldwide demand for energy, combined with the pressing environmental concerns associated with fossil fuel consumption, has accelerated the global transition toward renewable energy sources such as solar photovoltaic, wind power and fuel cells. While these resources provide clean and sustainable electricity generation, they are intrinsically intermittent and stochastic in nature, raising significant challenges in ensuring a stable and reliable power supply [1-4]. To address these limitations a hybrid energy system that integrate multiple renewable sources with complementary storage technologies such as batteries and supercapacitors have emerged as an attractive solution. In such systems, PV and fuel cell contribute clean generation, batteries provide medium-term storage and supercapacitors guarantee rapid dynamic response to transient events. However, the efficient coordination of these diverse components requires advanced supervisory strategies capable of dynamically adapting to time-varying operating conditions.

The key issue in hybrid energy systems is the optimal management of power flows. Traditional methods, like PI controllers, are straightforward but tend to be insufficient to cope with nonlinear dynamics, uncertainties, and high intermittency of renewable sources. These approaches can lead to ineffective use of storage devices, premature battery aging, or the inability to ensure system stability in changing operating conditions. Additionally, coordination between the supercapacitor and battery is essential. If not properly addressed, it can cause unbalanced charge-discharge cycles, thus decreasing the lifespan of storage devices and causing higher operating expenses. As such, there is a need for sophisticated supervisory strategies that not only balance power distribution but also maximize the reliability, efficiency and lifespan of the system. Fuzzy logic, with its ability to handle uncertainties and mimic human decision-making processes, has emerged as a promising solution. Unlike rigid classical control approaches, fuzzy logic enables flexible, rule-based decisions that can adaptively react to dynamic changes in the availability of resources, the state of charge (SOC) of storage systems and load demand.

The primary objective of this study is to develop, implement and test an improved method for managing energy in a hybrid renewable energy system. The system integrates solar panels and fuel cell, with battery and supercapacitor support. For this purpose, a fuzzy logic controller is developed to manage energy flow effectively and distribute loads efficiently among the

renewable sources, storage devices, and the grid. The performance of the fuzzy logic approach is thoroughly compared with a conventional PI-based energy management technique in terms of response time, stability, overall efficiency, and duration of storage longevity. The proposed approach is implemented and tested in MATLAB/Simulink under diverse conditions, taking into account variations in load demand and fluctuating weather conditions such as sunlight, temperature, and wind speed. Lastly, a comprehensive evaluation of the system's behavior in dynamic and steady states is performed, highlighting the advantages and merits of intelligent fuzzy logic management over conventional techniques.

The thesis is organized to lead the reader from fundamental principles through modelling, controller design and validation to final conclusions. Chapter I reviews the fundamentals of the renewable technologies considered in this study (photovoltaic, fuel cell), describes the principal components and conversion chains and recalls the operating principles relevant to system design. Chapter II develops the modelling and simulation framework detailed mathematical models are presented for the PV subsystem (cell to array), the fuel cell, the battery, the supercapacitor and the associated power converters. Chapter III presents the design and implementation of a Long Short-Term Memory (LSTM) controller for a photovoltaic generator, highlighting its ability to improve forecasting and control accuracy under variable environmental conditions. Chapter IV describes the integrated hybrid architecture and the supervisory control strategies. It details the classical energy-management scheme, the proposed fuzzy logic–based supervisory controller (membership functions, rule base and implementation in MATLAB/Simulink), the simulation scenarios used for validation and the comparative performance analysis in both transient and steady-state conditions. The thesis concludes with a final section that summarizes the main contributions, discusses limitations and practical implications, and outlines perspectives for future work such as experimental validation, real-time implementation and adaptive learning extensions.

Chapter I

State of the art of the hybrid energy production system

I.1. Introduction to hybrid energy

The increasing penetration of variable renewable resources has highlighted the operational limitations of stand-alone generation technologies such as pure solar or wind systems. Amidst this paradigm transition, hybrid renewable energy systems (HRES) have emerged as key options to enhance the reliability and sustainability of electricity supply [3].

Hybridization in renewable energy systems is primarily required to overcome the inherent shortcomings and intermittency of single-source energy systems. While renewable sources like solar and wind power offer great benefits, they also demonstrate intermittency and fluctuation in their energy supply. In the context of the global energy transition, hybrid energy systems (HES) have emerged as a promising solution HES combine two or more sources of energy to generate electricity. These systems can be used to provide a reliable and sustainable source of energy, especially in remote areas where access to the grid is limited or non-existent. HES can also be used to reduce greenhouse gas emissions and improve energy security [1].

Hybrid renewable energy systems exhibit a wide range of architectural configurations, yet they are all structured around a common set of fundamental design principles. Specifically, these systems are typically organized under hierarchical supervisory control schemes that coordinate power exchange among multiple generation and storage units, ensuring optimal operating efficiency while maintaining continuous real-time balance between electrical demand and available generation [2].

Multi-source renewable energy systems provide an effective approach for small to medium-scale stationary power generation. These systems integrate multiple renewable sources (e.g., solar and wind), resulting in minimal environmental impact and high energy efficiency. While architecturally more complex than single-source alternatives, multi-source configurations offer superior operational flexibility, improved reliability, and attractive economic returns [2-4].

HES are categorized according to their energy source composition. The main classifications include:

Energy source composition	System description	Reference
Solar wind hybrid systems	These systems combine solar and wind energy to generate electricity. Solar panels generate electricity from sunlight, while wind turbines generate electricity from wind.	[2],[3]
Solar diesel hybrid systems	These systems combine solar energy and diesel generators to generate electricity. Solar panels generate electricity from sunlight, while diesel generators provide backup power when the sun is not shining.	[2],[3]
Solar fuel-cell electrolyzer hybrid systems	These systems integrate photovoltaic arrays with hydrogen-based energy storage, where electrolyzers convert surplus solar electricity into hydrogen during periods of high generation, and fuel cells reconvert the stored hydrogen to electricity during periods of insufficient solar availability.	[4]
Solar wind battery fuel-cell electrolyzer diesel systems	These systems combine wind energy, solar energy, battery storage, hydrogen storage, and diesel generation to provide highly reliable electricity. wind turbines and solar panels generate electricity from wind and sunlight, batteries store excess energy for short-term use, electrolyzers produce hydrogen from surplus renewable power for long-term storage, fuel cells convert stored hydrogen back to electricity when needed, and diesel generators provide backup power during extended periods of low renewable generation.	[5]

I.2. Main components of hybrid systems

I.2.1. Renewable energy generators

Renewable energy is the energy generated from natural resources. Primary renewable resources include solar radiation, wind energy, hydropower, and geothermal heat all sustained by continuous natural processes. Unlike finite fossil fuel reserves, these energy sources offer sustainable, long-term power generation with minimal environmental impact. The global energy landscape has experienced a significant transition toward renewable sources in recent years. As illustrated in Figure I.1, renewable energy's contribution to global electricity generation has increased substantially from 23% in 2015 to 32% in 2024, representing a 9% gain over the nine-year period. This growth trend underscores the increasing viability and economic competitiveness of renewable technologies [6].

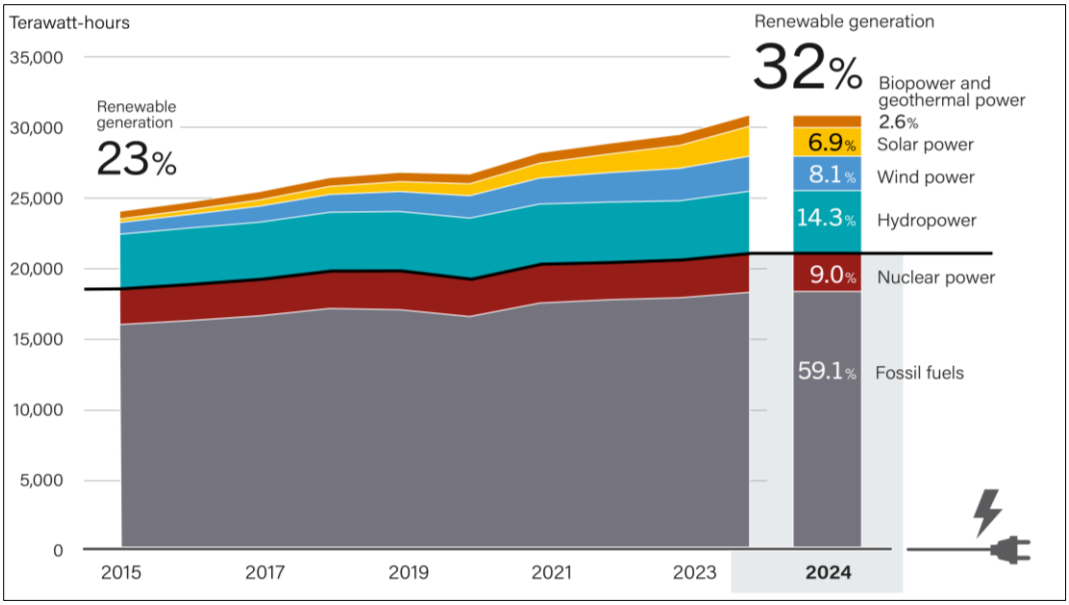

Figure I.1. Electricity generation by energy source 2015-2024 [6].

I.2.1.1. PV generator

Solar photovoltaic (PV) technology has emerged as a dominant driver of the global energy transition, exhibiting rapid and sustained growth over the past decade. by the end of 2024 [6], global PV capacity reached approximately 2247 GW, representing a substantial increase, with installed capacity nearly doubling since 2022 and more than tripling compared to levels prior to 2020 As illustrated in Figure I.2 .

The photovoltaic (PV) cell is the fundamental unit of a PV system. It is fabricated from semiconductor materials and directly converts incident light energy into electrical energy

through the photovoltaic effect. Figure I.3 illustrates a cross-section of a typical PV cell structure. A PV cell is made from a semiconductor material (such as silicon) and has a structure similar to a conventional diode. It consists of an N-doped upper layer and a P-doped lower layer forming a PN junction, which creates a potential barrier and an internal electric field. When photons strike the surface, they transfer energy to the material, generating electron–hole pairs that are separated by this field and collected at the metallic contacts. This process produces an electrical current and voltage, whose values depend on several parameters that will be discussed later [7].

A PV module consists of a set of PV cells elements mounted in series and / or in parallel in order to obtain electrical characteristics desired such as: the power, the short-circuit current I_{sc} or the open-circuit voltage V_{oc}.

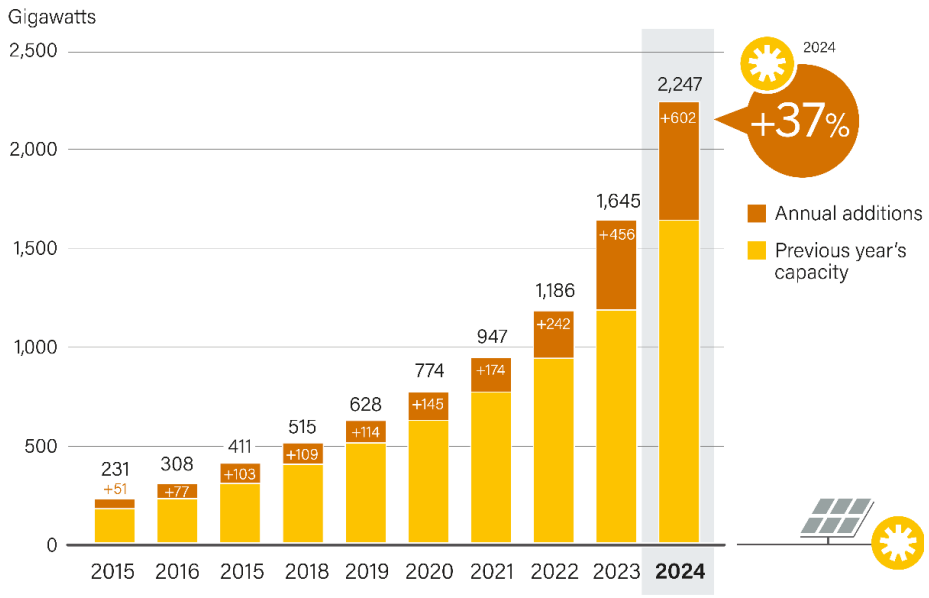

Figure I.2.PV global capacity and annual additions ,2015-2024 [6].

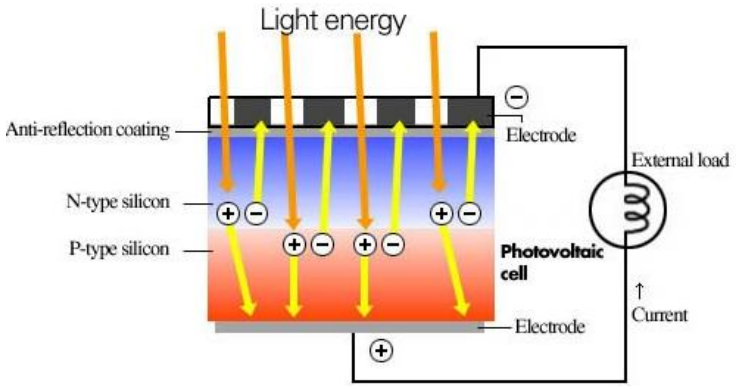

Figure I.3. Principle of photovoltaic cell operation [8].

I.2.1.2. Wind generator

Wind energy has emerged as one of the most rapidly expanding renewable energy sources globally, with cumulative installed capacity growing from 433 GW in 2015 to 1,135 GW in 2024 [6], as illustrated in Figure I.4. A wind generator, also known as a wind turbine, is a device that converts the movement energy of the wind into mechanical energy and then into electrical energy via a generator. Their functioning principles are straightforward. The wind turbine design is influenced by windmill technology as shown by Figure I.5. The rotor blades capture the kinetic energy of the wind and transmit the resulting rotational torque through a gearbox to the generator, housed within the nacelle alongside the brake, controller, and yaw drive system. The anemometer continuously monitors wind speed, while the yaw motor orients the nacelle to maintain optimal alignment with the prevailing wind direction, maximizing energy capture. The generated electrical power is then transmitted to the load via power cables routed along the tower structure [9].

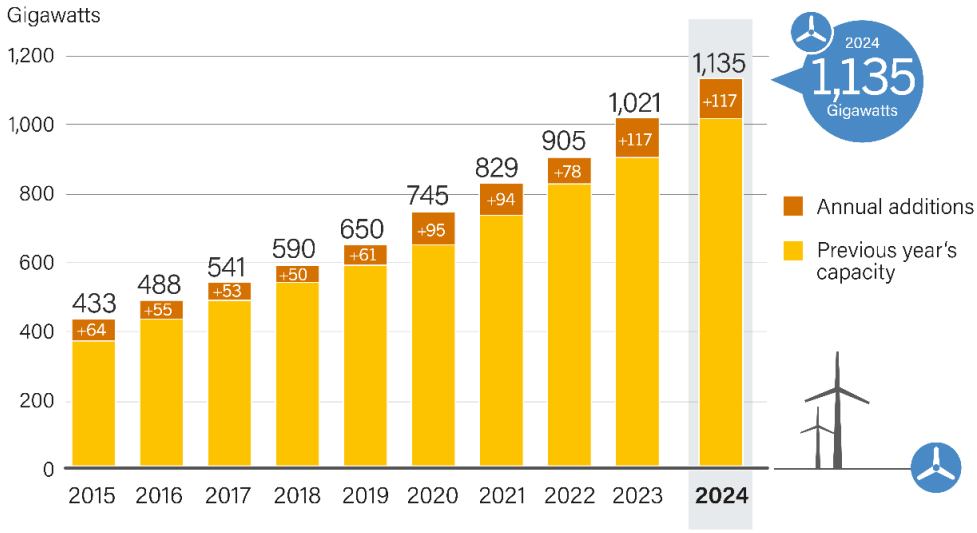

Figure I.4.Wind power global capacity and annual additions ,2015-2024 [6].

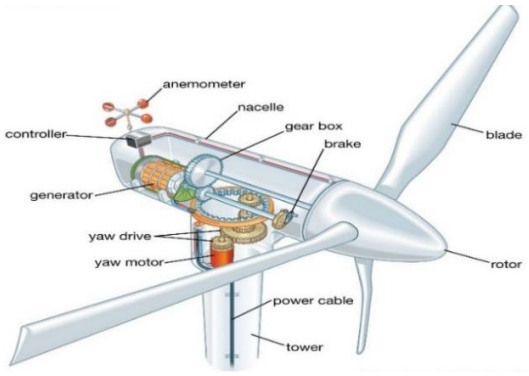

Figure I.5. Wind turbine [10].

I.2.1.3. Fuel cell

A fuel cell is an electrochemical generator that uses a chemical reaction to transform the chemical energy of a combustible (such as hydrogen, natural gas, carbon monoxide, and methane) into electrical energy. It consists of individual unit cells, each composed of two electrodes an anode and a cathode where electrochemical reactions occur. The electrodes are separated by an electrolyte that facilitates the transfer of ions and blocks the passage of electrons [11].

Practically a combustible fuel cell an electrical tension of between 0.7 and 0.8 V. As a result, in order to create stacks (modules) that have the necessary tension and power for the consumer, the cells must be assembled in series. Figure I.6 represent the operating principle of fuel cell.

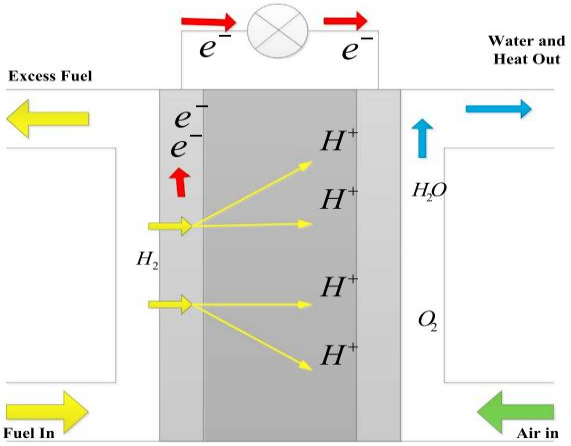

Figure I.6. Schematic diagram of a fuel cell [11].

I.2.2. Conventional energy generators (diesel, gas, etc.)

Conventional energies are forms of energy that are widely used to meet human production and consumption needs. Among these energies, the most widely used are nuclear energy and energy derived from fossil fuels. One of the electricity generation systems that is widely used in multi-source systems and is based on these energies is the diesel generator.

I.2.2.1. Diesel generator

The diesel generator is a device that can generate electricity by burning gasoil. As a result, this device relies on a primary power supply that is assumed to be available at all times. The use of this device in hybrid systems aims to mitigate any potential production insufficiency or power outage owing to a technical issue. The presence of a diesel generator is crucial in certain cases, especially for hybrid systems, where power outages can result in severe consequences and financial losses. Several applications make use of diesel generators. They have been widely

used as emergency power, as backup power, or as a source of electricity supply in isolated power systems. They are available in sizes ranging from 1 kVA to several thousand kVA. Because of its wide range, it is commonly used in various electrical applications and systems, particularly in autonomous systems to ensure uninterrupted power or emergency power. They are frequently used with other devices to meet electrical energy quality objectives [12].



Figure I.7. Diesel generator [13].

I.2.2.2. Gas generator

A gas generator is a type of generator that operates on gas as fuel instead of traditional fuels such as diesel or gasoline. Gas generators can run on various types of gas, such as natural gas, propane, liquefied petroleum gas (LPG), or biogas. They are used to generate electricity through the combustion of gas in an internal combustion engine [14].

I.2.3. Energy storage (batteries, supercapacitors)

Various technical solutions have been proposed to address the intermittency and variability inherent to renewable energy sources. Among these, electrical energy storage systems (EES) represent an effective approach for improving the stability and reliability of renewable-based power systems. By enabling the temporal decoupling between energy generation and consumption, storage technologies help maintain the balance between supply and demand within microgrids. In this context, batteries and supercapacitors play a crucial role in enhancing system performance.

I.2.3.1. Batteries

Batteries are utilized for electrochemical energy storage [15]. They use oxidation-reduction to store electrical energy at the charge, which is then returned to the discharge with a high yield (about 85%). They are distinguished by a nominal voltage under load that corresponds to the oxidation-reduction potential unique to this torque, and the second fundamental property is the C_{bat} capacity (Ah), which indicates the current required to fully charge a battery in a particular

number of hours. Two criteria make it possible to judge whether they are suitable for the desired application: the service life in terms of the number of charge and deep discharge cycles and their specific energies (mass or volume energy storable by the accumulators). Currently, batteries are classified into three groups based on the type of their electrodes: lead-acid, nickel-based, and lithium-based accumulators. Batteries can be used in a variety of applications based on its power, energy, and size [16]. They can be used for residential storage (a single house, a group of houses, and a neighborhood) or for large-scale network storage (several megawatt hours). Batteries can quickly address unexpected network imbalances by quickly absorbing power spikes over short periods of time.

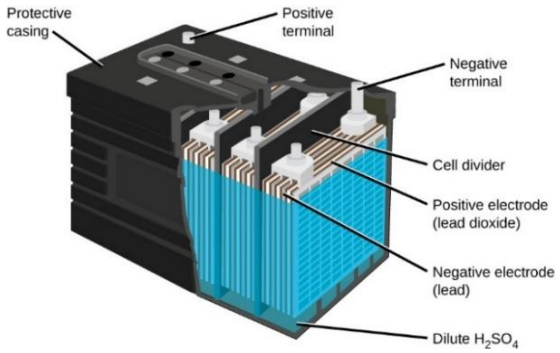

Figure I.8. Electrochemical battery [17].

I.2.3.2. Supercapacitor

Supercapacitor have been around for 20 years and serve as an alternative to batteries. They appear to be high-capacity condensers and work on the same principle as batteries [18].

A supercapacitor is made up of an electrolyte that separates two electrodes in a porous material, such as activated carbon, to multiply the specific surface. They are connected to an electron collector, which transports them from one to another in the electrical circuit based on the charge and discharge current. The charge is complete when the electrode reaches its dissociation potential. The electrode surface needs to be large enough to accommodate enough ions to enhance the component's capacity.

Supercapacitors can have capacities ranging from a few farads to thousands of farads, depending on the chemical components used in their design [19]. It has the same parameters as a battery, including a nominal full charge voltage of 1 V for water or 2.7 V for acetonitrile, and a specific energy of 0.1 to a few Wh/kg, which is significantly lower than that of batteries. Specific power ranges from 1 to 10 kW/kg, while batteries are limited to hundreds of W/kg for lead-acid and around 300W/kg for lithium-ion. Figure I.9 represent the operating principle of a supercapacitor.

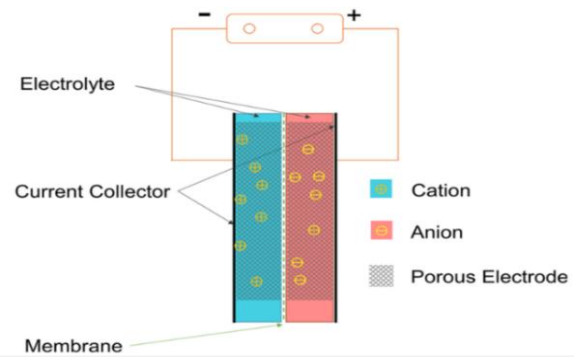

Figure I.9. Schematic illustration of a supercapacitor [20].

I.3. Common hybrid technologies and architecture

Based on their grid connection status, HRES can be broadly divided into three categories: hybrid micro-grid, autonomous systems, and grid connected systems. This classification is visually shown in Figure I.10 and offers various implications for the design, operation, and governmental regulation of HRES.

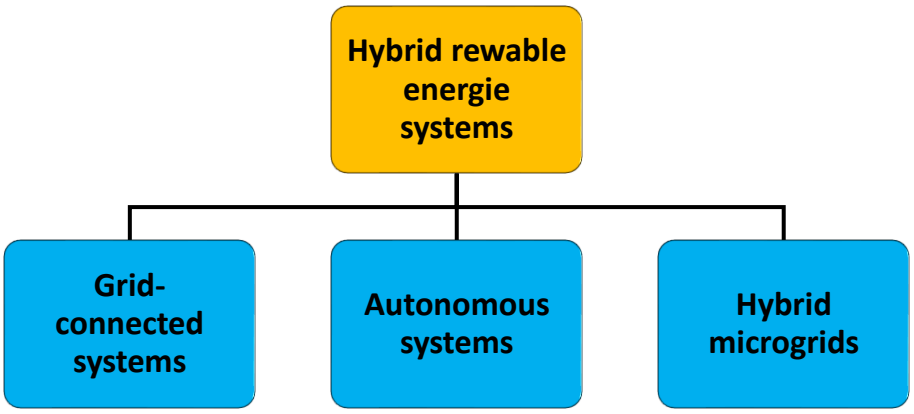

Figure I.10. Classified of common hybrid technologies and architectures.

I.3.1. Grid-connected systems

The centralized electrical grid is directly linked to the HRES. The capacity to feed excess electricity back into the grid, frequently taking advantage of feed-in tariffs or net metering laws, is the main benefit of an on-grid system. This kind of system may utilize the grid's current infrastructure and is typically easier to establish in terms of regulations as shown in Figure I.11.

Nonetheless, it is highly reliant on the stability of the grid and susceptible to disruptions from it. In urban and suburban regions with robust and dependable grid connectivity, on-grid systems are well-suited [21].

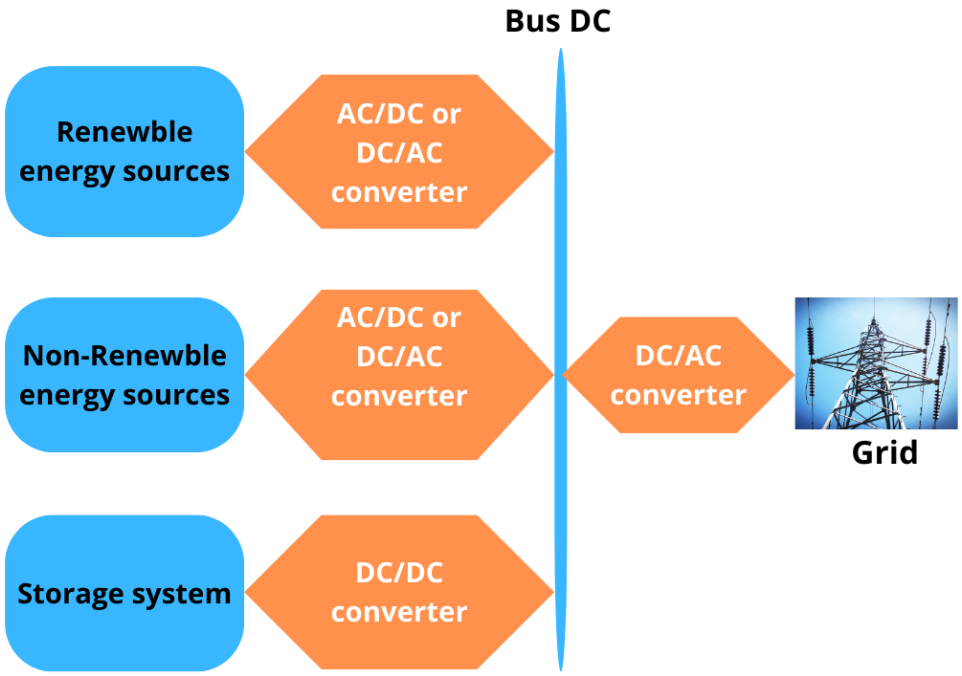

Figure I.11. Basic components of a grid connected system.

I.3.2. Autonomous systems for rural and remote applications

Autonomous systems produce energy on their own, independent of the electrical grid. Frequently employed to supply energy to locations that are hard to reach or do not have access to a power system (such as remote communities, islands, mountain retreats).

In rural areas particularly in the developing world, where more than 1billion people lack the essential energy services to satisfy the most basic needs and to improve their social and economic status. The cost of grid for rural electrification in area extension, sometimes very high due to a low-density level of population, leads often various organizations to explore alternative solutions.

The choice of diesel power generation has been considered for a long time as the most economical and reliable alternative, however this solution is not always the most profitable and induces several environmental and practical nuisances for the user: high operating costs energy dependence for the user (and for the country), fuel transportation problems, complicated maintenance, useful life of five years but frequently less due to maintenance problems no guarantee of uninterrupted generation [22].

A renewable energy system (mainly PV or wind) may be a good solution to supply small and medium energy loads. It can provide an uninterrupted supply of electricity (particularly attractive for systems as telecommunications security installations, water supply and cooling), it is easy to install and requires a low maintenance and has a high reliability. It particularly than

an engine generators utilization. As shown in Figure I.12 to supply the energy required by the water pump, a hybrid system has been applied, consisting of a photovoltaic energy generator as the primary source and a battery as a back-up system that works to store energy during energy availability and discharge it during energy shortages [23].

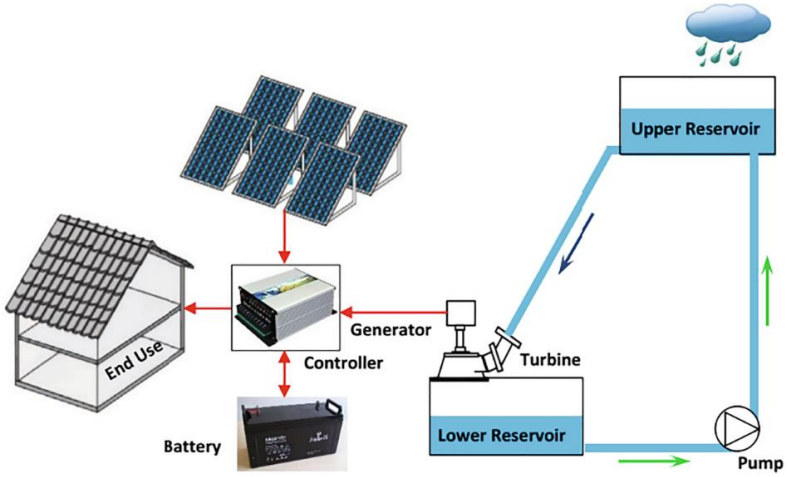

Figure I.12. Stand-alone hybrid energy system [23].

I.3.3. Hybrid micro-grids

First presented in the technical literature [24],[25]. The micro-grid concept offers a dependable way to integrate distributed energy resources, such as Energy Storage Systems with controllable loads. The main grid would view such a micro-grid as a single unit that would react to the proper control signals.

A micro-grid is a localized energy system that may function both independently and in collaboration with the central grid, falling in between on-grid and off-grid systems. Energy storage technologies with a variety of renewable and maybe conventional energy sources are frequently included in micro-grids.

The hybrid micro-grid is the combination of an AC micro-grid with a DC micro-grid as shown in Figure I.13. The AC micro-grid can be composed of a renewable source (wind energy) and a traditional source (diesel generator) and low voltage network, in addition to the storage system (flywheel) and the AC loads. As for the DC micro-grid, it can contain two renewable sources (photovoltaic energy + fuel cell) and a storage system (battery) in addition to the DC loads. Electrical energy can also be exchanged between the two micro-grids via AC/DC converters. The advantage of this installation is that it increases the efficiency of the system.

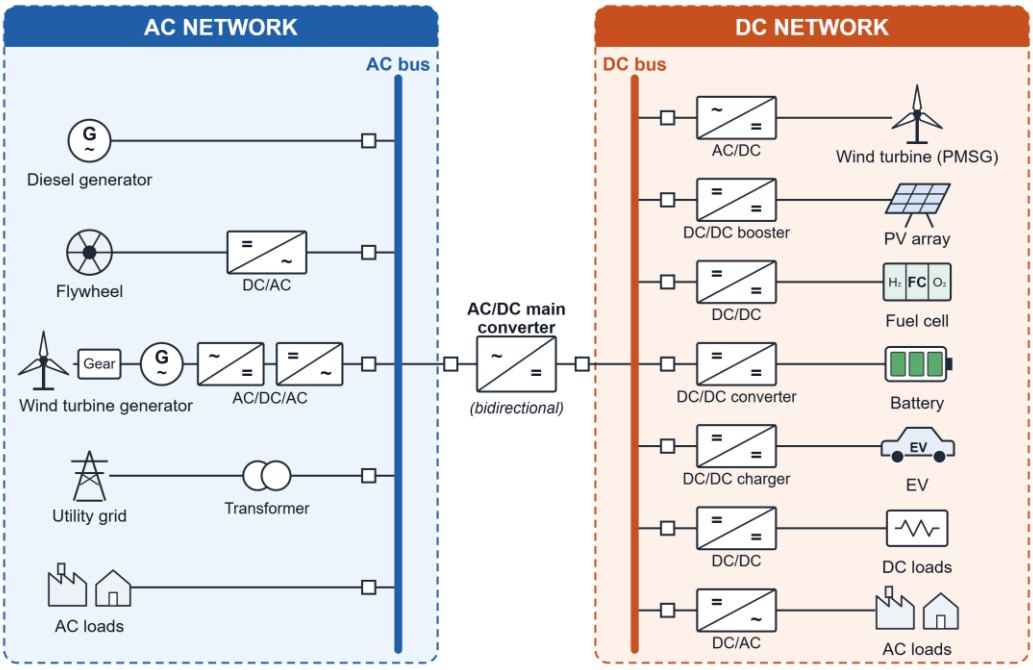

Figure I.13. Schematic diagram of a hybrid micro-grid [25].

I.4. Advantages and challenges of hybrid systems

I.4.1. Energy efficiency and emissions reduction

The primary benefit of hybrid technologies is their ability to continuously provide the load with the energy it needs and, wherever feasible, generate the greatest amount of energy from renewable sources. HRES can:

- Improve stability and dependability by combining complementary energy sources that peak at various times like wind and solar power, to produce a steady and reliable power production. By doing this, a more dependable energy source is ensured, lowering the possibility of power outages during times of low sun or wind [26].
- Increases energy availability: Seasonal changes in renewable energy generation are a result of weather patterns in many places. In order to help satisfy ongoing energy demands, hybrid systems that incorporate several sources can offer a more consistent energy supply throughout the year [27].
- Increase efficiency because, during certain times of the year, some renewable energy sources like solar panels might provide too much electricity. Energy storage devices can be integrated to store excess energy and use it during periods of low output. This improves system efficiency and minimizes waste.

- Help maintain grid stability, as intermittent renewable energy sources can strain power grids by supplying electricity during peak demand, reducing congestion and improving overall stability [28].
- Benefits distant and off-grid communities. Combining multiple renewable sources in areas with restricted access can create enough power without relying on costly fuel-based generators [29], [30].
- Offer a path to a cleaner energy future. Integrating renewable sources with low-carbon backup options, such as battery storage or cleaner fossil fuel technologies, can balance energy supply and demand, gradually lowering reliance on fossil fuels [31].

I.4.2. Challenges of hybrid systems

While HRES provide a robust solution for mitigating the stochastic and intermittent nature of individual renewable sources, their implementation entails significant technical and economic challenges. The following sections detail the primary drawbacks associated with system hybridization:

I.4.2.1. Technical Challenges

The integration of multiple energy sources introduces a range of technical, operational, and infrastructural challenges that must be carefully considered during both the design and implementation stages. The principal technical challenges encountered in the design and implementation of HRES can be summarized as follows:

- Different energy sources may require specific control and management systems to be integrated seamlessly.
- Renewable sources like solar and wind are intermittent, making prediction and management more complex.
- Building new infrastructure or modifying existing infrastructure for HRES might be challenging. Energy Storage Choosing, integrating, and managing systems that maintain energy reliability can be hard [32].

I.4.2.2. Cost

Hybrid renewable energy systems (HRES) often require higher initial capital investment compared to single-source systems due to the integration of multiple technologies and associated power electronics. Furthermore, the inherent variability of renewable resources can affect the predictability of investment returns, thereby increasing financial risk. In addition,

some HRES technologies remain at relatively early stages of development, which contributes to economic uncertainty and can hinder large-scale deployment [32].

I.4.2.3. Environmental Challenge

The integration of multiple renewable energy sources within a hybrid system may raise specific environmental concerns, particularly regarding land use. Large-scale deployment of solar and wind systems often requires significant surface area or land with particular characteristics, which can lead to conflicts with agriculture, biodiversity preservation, or urban development. Moreover, accurate assessment of renewable resources such as wind speed and solar irradiation is essential to ensure the system's reliability and efficiency. However, these assessments are often challenging due to spatial and temporal variability, leading to potential mismatches between expected and actual performance.

I.4.2.4. Regulatory & Policy Challenges

The deployment of Hybrid Renewable Energy Systems (HRES) is not only a technological challenge but also deeply intertwined with the regulatory and policy frameworks of the host country. Policies governing energy markets, grid integration, and environmental standards directly influence the feasibility, scalability, and long-term sustainability of such systems. In many cases, the rapid advancement of renewable technologies has outpaced the evolution of regulatory frameworks, leading to gaps, inconsistencies, and barriers to adoption. Various energy sources may be subject to different policies and regulations, complicating system design [33]:

- **Grid Integration Policies**

  The expansion of large-scale hybrid plants is frequently obstructed by existing grid bottlenecks and a slow rate of transmission infrastructure development. Traditional grids were designed for centralized fossil-fuel generation, and their regulatory structures are often inadequate for managing decentralized, intermittent renewable resources. Issues such as grid code compliance, connection procedures, and energy dispatch priorities become critical. For example, some jurisdictions impose restrictive limits on renewable penetration, while others lack clear compensation mechanisms for surplus energy exported to the grid. Without harmonized grid policies that encourage flexibility and smart grid deployment, the integration of hybrid systems remains constrained. This regulatory inertia not only affects technical performance but also undermines investor confidence in renewable energy markets [33].

- **Licensing and Standards**

  The absence of standardized regulations for hybrid systems introduces further uncertainty in project licensing and operational compliance. Unlike conventional single-source plants, HRES involve complex interconnections of multiple technologies, requiring unique safety, quality, and interoperability standards. In many countries, regulatory authorities have yet to establish guidelines that address the hybrid nature of these systems, resulting in delays in project approval and additional administrative burdens. Moreover, differing certification requirements across regions create barriers to international collaboration and technology transfer. The lack of clarity in licensing frameworks discourages innovation and slows down the pace at which hybrid renewable solutions can be scaled.

I.5. Case studies and real-life applications

I.5.1. Notable projects around the world

The application of hybrid systems is a very dynamic field, numerous demonstration projects on such systems have been carried out globally for a variety of purposes, including the electrification of remote villages, the operation of remote telecommunications units, and the creation of micro-grids for the safe and clean production of electricity in urban areas [34]. A brief summary is provided of seven representative applications of hybrid systems and micro-grid test facilities (deploying hybrid systems) from around the world. These applications vary in purpose and system configuration.

Notable project	Project description	Reference
Utsira Island, Norway	An autonomous hybrid wind-hydrogen-fuel-cell system with flywheel and battery storage and a hydrogen engine supplies power to the island residents.	[35]
Kahua Ranch, Hawaii Hydrogen Power Park, USA	The Hawaii Hydrogen Power Park program initially funded the development of this hybrid wind-PV-electrolyzer-FC energy plant for technological validation and research. Kahua Ranch on Hawaii Island receives electricity from the system that emits no emissions	[36]
Starkenburger Lodge, Austria	A completely off-grid hybrid PV-storage system, including a CHP-based engine, supplies the power demand of the remote Alpine Lodge in the Austrian Alps.	[37]
Fuel cells and Energy Networks of Electricity, heat, and hydrogen, Japan (Project NEXT 21)	By the end of 2009, around 5000 PEMFCs (powered by natural gas) had been placed in private homes as test installations. The PEMFC units supply the residences with hot water and power.	[38–40]
The Kythnos Island micro-grid project, Greece	The system is a diesel-engine, single-phase PV micro-grid that is installed on the island to give the locals uninterrupted power. The system is used to test the micro-grid's power management and centralized and decentralized control in islanded mode.	[41]
The Hachinohe micro-grid project, Japan	The purpose of this renewable-energy-based micro-grid, built in the urban city of Hachinohe, is to investigate its grid integration and stabilization, as well as control and reliable operation in islanded mode	[42]
Wind $2H_2$ Project, National Wind Technology Center (NWTC) at the National Renewable Energy Laboratory(NREL), USA	In March 2007, the Wind $2H_2$ system received approval for its inaugural demonstration operation. By using electrolyzes, the system directly generates hydrogen from RE sources. The produced hydrogen is kept in high-pressure storage tanks where it can be utilized as a fuel for vehicles and a medium for storing energy	[43]

I.5.2. Feedback and lessons learned

Hybrid renewable energy systems could benefit greatly from BESS technologies. Many experts are working on improving the coordination and development of BESS energy storage systems for use in micro-grids to manage the energy balance between supply and demand by storing energy during off-peak hours at a lower cost. Although its potential is recognized, developing an efficient BESS suitable for micro-grid applications remains a major challenge.

The management techniques used in hybrid systems are chosen in line with the goals of every investigation. Since they enable analysis of both technical (such as duration, demand fulfilment, and performance) and economic (such as minimizing system costs, increasing savings, and lowering the cost of energy) aspects of hybrid renewable energy systems to achieve an optimal configuration, most researchers concentrate on techno-economic objectives. Numerous techniques, including fuzzy logic, neural networks, particle swarm optimization, are used to monitor the parts of the hybrid renewable energy system in order to accomplish these goals. These methods enable the efficient assessment and optimization of hybrid systems' performance.

PV-Wind-distributed generator was the most widely utilized generation source configuration because it had the highest cost-benefit ratio and dependability.

Residential locations are where these systems are most frequently used because many of the nations where these systems are researched have weak or nonexistent electrical services. The isolated hybrid network design is the most used one.

I.6. Current trends and innovations

I.6.1. New technologies and materials

These studies [44-49] evaluates new concerns and explores the literature on hybrid energy systems for buildings. Hybrid energy systems integrate energy technologies to improve environmental performance, efficacy, and flexibility while reducing costs. They provide a practical choice for establishments hoping to increase revenue and produce other useful goods. By utilizing hybrid systems to target applications that are challenging to decarbonize and incorporate extra renewable energy, significant reductions in greenhouse gas emissions can be accomplished.

I.6.2. Future prospects and emerging areas of research

Below is a sample list of upcoming research topics that may have an impact on the generation and management of RE power:

Technology Type	Future Prospects (Inferred)	Reference
AI-driven optimization & control	the development of intelligent control systems, sustainable materials, and efficient recycling processes to ensure the widespread adoption and long-term viability of HESS.	[44]
Agrivoltaics	Highly likely to become an industrial standard for sustainable agriculture and decentralized rural grids in arid regions.	[45]
Floating Photovoltaics (FPV)	Expected 20% annual increase in deployment, particularly in Asia, becoming a major utility-scale alternative where land is scarce.	[46]
Next-Generation Storage	Research is shifting toward technologies such as solid-state batteries, hydrogen storage, and pumped hydro storage to enhance cost-effectiveness.	[47]
Building Integrated PV (BIPV)	Likely to become a standard for net-zero energy buildings and urban decentralized grids as semi-transparent window technology matures	[48]
Blockchain Technology	This is emerging as a tool for peer-to-peer (P2P) energy trading, providing secure and transparent decentralized platforms for prosumers to trade energy autonomously	[49]

I.7. Energy Transition and the potential of Hybrid Energy in Algeria

Figure I.14 highlights the Algerian approach to gradually incorporating renewable energy sources into the energy mix while maintaining some reliance on fossil fuels. This explains the government's approach to broadening the country's energy sources and progressively incorporating renewable energy into the country's overall energy and economic system.

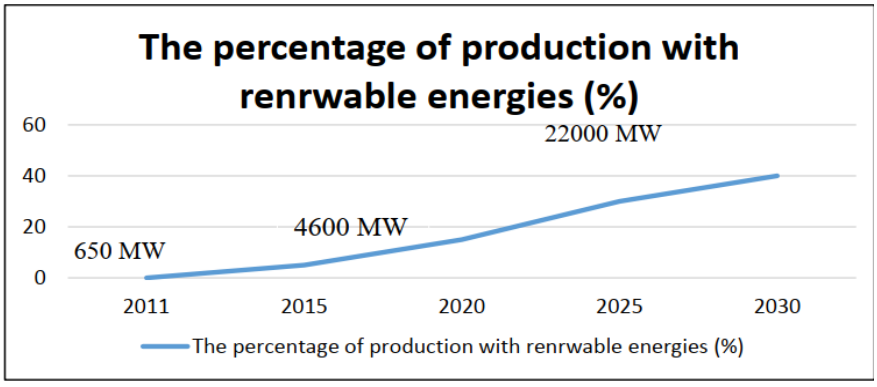

Figure I.14. Expected penetration rate of renewable energies in national production [50].

Algeria, like many other nations in the globe, aims to employ renewable energy sources to improve its energy security within the context of the dynamics of energy transition by diversifying its energy mix and lowering its reliance on fossil fuels. Because of the country's abundance of sunshine and high winds in some locations, renewable energy sources, particularly solar and wind energy, have a lot of promise [50].

I.7.1. Adoption of Hybrid Energy in Algeria

One of the main steps towards ensuring Algeria has energy security is the country's transition to renewable energy. The nation has abundant solar and wind resources that may be used to generate sustainable energy.

Renewable energy projects to generate electricity for the national market will be carried out in two phases:

- ✓ First phase 2015 - 2020: This first phase will see the implementation of 4,000 MW of photovoltaic and wind energy, as well as 500 MW of energy from biomass, combined heat and power and geothermal energy.
- ✓ Second phase 2021 - 2030: The development of the electrical connection between the North and the Sahara (Adrar), will make it possible to install large-scale renewable energy stations in the areas of In Salah, Adrar, Timimoun and Bechar and integrate them into the national energy grid. By then, solar thermal energy could be economically viable. Table I.1 shows the cumulative capacity of the renewable energy program, by type and phase, over the period 2015 - 2030.

Table I.1. National Renewable Energy and Energy Efficiency Program 2015-2030 [51].

Energy Sources	Phase-One2015-2020 [MW]	Phase-Two 2020-2023[MW]	Total [MW]
Solar cells	3000	10575	**13575**
Wind	1010	4000	**5010**
Cogeneration	150	250	**400**
Solar thermal	0	2000	**2000**
Biomass	360	640	**1000**
Geothermal	5	10	**15**
Total	4525	17475	**22000**

I.7.2. Integration of Hybrid Energy Systems in Algeria

- ✓ Hybrid renewable energy projects carried out: The hybrid electric power plant (gas–solar) of Solar Power Plant (SPP1) in Hassi R'Mel of 150 MW of which 25 MW in solar thermal (CSP), commissioned in July 2011.
- ✓ Through a foreign partnership strategy between Algerian Energy Society and the Spanish company Abengoa [52], Algeria is aiming to create three hybrid solar energy production centers, to be built according to the specifications listed in Table I.2.

Table I.2. Table hybrid solar energy projects in Algeria [52].

Region	Capacity (MW)	Estimated cost (million euros)
Second solar power plant El Maghir	80	322
Third solar power plant EL Naama	70	285
Fourth solar power plant Hassi el Rmel	70	285

1.7.3. Institutional Framework for Renewable Energy Development in Algeria

Algeria has created national policies to support and advance renewable energy as a component of sustainable development. These policies rely on a collection of organizations and businesses, each of which is in charge of creating renewable energy within their own areas of specialization. To further promote study in this area, various research centers have been formed in Algeria, each will be outlined separately:

- **The National Agency for the Promotion and Rationalization of Energy Use (APRUE):** It was founded on August 25, 1985, with the intention of carrying out the state's energy-related policies, particularly those pertaining to industry, transportation, and agriculture, as well as encouraging the use of renewable energy sources and sector-specific energy-related programmers [53].
- **The Solar Equipment Development Unit:** On January 9, 1988, this unit was founded in Tipaza. It is in charge of creating solar equipment and experimental models of solar equipment with thermal effects for use in industry, agriculture, and the home. It also produces solar equipment with voltage illumination for use in agriculture and the home [54]. It is also in charge of creating mechanical, thermal, and electrical systems that support the creation of solar equipment.
- **Silicium Technology Development Unit:** Under the direction of the Ministry of Higher Education and Scientific Research, this entity was founded in 1988. Its goal is to carry out innovative, training, assessment, and scientific research in the areas of material sciences and semiconductor devices for a variety of applications. Additionally, it works with academic institutions to advance information and convert it into technical know-how and goods required for social and economic recovery [55].
- **Center for Development of New and Renewable Energies:** The Centre in Bouzareah was established on March 28, 1998 by the Ministry of Higher Education and Scientific Research. The main objectives of the center are to carry out research on renewable energy, particularly solar energy, and to create plans for using these energy sources.
- **The Applied Research Unit for Renewable Energies (CDPER): (**CDPER) is a 1997-founded research organization in Algeria. The center is dedicated to promoting renewable energy technologies as a means of furthering sustainable development. CDPER conducts research and offers training on renewable energy in Algeria in partnership with universities and research centers.
- **The Algerian Company for New Energies (CANE):** In Algeria, (CANE) is a state-owned company that specializes in the planning, execution, and administration of renewable energy projects. The goal of CANE is to support sustainable development and aid in the nation's energy transition by broadening its energy sources. The firm is in charge of putting different renewable energy projects, such as hydroelectric, solar, and wind power facilities, into operation in Algeria. In order to promote the use of renewable energy in Algeria and to further research and development into this field, CANE also works with national and international partners. (CANE, the Algerian Company for New Energies, s.d).

- **Applied Research Unit in Renewable Energy in Desert Regions:** Under the umbrella of the Renewable Energy Development Centre, this unit was established in 2004. It takes part in all technological development and scientific research projects that the National Programme for Research in Renewable Energies section undertakes. It focuses on carrying out studies to advance and improve the application of renewable energy sources in arid areas.
- **Algerian Institute of Renewable Energy:** Since this school provides training in subjects including engineering, security and safety, energy audits, and project management, it mainly supports the state's training initiatives in the field of renewable energy.

I.7.4. The legal and legislative framework for renewable energy in Algeria

In this regard, Algeria has created a number of incentive systems inside legislative frameworks to control and specify the functions of different organizations engaged in the most efficient use and investment of renewable natural resources. Among the most significant statutes are:

- **The Decree dated 28/12/1988**: About the Renewable Energy Center's linkage with solar equipment development divisions.
- **Law N° 02-01 dated February 5, 2002:** Has to do with gas delivery to the general population and power. The laws are regarded as the first to address the sale of energy generated from renewable sources, encourage the utilization of renewable energies, and include the environmental obligations outlined in them [55].
- **Law N° 04-09 dated August 4, 2004:** Focuses on advancing renewable energy sources within the context of sustainable development. It calls for the creation of a national programme to support renewable energy sources as well as the encouragement and advancement of their advancement. The law also creates a national observatory for renewable energy, whose job it is to advance and promote these sources of energy [56].
- **Presidential Decree N° 12-416, dated December 11, 2012**: Comprises the approval of the agreement of understanding in the areas of energy management and renewable energy between the governments of Algeria and Tunisia. This entails working together to encourage the use of renewable energy sources and reduce energy consumption in both nations.
- **Decree N° 17-89, dated February 26, 2017:** This lays forth the process for releasing tenders for the generation of renewable energy or those resulting from cooperative production and the unification of the national power supply system [57].

  Executive Decree N° 20-322 of November 22, 2020: Outlines the authority of the Minister of Renewable Energies and Energy Transition [58].

- **Executive Decree N° 20-323 dated November 22, 2020**: It controls the Ministry of Energy Transition and Renewable Energies' core administration [59].

I.8. Regulations, policies and incentives

I.8.1. Government and international initiatives

The objectives of the markets, policy, and regulation research area are to evaluate regulations, policies, ownership structures, and market products that are emerging or needed to ensure efficient operation of HES. To relate the greater sense of urgency for the markets, policy, and regulation opportunities, they are presented prior to those for valuation and technology development. In other words, the sudden rise in HES is challenging conventional approaches in markets, policy, and regulation. Markets, policy, and regulation research topics related to HES extend across topic areas and jurisdictions, from federal regulation and wholesale markets to state utility regulation, state policy and local regulation.

I.8.2. Standards and protocols for hybrid integration

The following steps can be considered among the standards and protocols for hybrid integration of renewable energies [52]:

- Study of loads and requirements: A study is carried out precise electrical load in terms of type, quantity, nature and relationship with time. An important parameter in the design of the system is to determine the amount of load loss allowed.
- Evaluation of sources: In order to choose the most appropriate source from among those available in the area to be supplied with electricity, it is necessary to evaluate the sources (solar, wind, etc.). Data on each of these sources must be available for evaluation.
- Technology assessment: Once the sources to be applied have been identified, research is carried out and the best technological options for these sources are determined.
- Determination of system components: The process of determining the system components includes determining the power of each component as well as the optimum way of connecting these components.

I.9. Conclusion

Throughout this chapter, we have examined the fundamental principles, components, architectures, advantages, and challenges associated with hybrid energy technology. From component plays a crucial role in shaping the performance and viability of hybrid systems. We have also delved into common hybrid technologies and architectures, including hybrid micro-grids, autonomous systems, and grid-connected installations. Case studies and real-life applications from around the world have provided valuable insights into the practical implications of hybrid energy technology, current trends and innovations underscores the dynamic nature of hybrid energy production, the potential of hybrid energy systems to facilitate sustainable development and address energy challenges remains significant. Finally, the last section of this chapter is about the specific context of Algeria. The adoption of hybrid energy systems presents an opportunity to diversify the energy mix, enhance energy security, and promote economic development while mitigating environmental impacts. By embracing hybrid energy technology and leveraging supportive policies. In the next chapter, we will discuss the components of the proposed hybrid system and their modelling.

Chapter II

Modelling of multi-source system: different production systems

II.1. Introduction

Modeling is a mathematical technique used to represent a technological process. The goal is to theoretically study the behavior of particular parameters and optimize them while adhering to a given constraint. To this end, modeling the multi-source energy system is required to establish a direct relationship between the energy produced by the system and the demand for its use. While the estimation of the system's adaptability properties to each period of the year is based on a theoretical and empirical study. The system proposed in this study is a hybrid multi-source system with a storage system. It consists of a photovoltaic generator, a fuel cell, a battery and a supercapacitor. In the sections that follow, we will outline the well-detailed mathematical models for each of these many system components.

II.2. Definition of multi-source system modelling

Multi-source system modeling refers to the process of creating mathematical or computational models that represent systems powered or influenced by multiple sources of energy, inputs, or factors [59].These systems often involve diverse energy sources such as solar, wind, fuel cell, and battery storage, among others.

II.3. Study, analysis and choice of the final system architecture

According to the electric bus , we distinguish three architectures or bus configurations in hybrid systems:

II.3.1. AC coupling

The solution traditionally used in electrical systems is to transmit power in AC form, as shown in Figure II.1. In the AC bus topology, all production sources are connected to the AC bus via converters. This configuration offers better performance than the previous one, since decoupling the different sources of production would allow them to act quite independently of each other. However, the efficiency of the system as a whole is low, because a certain amount of energy is lost through the use of static converters, and this type of combination complicates the control system.

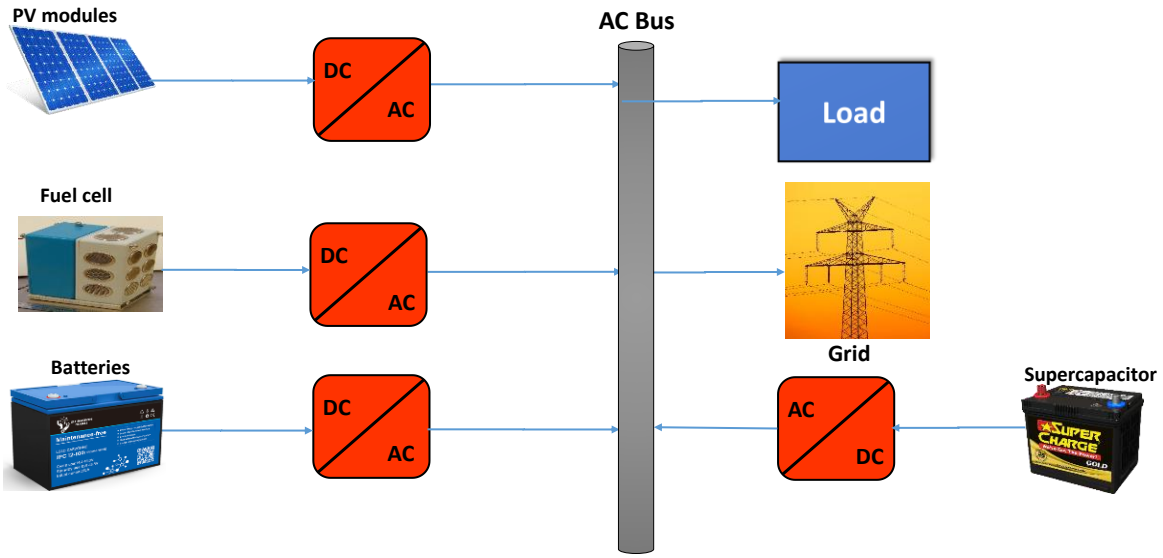

Figure II.1. The structure of the hybrid system with bus AC.

II.3.2. Mixed DC/AC coupling

For distributed systems, in a micro-grid, or in an isolated site, a good solution may be the mixed coupling, associating a continuous bus, and an alternating bus [59]. The load(s) may, depending on the case, be continuous or alternating. This solution makes it possible to connect each one to the bus which corresponds to it, then to exchange the power between the buses by means of reversible DC/AC converters, as shown in Figure II.2.

When the load level is low, either source can generate the energy required. However, the two sources can operate in parallel during peak loads.However the implementing of this system is relatively complicated because of the parallel operation (the inverter must be able to operate both autonomously and non-autonomously, synchronising the output voltages with the output voltages of the AC generator).

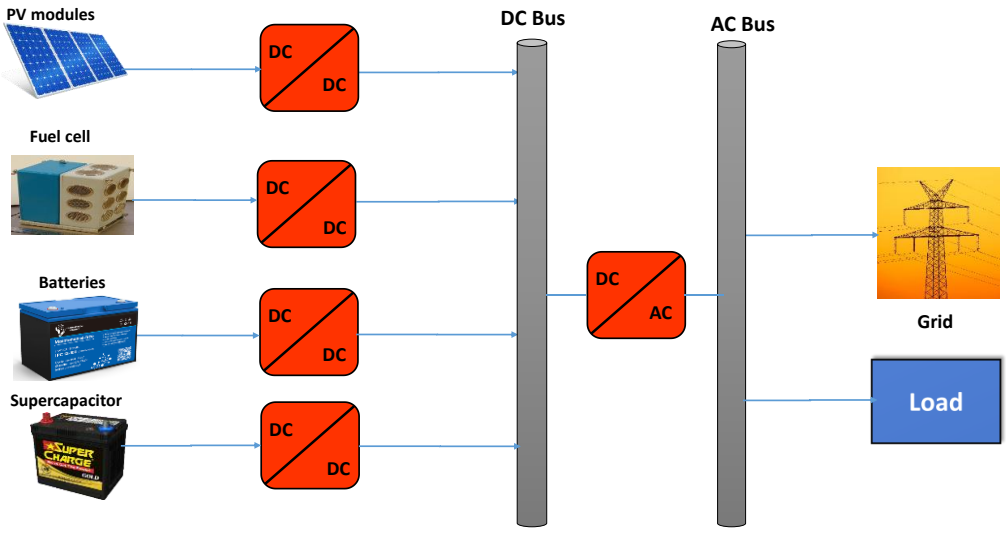

Figure II.2. The structure of the hybrid system with mix bus AC and bus DC.

Thus freed from the constraints of waveform, the continuous storages can more efficiently manage the energy of the system thanks to DC / DC converters, and the processing of the photovoltaic power is simplified.

II.3.3. DC coupling

Figure II.3 shows the DC bus structure of a hybrid system. In this architecture, the energy supplied by each system source feeds a DC bus through DC/DC converters. with a grid system connected to the DC bus via an inverter. The advantage of this topology is the simplicity of control compared with other configurations. And the photovoltaic panel can be optimally sized to operate at maximum power during the demand for power.

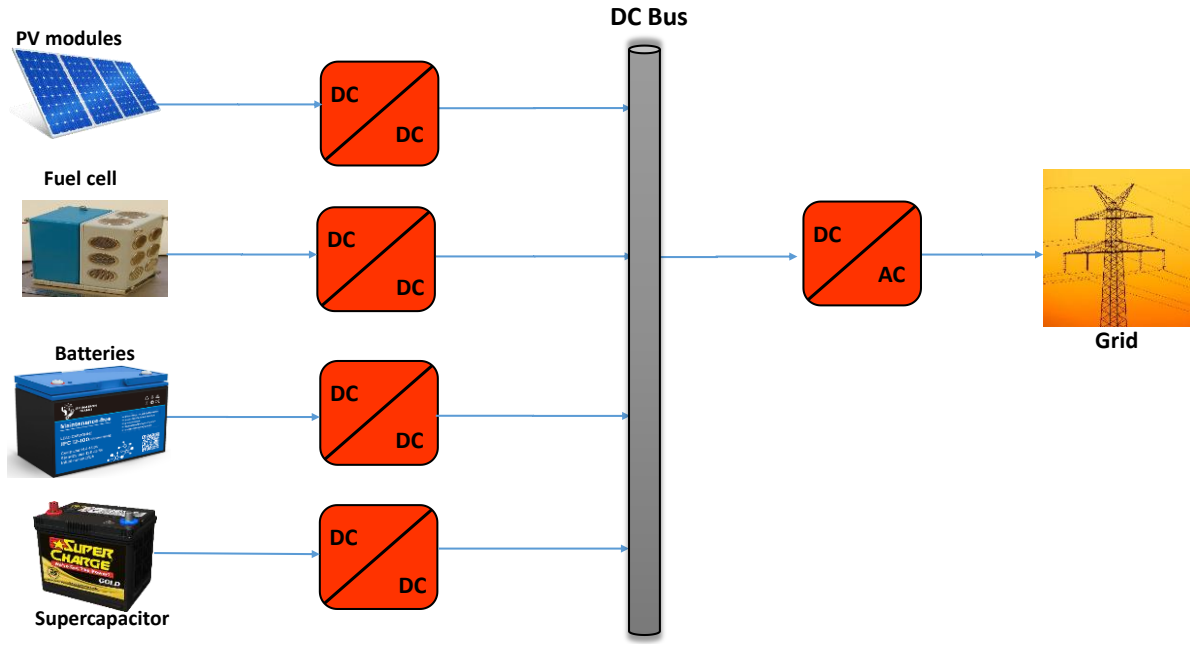

Figure II.3. The structure of the hybrid system with DC bus.

II.4. Development of energy source models

II.4.1. Photovoltaic System Modelling

A solar cell is a semi-conducting PN junction that generates electricity via photovoltaic effect. Figure II.4 shows the single diode model of a PV cell in a static configuration, a PV cell is composed of a current source, a diode, and two resistors: R_{sh} in parallel with the current source and diode, and R_s in series connection.

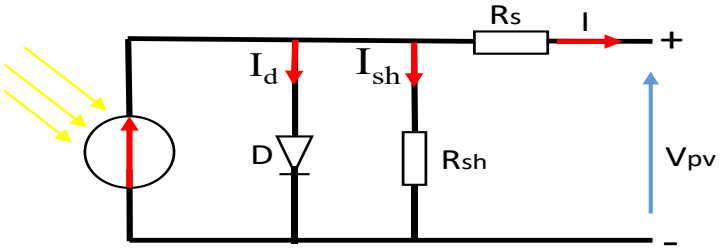

Figure II.4. Equivalent electrical diagram of a PV cell.

Equation (II.9) uses Kirchhoff's current law to define the output current of the solar cell:

$$I_{pv} = I_{ph} - I_d - I_{sh} \quad \text{(II.1)}$$

Where I_d is the diode saturation current, I_{ph} is the incoming photon current, and I_{pv} is the PV cell's output current.

Figure II.4 presents a PV cell, which includes a controlled current source I_{ph}, a diode I_d, and internal resistances (R_s and R_p). The controlled current source depends on solar irradiation and cell surface temperature, as shown below:

$$I_{ph} = \left[I_{ph,T_{ref}} + \sigma_I\left(T_c - T_{ref}\right)\right]\left(\frac{G}{G_{ref}}\right) \quad \text{(II.2)}$$

Where:

$$I_{ph,T_{ref}} = \frac{R_{sh}R_s}{R_{sh}} I_{sh,T_{ref}} \quad \text{(II.3)}$$

Photovoltaic cells are connected in a serial configuration to create a photovoltaic module [60]. For a module with N_s cells connected in series and N_p cells connected in parallel, the module's current can be calculated based on its tension as follows:

$$\boldsymbol{I_{PV} = I_{ph}N_p - I_0N_p\left\{exp\left[\frac{V_{pv}+I_{pv}R_s\left(\frac{N_s}{N_p}\right)}{mV_T}\right] - 1\right\} - \frac{V_{pv}+I_{pv}R_s\left(\frac{N_s}{N_p}\right)}{R_p\left(\frac{N_s}{N_p}\right)}} \quad \text{(II.4)}$$

Where:

$$I_0 = \frac{I_{sh,T_{ref}}+\sigma_I\left(T_c-T_{ref}\right)}{exp\left(\frac{V_{oc,T_{ref}}+\sigma_V\left(T_c-T_{ref}\right)}{mV_T}\right)-1} \quad \text{(II.5)}$$

The thermal voltage of a PV module is defined as ($V_T = \frac{N_sKT_c}{q}$). K represents the Boltzmann constant (1.380×10^{-23} Joules/Kelvin), q represents electron charge (1.602×10^{-19} C), and T_c denotes module temperature.$I_{ph,T_{ref}}$represents photocurrent,$I_{sh,T_{ref}}$the short-circuit current, and

$V_{oc,T_{ref}}$ the open-circuit voltage at STC. The relative temperature coefficients for current and voltage are α_I and α_V, respectively [61].

II.4.1.1. I-V characteristic curve

At a constant temperature of 25°C and constant solar radiation of 1000 W/m^2. The I-V characteristic of the photovoltaic system is represented by the I(V) curve shown in Figure II.5 where:

- ✓ Point 1: The current is at its maximum (I short-circuit) while the voltage is zero
- ✓ Point 2: The cell produces the maximum power possible thanks to optimum operation.
- ✓ Point 3: The voltage is at maximum (V open circuit) while the current is zero.

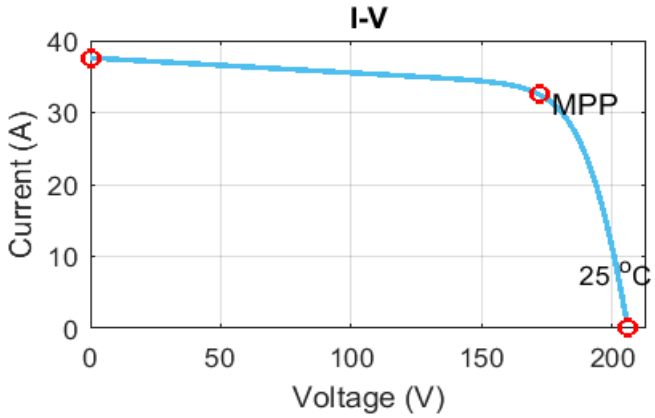

Figure II.5. Typical I-V characteristic of a solar module.

II.4.1.2. P-V characteristic

The P(V) characteristic of the photovoltaic system is represented by the P(V) curve shown in Figure II.6 at a constant temperature of 25°C and constant solar radiation of 1000 W/m^2 . In this way, the power of the photovoltaic system increases until it reaches the optimum value MPP and then decreases as a function of the change in voltage.

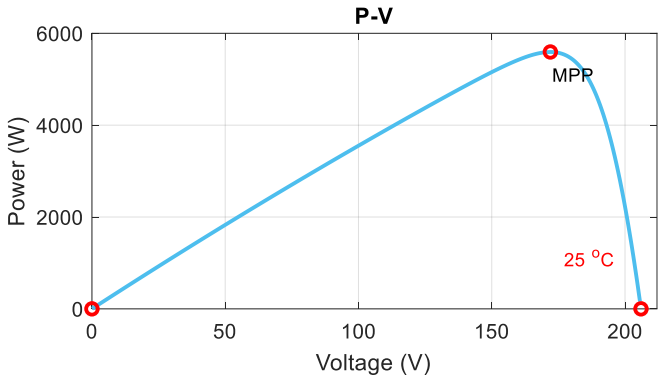

Figure II.6. Typical P-V characteristic of a solar module.

II.4.1.3. Irradiance Influence on P-V and I-V curves

Figure II.7 displays the electrical characteristics of the PV module at varying irradiance levels (ranging from 0 W/m^2 to 1000 W/m^2). The temperature remains constant at 25°C. Higher solar irradiance leads to higher I_{SC} and P_{MPP} levels. The MPP voltage (V_{MPP}) and open circuit voltage (V_{OC}) increase slightly. Weather conditions have a significant impact on the electrical performance of PV modules, as previously demonstrated. P-V and I-V curves show nonlinear characteristics. PV module output power/current depends on three factors: PV operating voltage, temperature, and irradiance. Irradiance directly affects short-circuit current, but temperature has a greater impact on MPP voltage.

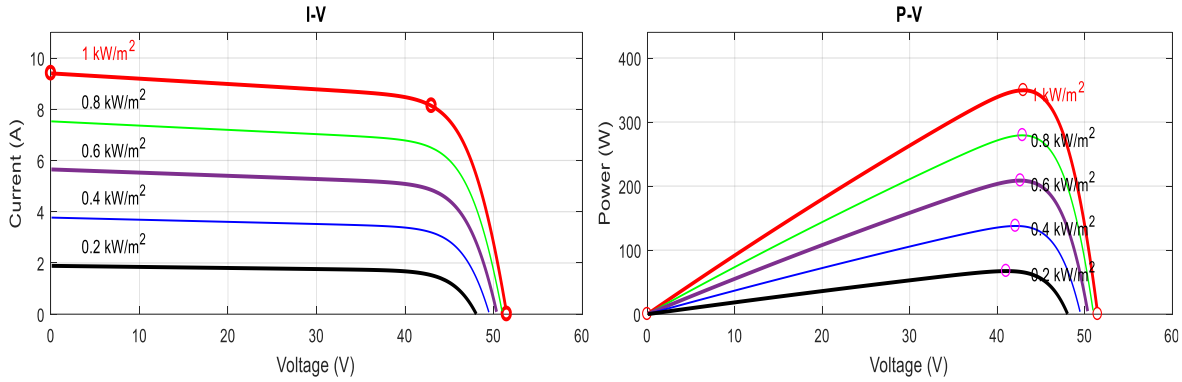

Figure II.7. Effect of variable irradiance on the P-V and I-V characteristic curve.

II.4.1.4. Temperature Influence on P-V and I-V characteristics

Simulation tests on a typical PV module show how environmental conditions (G and T) affect the electrical characteristics. In simulation, a single diode PV model is used. The P-V and I-V curves are presented and discussed. Figure II.8 displays the P-V and I-V characteristics at temperatures ranging from 0 to 50°C, with a constant irradiance of 1000 W/m^2 . It is observed that the short-circuit current and output power increase proportionally with irradiance intensity, whereas the open-circuit voltage exhibits a less pronounced variation.

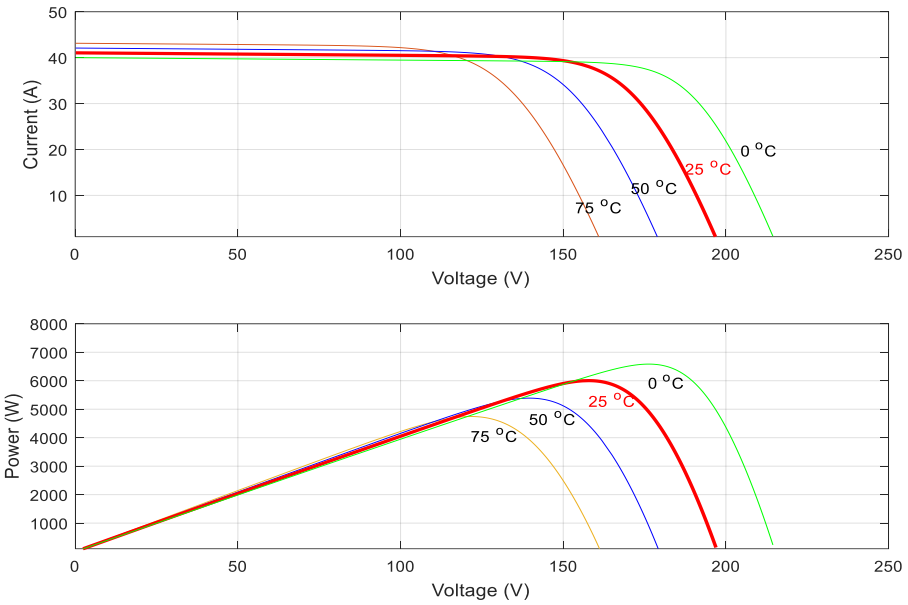

Figure II.8. Effect of variable temperature on the P-V and I-V characteristic curve.

II.4.2. Fuel cell modelling

In this thesis, a proton exchange membrane fuel cell (PEMFC) is used as shown in Figure II.9. The fuel cell uses hydrogen generated from renewable energy sources is proposed as preferable due to its advantages like zero-emission and high capacity. A Proton Exchange Membrane (PEM) fuel cell consists of three layers: anode, cathode, and electrolyte. The operation of the fuel cell, hydrogen is fed to the anode, which is subjected to an electrochemical reaction to produce protons and electrons. Meanwhile, oxygen is fed to the cathode to take part in the reduction reaction. Hydrogen is converted to protons and electrons at the anode catalyst layer, which is composed of platinum and supported by a carbon backbone [62].

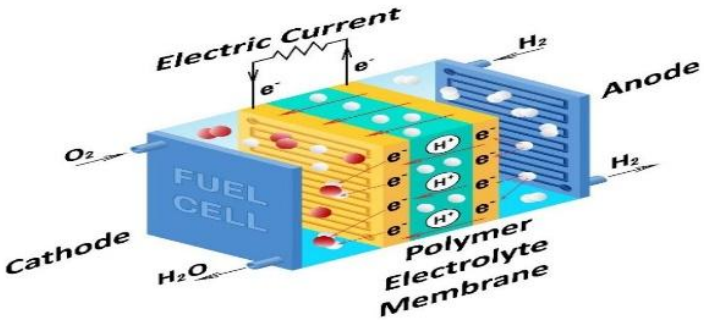

Figure II.9. Schematic diagram of a fuel cell.

The PEM fuel cell works according to the following reactions:

- At the anode, hydrogen is oxidised to protons :

$$H_2 \rightarrow 2H^+ + 2\,e^- \qquad \text{(II.6)}$$

- At the anode, oxygen is reduced as follows:

$$O_2 + 4\,e^- \rightarrow 2O^- \quad \text{(II.7)}$$

- At the cathode, protons react with oxygen to form water and absorb electrons [63].

$$\frac{1}{2}O_2 + 2H^+ + 2\,e^- \rightarrow H_2O \quad \text{(II.8)}$$

The equation for the overall electrochemical reaction of a feul cell :

$$H_2 + \frac{1}{2}O_2 \rightarrow H_2O + Electricity + HEAT \quad \text{(II.9)}$$

The polarization curve of the PEMFC operating at 70 °C is presented in Figure II.10. The curve is divided into three characteristic regions: activation losses, ohmic losses, and concentration losses [64]. Activation polarization arises from the sluggish kinetics of the electrochemical reactions at the electrodes. Ohmic polarization is associated with internal resistances within the membrane, electrodes, and current collectors, leading to a linear voltage drop. At high current densities, mass transport limitations in delivering reactants to the catalyst layer dominate, resulting in concentration polarization.

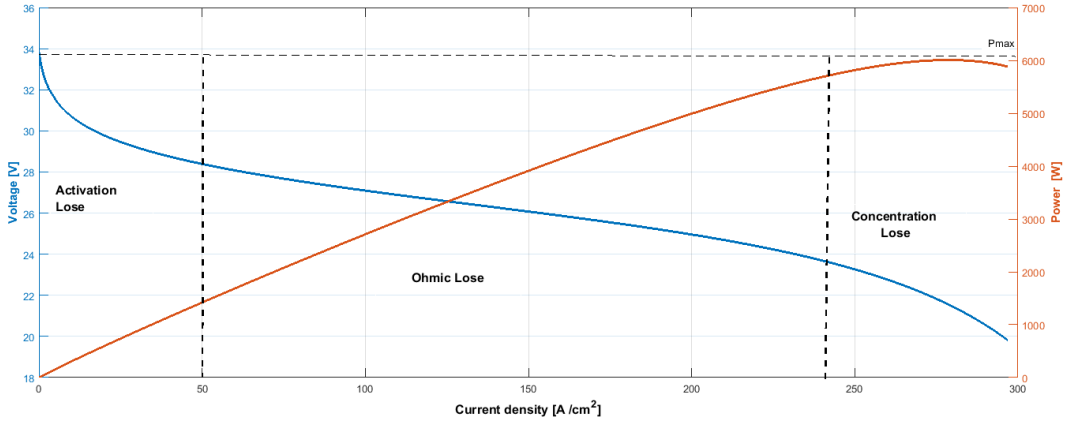

Figure II.10. Polarization and power density curves of a PEMFC at 70 °C.

By grouping together all the losses causing voltage drops in a PEM fuel cell, the voltage of a cell can be expressed by the following equation:

$$V_{FC} = E - \eta_{act} - \eta_{ohm} - \eta_{conc} \quad \text{(II.10)}$$

II.4.2.1 Activation losses

These losses occur during the initiation of the chemical reactions on the electrode surfaces. It is most dominant at low current densities. The activation voltage drop is given in the following form:

$$\eta_{act} = A.ln\left\{\frac{I_{cell}+I_n}{I_0}\right\} \quad \text{(II.11)}$$

Where: A is the Tafel coefficient, $I_{cell}$is the current delivered by the fuel cell, I_0 is the exchange current density at the cathode since the cathodic overvoltage is greater than that of the anode and I_n the internal current to take account of any gas and/or electrons passing through the electrolyte.

II.4.2.2. Ohmic losses

During proton passage, the internal resistances of the electrodes and membrane resistance cause ohmic losses.

$$\eta_{ohm} = R(I_{cell} - I_n)_{int} \quad \text{(II.12)}$$

$$Relc_{mem_{int}} \quad \text{(II.13)}$$

Where R_{int} is the total resistance of the fuel cell, $R_{elc}$the specific electrode resistance and R_{mem} is the specific proton resistance of the membrane.

II.4.2.3. Concentration losses

The concentration losses are given by equation (II.18). This voltage is expressed as a function of a limiting current I_L for which, as all the fuel is used, its pressure would fall to zero, and a constant B called the transport or mass transfer constant.

$$\eta_{conc} = -B.ln\left\{1 - \frac{I_{cell}+I_n}{I_L}\right\} \quad \text{(II.14)}$$

Typically, a PEM fuel cell generates little electrical power. To generate more power, the cells are connected in series and parallel to form a module [65]. The total voltage delivered by a PEM module is expressed as:

$$U_{cell} = N_s.V_{cell} = N_s.\left[E - A.ln\left(\frac{I_{cell}+I_n}{I_0}\right) - R_{int}.(I_{cell} + I_n) + B.ln\left(1 - \frac{I_{cell}+I_n}{I_L}\right)\right] \quad \text{(II.15)}$$

II.4.3. Storage system modelling

The backup energy storage system is designed to ensure load demand coverage during periods of unavailability or insufficient renewable generation in the hybrid system. In this work, a hybrid storage system is implemented by combining a battery and a supercapacitor. It is necessary because no single storage technology is perfect. This configuration efficiently addresses both long-term energy supply and short-term power fluctuations, as summarized in Table II.1.

Table II. 1. Comparative Characteristics of Batteries and Supercapacitors.

Feature	Battery	Supercapacitor
Energy Density	High (long-term storage)	Low
Power Density	Medium	Very high (fast charge/discharge)
Cycle Life	Moderate (thousands of cycles)	Very long (millions of cycles)
Response Time	Slow (seconds)	Very fast (milliseconds)

The supercapacitor supports the battery during charging and discharging transients caused by variations in energy demand and climatic conditions [66]. Both storage units are interfaced with the DC bus through bidirectional DC–DC step-down converters, enabling bidirectional current flow, as illustrated in Figure II.11.

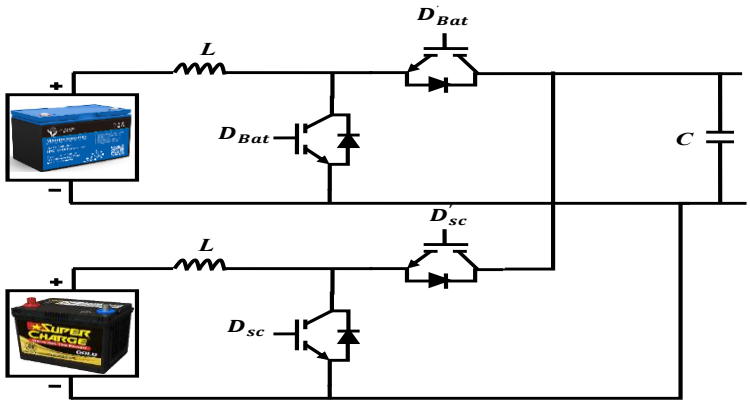

Figure II.11. Proposed hybrid energy storage system.

II.4.3.1. Battery modelling

The lead-acid battery used in this study is adopted. The equivalent circuit of the battery is shown in Figure II.12. In order to ensure that the load obtains the necessary energy in all circumstances, the additional energy generated compared with that required for charging would be stored (battery charging) and used as a supplement (battery discharging).

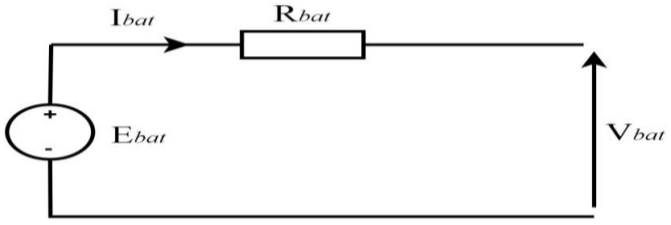

Figure II.12. Equivalent battery circuit.

The following relationship gives the expression for the voltage at the battery terminals (V_{bat}):

$$V_{bat} = E_{bat} - T_{bat(t)} \cdot I_{bat} \quad \text{(II.16)}$$

Internal battery parameters, such as battery current, battery hysteresis throughout the charge and discharge cycles, and extracted capacity, all affect the voltage of the nominal load during charging or discharging of the battery [67].

- **Battery charge model:**

When the power from renewable sources (photovoltaic) or backup sources (fuel cells) is greater than the load, the batteries are in a state of charge [68], and the capacity of the batteries at time t can be given by :

$$C_{bat(t)} = C_{bat(t)}(t-1).(1-\alpha) + \left(\frac{P_{pv}(t)+P_{fc}(t)+P_L(t)}{\eta_{inv}}\right)\eta_{bat} \quad \text{(II.17)}$$

$C_{bat(t)}$ and $C_{bat(t)}$ (t-1) are the quantities of battery charging and discharging at times (t) and (t-1) respectively, σ is the hourly rate of spontaneous charging, P_{pv} is the photovoltaic generator power, P_{fc} is the fuel cell generator power, P_L is the load demanded at time t, η_{bat} and η_{inv} are the inverter and battery efficiencies successively.

During charging, the efficiency is between 0.65-0.85 depending on the current load, whereas during discharging, the battery efficiency is set equal to 1.

- **Battery discharge model:**

When the load demand is greater than the power generated, the capacity of the batteries at time t can be expressed as follows:

$$C_{bat(t)} = C_{bat(t)}(t-1).(1-\sigma) + \left(\frac{P_L(t)}{\eta_{inv}-P_{pv}(t)+P_{fc}(t)}\right) \quad \text{(II.18)}$$

At any given time, the amount of charge in the batteries is subject to the following constraints:

$$C_{bat_min} \leq C_{bat} \leq C_{bat_max} \quad \text{(II.19)}$$

Here, the maximum battery capacity takes the value of the nominal battery capacity

$$C_{bat_max} = C_{bat,N} \quad \text{(II.20)}$$

while the minimum allowable capacity is defined by the depth of discharge (DOD):

$$C_{bat_min} = (1-DOD).C_{bat,N} \quad \text{(II.21)}$$

The maximum value of the state of charge (SOC) is equal to 1, and the minimum is determined by the maximum depth of discharge, SOC_{min}=1-DOD.

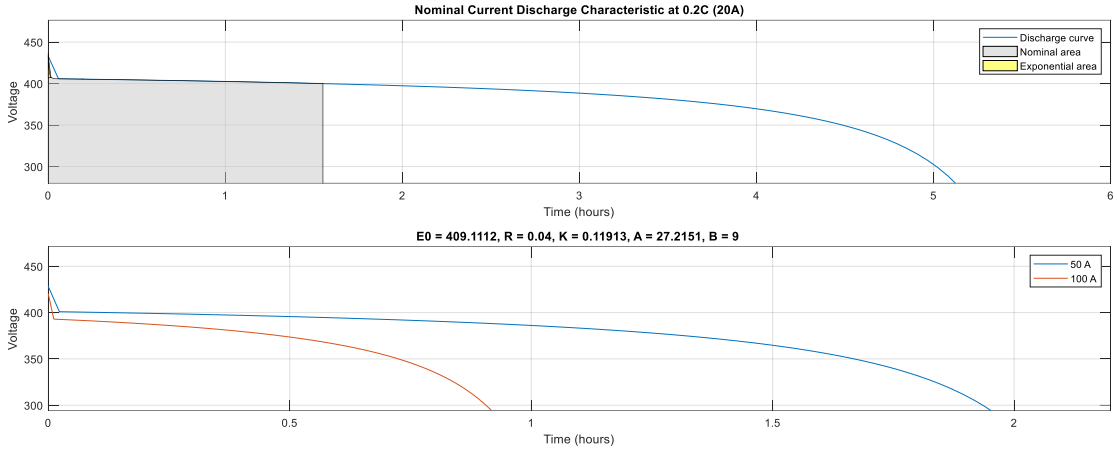

Figure II.13. Battery discharge characteristics under nominal and variable load currents.

II.4.3.2. Modeling of supercapacitor

Supercapacitor is a new technology for energy storage systems. Energy is stored using static charge rather than the battery's inherent electrochemical process.

In a matter of seconds during fast charge and discharge cycles, the R_1C_1 cell determines the supercapacitor's immediate behavior. R_2C_2 is the slow branch's representation. Within minutes, the first long-range cell is completed, and at the conclusion of the charge or discharge, the internal energy distribution is described [69]. The voltage of the SC is given by the following equation, ignoring the leakage current:

$$U_{sc} = N_{S\text{-}sc} V_{sc} = N_{S\text{-}sc} \left(V_1 + R_1 \frac{I_{sc}}{N_{P-sc}} \right) \quad \text{(II.22)}$$

Where V_{SC} and I_{SC} are the voltage and current of the elementary supercapacitor, respectively, and U_{SC} and I_{SC} are the voltage and current of the SC pack, respectively. The number of parallel and series branches of the SC_s connections are denoted by $N_{P\text{-}sc}$ and $N_{S\text{-}sc}$. In the secondary capacity C_2, the voltage v_2 is provided by:

$$V_2 = \frac{1}{C_2} \int I_2 dt = \frac{1}{C_2} \int \frac{1}{R_2} (V_1 - V_2) dt \quad \text{(II.23)}$$

II.4.3.2 Supercapacitor state of charge (SOC)

The state of charge (SOC) of the supercapacitor is determined as follows [II.28] :

$$SOC_{sc-min} \leq SOC_{sc} \leq SOC_{sc-max} \quad \text{(II.24)}$$

Where:

SOC_{sc-max} and SOC_{sc-min} represent the maximum and minimum SOC of the SC.

II.4.4. Modelling the various power converters

In an HES, converters are used to charge storage systems, convert direct current to alternating current, and more. The three main types of converters found in HESs are rectifiers, inverters and choppers. Rectifiers convert alternating current into direct current. Charging batteries from an alternating current source is often used in HSEs. These tools are relatively simple, affordable and effective.

II.4.4.1. Modeling of the boost converter

A step-up boost converter, is a DC-DC switching converter whose output voltage is greater than its input voltage. PV arrays with low output voltages that must be raised in order to be synchronized with the grid voltage typically require this kind of conversion. To create a successful MPPT algorithm, the power conversion stage's dynamic behavior is crucial.

We have two subsystems that use the boost converter:

- The PEM fuel cell is connected to the DC bus thanks to a boost converter in order to control the DC bus voltage at a reference value in the case of lack of energy.
- The wind turbine itself connected to the DC bus thanks to a booster chopper to make operate the wind generator at the maximum power point.

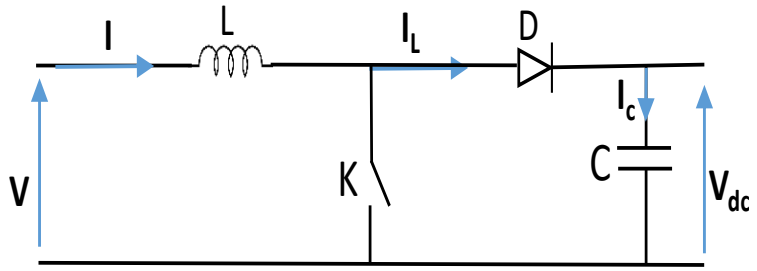

Figure II.14. Schematic diagram of a boost converter.

Figure II.14 shows a schematic diagram of a boost converter. The operation of a boost converter can be divided into two switching phases depending on the state of the switch K (open/closed). Each state is represented by a differential equation.

For the first period: K is closed

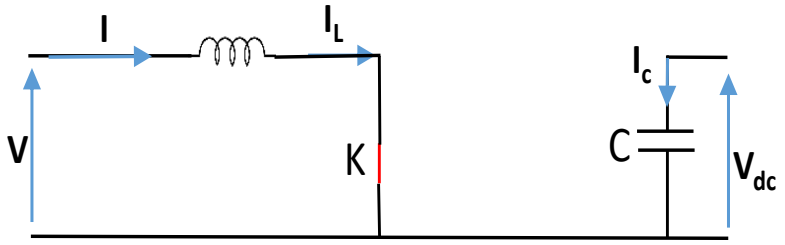

Figure II.15. Equivalent circuit of a converter in the closed state.

$$\begin{Bmatrix} v = L\dfrac{dI}{dt} \\ 0 = C\dfrac{dV_{dc}}{dt} + I_{dc} \end{Bmatrix}$$

For the second period: K is opened

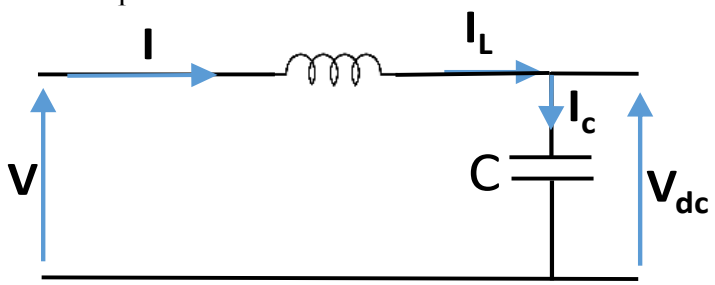

Figure II.16. Equivalent circuit of a converter in the opened state.

$$\begin{Bmatrix} V = L\dfrac{dI}{dt} + V_{dc} \\ I = C\dfrac{dV_{dc}}{dt} + I_{dc} \end{Bmatrix}$$

We consider that the switches used in this study are perfect. We can represent the converter by a system of equations:

$$\begin{Bmatrix} L\dfrac{dI}{dt} = V - (1-u)V_{dc} \\ C\dfrac{dV_{dc}}{dt} = (1-u)I - I_{dc} \end{Bmatrix}$$

Where u is the state of switch K, given by:

u=1, when switch K is closed (Figure II.15),

u=0, when switch K is open (Figure II.16).

II.4.4.2. Modelling of Bidirectional converter

In our work, the bidirectional converter is an essential element for controlling the charge and discharge of an energy storage system (battery + supercapacitor).

The reversible converter used in the storage system is a reversible power transfer, to charge and discharge the battery. The schematic diagram of a bidirectional chopper is given in Figure II.17, with the first direction corresponding to discharge mode (as a boost converter). The converter transfers energy from the battery to the DC bus when there is a shortfall in renewable energy production.

The second represents load mode (as a buck converter). When there is an excess, the bidirectional converter transfers the excess power from the DC bus to the battery, regulates the DC bus voltage and controls the power flow.

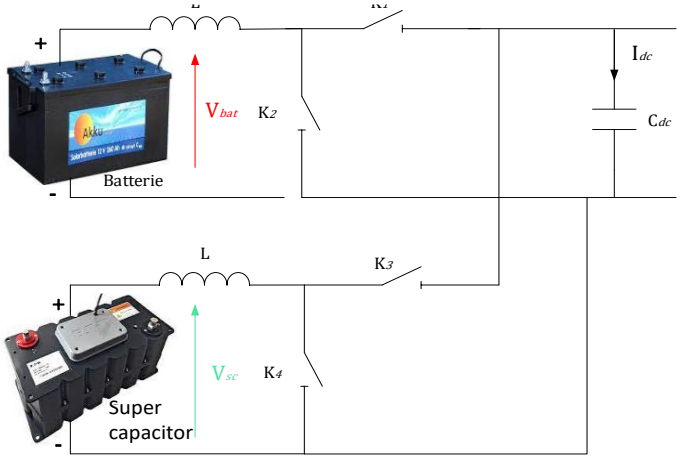

Figure II.17. Electrical diagram of the bidirectional DC/DC chopper.

II.4.4.3. Modelling the inverter

The output current from the inverters is not sinusoidal, but it will be filtered. The voltage generated by the inverter is filtered using the filter R_f,L_f.

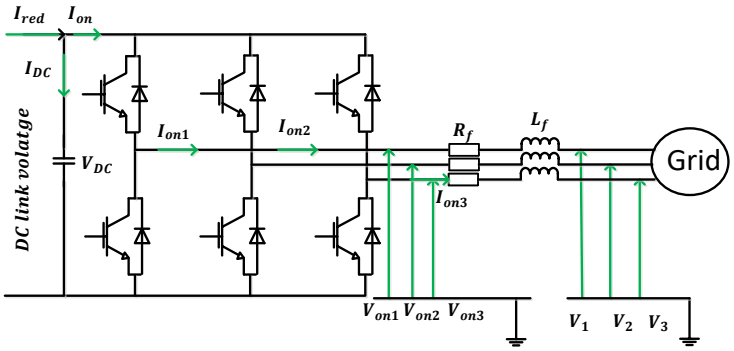

Figure II.18. Voltage converter operating in inverter mode.

Classification of inverters

- **Three-phase model:**

Following the same approach as above, the model can be written as follows:

$$L_f \frac{dI_{on1}}{dt} + I_{on1}R_f = V_1 - V_{on1}$$
$$L_f \frac{dI_{on2}}{dt} + I_{on2}R_f = V_2 - V_{on2}$$
$$L_f \frac{dI_{on3}}{dt} + I_{on3}R_f = V_3 - V_{on3}$$
$$C\frac{dV_{DC}}{dt} = I_{on} - I_{red}$$
$$C\frac{dV_{DC}}{dt} = \sum_{1}^{3} \frac{S_i I_{oni}}{2} - I_{red}$$

• **Model in Park's frame of reference**

In this case, we obtain:

$$\begin{cases} L_f \dfrac{dI_{ond}}{dt} + I_{ond}R_f = V_{sd} - S_d \dfrac{V_{DC}}{2} \\ L_f \dfrac{dI_{onq}}{dt} + I_{onq}R_f = V_{sq} - S_q \dfrac{V_{DC}}{2} \\ C \dfrac{dV_{DC}}{dt} = I_{on} - I_{red} \\ I_{on} = \dfrac{1}{2}\left[S_d I_{ond} - S_q I_{onq}\right] \end{cases}$$

II.4.4.4. Modelling the DC bus

The continuous bus is typically regarded as incapable in modeling. We completed the coupling of sources in accordance with the continuous bus configuration after all fundamental models had been described.

The power supplied by the system sources is collected in the DC bus as shown in Figure II.19. After describing each basic model, we coupled the sources according to the DC bus layout, counted as a capacitance in the modelling.

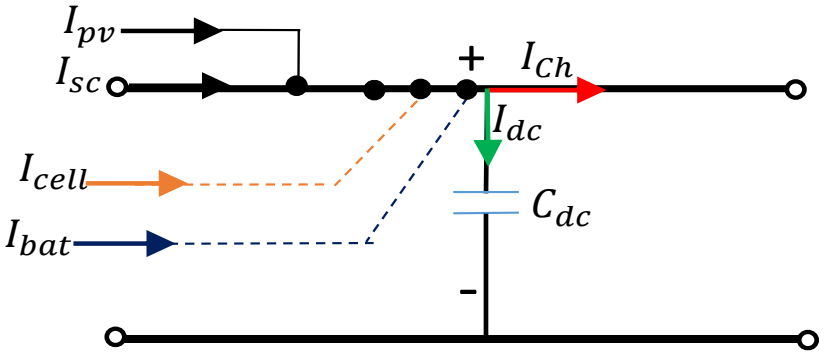

Figure II.19. Electrical diagram of the DC bus.

The current in the bus is given by the following equation:

$$\frac{dV_{dc}}{dt} = \frac{1}{C} I_{dc} \qquad \text{(II.25)}$$

Where : $I_{DC} = I_{pv} + I_{cell} \pm I_{Bat} \pm I_{sup} - I_{ch}$

• I_{pv} : Photovoltaic generator current.

• I_{cell} : Fuel cell current.

• I_{Bat} : Battery current.

• I_{sc} : Supercapacitor current.

• I_{ch} : The load current.

II.5. Evaluation the components of the hybrid system

The hybrid energy system studied is described in Figure II.20. The system consists of two renewable energy sources and a hybrid energy storage system. The first source is a photovoltaic generator coupled to a DC-DC boost converter; the second source is a fuel cell connected to a DC-DC boost converter. As for the HESS, it consists of a lead-acid battery and a supercapacitor, both coupled to its own bidirectional converter (DC/DC), and a load shedder (resistor) is used to protect the storage system against overloads. The aim of this system is to supply the necessary power to the grid by connecting the above components in parallel with bus-DC. Thanks to the inverter (DC/AC) connected to the grid, the DC voltage is converted into AC voltage.

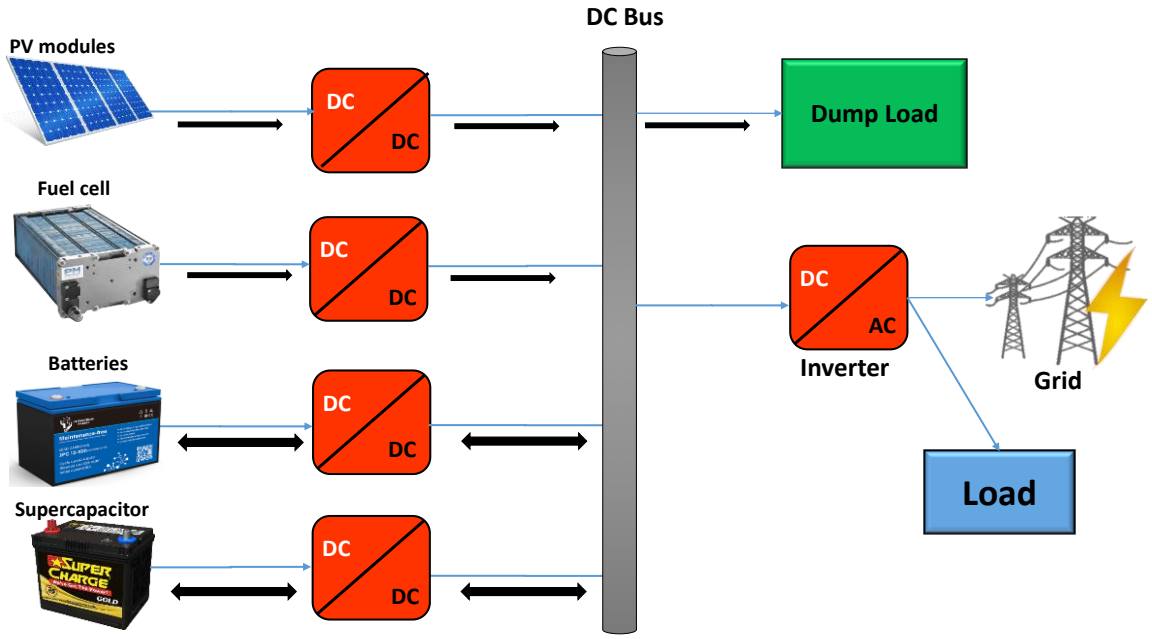

Figure II.20. The structure of the hybrid energy system studied.

II.6. Conclusion

In this chapter, we have modelled a multi-source system consisting of a PV generator, a fuel cell, a storage system and converters. A DC bus connects each of these components. The key concepts surrounding the technology used in the HRES and the numerous models have been provided in this context. In order to use renewable resources as efficiently as possible, the components of the HRES must be operated and sized to take account of variations in load. The following chapter provides details on advanced control design, beginning with the LSTM-based controller for photovoltaic generation and extending to the comparative study of classical and fuzzy logic–based energy management strategies for the overall hybrid system.

Chapter III

LSTM Controller Design for a PV system

III.1. Introduction

The increasing demand for clean energy and the urgent need to reduce greenhouse gas emissions have intensified global interest in renewable energy systems, particularly photovoltaic (PV) technologies [70]. PV systems offer significant environmental and economic benefits, but their efficiency is highly dependent on operating conditions such as irradiance, temperature, and shading [71]. To extract maximum power from PV systems under varying conditions, reliable Maximum Power Point Tracking (MPPT) algorithms are essential. Traditional MPPT techniques, such as perturb and observe (P&O) and incremental conductance (INC), are widely used due to their simplicity. However, they often suffer from oscillations around the MPP and slow dynamic response, especially under rapidly changing environmental conditions. In recent years, artificial intelligence (AI)-based MPPT strategies have gained attention due to their adaptability and data-driven nature [72]. Most of these approaches focus on generating optimal reference signals, but few address the challenge of maintaining high tracking performance across all operating regions of the PV system.

In this chapter, we present a simulation-based MPPT controller built using Long Short-Term Memory (LSTM) neural networks. The model is trained using data generated from optimally tuned PI controllers, each operating in a specific voltage region of the PV system. This enables the LSTM controller to learn region-specific dynamics and generalize its control behavior across a wide range of scenarios.

III.2. Maximum power point tracking

The amount of energy that can be extracted from renewable energy sources, including photovoltaic (PV), hydroelectric and wind energy conversion systems (WECS), fluctuates throughout the day and depends on climatic conditions wind speed (for wind energy conversion systems), radiation and temperature (for PV systems) [73]. There is an optimum operating point at which the maximum power from these systems can be extracted.

Solar cells exhibit non-linear V-I properties that vary with solar radiation and temperature. The V-I and V-P characteristics of solar cells have a unique point known as the Maximum Power Point [74]. At this point, the entire system, including the solar panel, generates maximum power and operates more efficiently. The MPP of a solar cell is undefined, but may be calculated using certain algorithms. To perform these computations and methods, the Maximum Power Point Tracking (MPPT) system has been developed.

III.3. Control of photovoltaic power generation systems

To drive the PV system to its maximum power (MPP), the two-loop control strategy is commonly used in control systems with good transient performance. This strategy consists of two primary loops: the seeking loop and the tracking loop. The seeking loop continuously calculates and updates the MPP reference value using an MPPT algorithm, ensuring that the system adapts to changes in irradiance and temperature. The tracking loop rapidly follows the reference provided by the seeking loop, adjusting converter control variables to achieve stable and efficient operation with minimal oscillations. This decoupling between reference generation and tracking enhances system stability, speed, and responsiveness, particularly under dynamic environmental conditions [75],[76].

As a result, a suitable control system should be designed to drive the PV cells to their maximum power points (MPP) in order to maximize the efficiency of this conversion.

III.3.1. State of the art on different MPPT techniques (Seeking Loop)

Maximum Power Point Tracking (MPPT) techniques are essential for optimizing the energy extraction from photovoltaic (PV) systems, ensuring they operate at their highest efficiency under varying environmental conditions. Over the years, Several MPPT techniques have been developed, broadly classified into conventional and advanced methods. These techniques differ in terms of tracking speed, complexity, and efficiency, with advanced methods often leveraging artificial intelligence and optimization algorithms to improve performance [77].

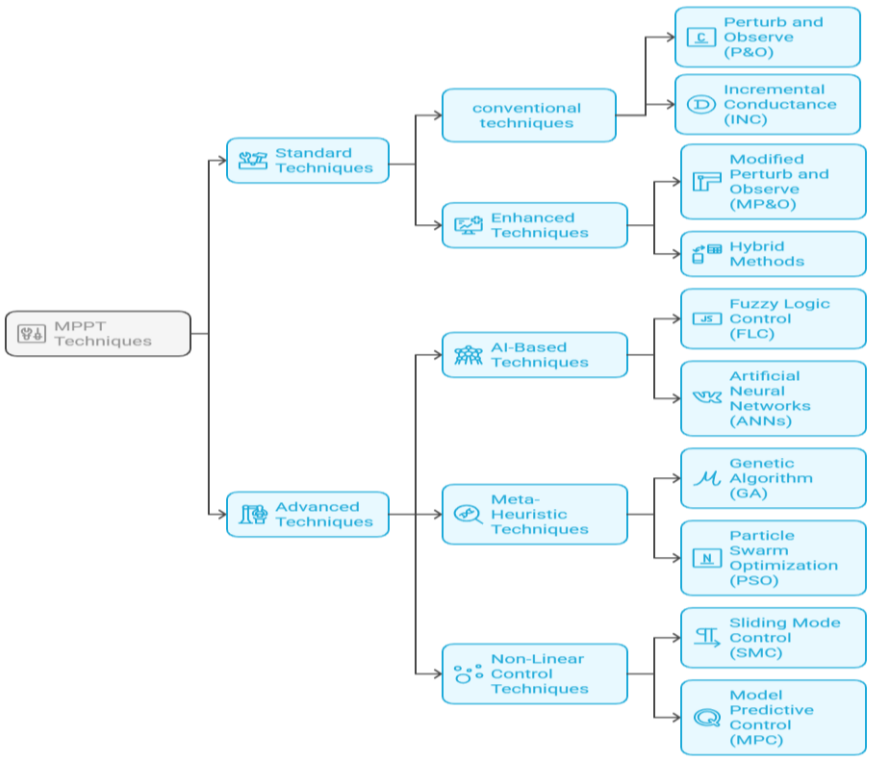

Figure III.1. Classification of MPPT techniques.

III.3.1.1. Conventional techniques

Conventional MPPT techniques are well-established and widely used due to their simplicity and ease of implementation. These methods are generally categorized into standard and enhanced conventional MPPT techniques [78].

Standard conventional MPPT techniques include fundamental approaches such as:

- **Perturb and Observe (P&O):** The Perturb and Observe (P&O) algorithm remains the most extensively applied maximum power point tracking (MPPT) technique in photovoltaic (PV) systems, primarily owing to its algorithmic simplicity, low computational requirements, and ease of implementation in embedded systems [79]. The underlying principle consists of incrementally perturbing the duty cycle of the associated DC–DC converter and observing the resulting variation in output power. When an increase in power is detected, the perturbation is maintained in the same direction; conversely, a reduction in power necessitates a reversal of the perturbation direction, thereby facilitating convergence toward the maximum power point (MPP).

  Despite its widespread use, the classical P&O algorithm is constrained by intrinsic limitations. First, its reliance on continuous perturbation induces oscillatory behavior around the MPP, which inevitably compromises steady-state efficiency. Second, the method is highly sensitive to irradiance and temperature transients. Under rapidly varying environmental conditions, the algorithm may erroneously interpret fluctuations as responses to its own perturbations, leading to divergence from the true MPP and, consequently, significant energy losses. [80].

- **Incremental Conductance (INC):** Incremental Conductance MPPT addresses the limitations of the P&O MPPT approach. The MPP is calculated by comparing the solar PV array's instantaneous conductance to the incremental conductance , leading to more accurate tracking under rapidly changing irradiance conditions [81]. At MPP of the PV source, it holds that:

$$\frac{\partial Ppv}{\partial Vpv} = 0 \Rightarrow \frac{\partial\,(Ipv \cdot Vpv)}{\partial Vpv} = I_{pv} + \frac{\partial \mathrm{Ipv}}{\partial Vpv} V_{pv} = 0 \Rightarrow \frac{\partial \mathrm{Ipv}}{\partial \mathrm{Vpv}} = -\frac{Ipv}{Vp}$$

  However, the IC control process is rather complicated, and the tracking performance will be somewhat impacted by the speed and accuracy of the measurements. In addition, the tracking error is proportional to the step size of the voltage increase.

- **Open Circuit Voltage (OCV):** This technique estimates the MPP voltage as a fixed percentage (typically 75-80%) of the open-circuit voltage of the PV array, reducing computational complexity but at the cost of lower accuracy [82]. One of the simplest and least expensive ways to maximize the power point of a solar panel is to use the constant voltage method. As was previously mentioned, temperature and solar radiation intensity affect panel voltage. There is a linear relationship between V_{MPP} and V_{oc} that can be expressed by: $V_{MPP} = K_V.V_{OC}$. Where V_{oc} is the open circuit voltage, which the manufacturer of the solar PV panel provides. V_{MPP} is the voltage at the maximum power point K_v normally lies between 0.7 and 0.82. If there is any error, the instantaneous input voltage from the panel is compared to the reference voltage, amplified, and used as a duty cycle that is fed into the DC-DC boost converter.

- **Short Circuit Current (SCC):** In this method, the MPP current is estimated as a fraction of the short-circuit current, making it easy to implement but less efficient under varying environmental conditions. This technique takes advantage of the presumption that there is a linear relationship between the cell-short circuit current (I_{SC}) and the cell current corresponding to the maximum power (I_{MP}). The formula for this relationship is $I_{MP} = K.I_{SC}$. Where K is referred to as the current factor. The module's MPP current is approximately 90% of its short circuit current [83].

III.3.1.2. Enhanced conventional MPPT techniques

Enhanced conventional MPPT techniques aim to address the limitations of standard methods by improving tracking accuracy, efficiency, and adaptability under varying environmental conditions. These methods are designed to reduce steady-state oscillations, improve convergence speed, and enhance the robustness of the MPPT process. Some of the commonly used enhanced conventional MPPT techniques include adaptive algorithms, hybrid approaches, and temperature-compensated methods [84].

- **Modified Perturb and Observe (MP&O)**: This variation of P&O incorporates adaptive step-size control to enhance tracking speed and reduce steady-state oscillations [85]. Unlike the traditional P&O, MP&O dynamically adjusts its perturbation step size based on system conditions, leading to improved efficiency and reduced power losses under rapidly changing irradiance.

- **Modified Incremental Conductance (M-INC)**: In [86] employed adaptive algorithms and predictive models, this method refines the accuracy of INC under fast-changing irradiance conditions. M-INC techniques incorporate real-time data processing and optimization strategies to enhance responsiveness and minimize oscillations at the MPP.
- **Hybrid Methods**: Combining different conventional techniques, such as P&O with OCV, enhances reliability and reduces the drawbacks of individual methods. Hybrid approaches leverage the strengths of multiple MPPT techniques, improving overall tracking accuracy and system adaptability [87].

III.3.1.3. Advanced techniques

With the growing demand for higher efficiency and adaptability in MPPT, advanced techniques leveraging artificial intelligence, meta-heuristic algorithms, and nonlinear control methods have been developed. These methods aim to improve convergence speed, accuracy, and robustness under dynamic environmental conditions [88]. Artificial intelligence-based approaches, such as fuzzy logic and neural networks, enable adaptive learning mechanisms that enhance MPPT performance in real-time [89]. Meanwhile, meta-heuristic algorithms, including particle swarm optimization (PSO) and genetic algorithms (GA), offer global search capabilities that efficiently track the maximum power point even under partial shading conditions [90]. Furthermore, nonlinear control techniques, such as sliding mode control and model predictive control, provide enhanced stability and fast transient response, making them suitable for highly dynamic scenarios [91].

III.3.1.3.1. Techniques based on artificial intelligence

Artificial intelligence (AI)-based MPPT techniques improve tracking performance by incorporating machine learning and computational intelligence approaches [92]. These include:

- **Fuzzy Logic Control (FLC)**: Fuzzy logic, that is, the reasoning algorithm that falls under artificial intelligence, aims to replicate human reasoning and decision-making processes in machines. The algorithm enables altering duty cycles dynamically, which improves response time and the system's ability to adapt to changing irradiance conditions [93]. This method is advantageous because of quicker response time, lesser steady state oscillations, and improved performance during drastic shifts in the environment. The effectiveness of this method highly depends on how well the fuzzy rule base and membership functions are designed.

- **Artificial Neural Networks (ANNs)**: ANNs are trained using historical data to predict the optimal MPP, offering superior tracking under non-uniform shading and dynamic weather conditions. Artificial neural networks (ANNs) have lately been applied in physical systems [94]. ANN can be compared to the way neurons process information in the human brain. An ANN is made up of a single artificial neuron and other essential components. ANN is an experience-based methodology that leverages data to uncover patterns or links for training and learning, unlike other program-based strategies.

- **Deep Learning Approaches**: These utilize more sophisticated structures of neural networks like convolutional and recurrent neural networks (CNNs and RNNs) in order to improve the precision and robustness of tracking in practical environments [95] . Deep learning models can analyze large volumes of data to identify trends in PV parameters and predict the best MPP in real time. They surpass traditional approaches in dealing with non-uniform irradiance or partial shading positions owing to their ability to multitask complex high-dimensional feature extraction. Nevertheless, their performance hinges on high investment computing systems and large amounts of training data to be fully effective.

III.3.1.3.2. Techniques based on the meta-heuristic approach

Meta-heuristic algorithms are inspired by natural and evolutionary processes and are used for optimizing MPPT control strategies [96]. These algorithms are particularly effective in solving complex, non-linear, and multi-modal optimization problems inherent in photovoltaic (PV) systems [97]. Unlike conventional methods, meta-heuristic approaches do not rely on gradient information, making them highly adaptable to dynamic environmental conditions, including partial shading and temperature variations. Common techniques include:

- **Particle Swarm Optimization (PSO)**: A population-based optimization technique mimicking bird flocking behavior to efficiently locate the global maximum power point [98]. The algorithm is a simplified model of flock or school behavior. A swarm's individual particles stand in for potential answers. At each cycle's end, the particles have repositioned themselves based on their nearest P_{best} and the G_{best} data. Each particle's new position (X_i) is influenced by a velocity factor, as shown in equation (III.1):

$$X_i\ (\mathrm{t+1}) = X_i\ (\mathrm{t}) + V_i\ (\mathrm{t+1}) \qquad \text{(III.1)}$$

V_i stands for the perturbation factor as shown in equation (III.1):

$$V_i\,(t+1) = V_i\,(t) + c_1\, r_1\,[P_{best} - X_i\,(t)] + c_2\, r_2\,[G_{best} - X_i\,(t)] \qquad \text{(III.2)}$$

PSO is an effective method. However, because of its limited capacity for exploration, it might become stuck in local optima. Additionally, when particles have already converged to a particular solution.

- **Genetic Algorithm (GA)**: GA is a meta-heuristic optimization technique that uses biological behavior and evolution to find answers. Holland first proposed this strategy in 1975 using the survival of the fittest theory [99]. In general, GA uses fixed-length strings to model the candidates' solutions, or "chromosomes," in the problem search space. A constant population of genes that can be displayed as binary or real codes makes up a chromosome. Through competition, the chromosome population progressively changes over generations in the algorithm process. Selection, crossover, and mutation are the three ways that genetic operators are used to accomplish this evolution. The process of evolution ensures that the chromosome with the highest fitness survives and mates with the next generation. GA optimization has been applied to various optimization issues, including MPPT that the renewable energy industry faces. GA can quickly converge on a variety of optimization problems. Furthermore, the technique performed satisfactorily in lowering the likelihood of becoming stuck in the local optimum. However, it is not advised to use this approach to optimize problems that are extremely large or complex.

- **Ant Colony Optimization (ACO)**: is a probabilistic algorithm that searches for global solutions to stochastic problems. In [100] Dorigo and Gambardella introduced the algorithm in 1997, based on ant foraging behavior to determine the optimal path to food. This technique models the foraging behavior of ants to find optimal duty cycle values for MPPT. The ACO-based MPPT technique uses each location to represent the voltage value of the PV array. The f(x) objective function evaluates each ant's fitness based on the output power of the PV array and its voltage value.

- **Grey Wolf Optimization (GWO)**: Based on the hunting behavior of grey wolves, GWO efficiently tracks the MPP with minimal oscillations [101]. It is a nature-inspired optimization technique that mimics the hunting behavior of humpback whales. Preferring to live in packs, grey wolves are regarded as the top predators. Alpha (α), beta (β), delta (δ), and omega (ω) are the four types of grey wolves used to mimic the

leadership hierarchy. We use the alpha (α) as the fittest solution when designing GWO to model the social hierarchy of wolves mathematically. As a result, beta (β) and delta (δ) are the names of the second and third best solutions, respectively. It is assumed that the remaining candidate solutions are omega (ω). The GWO algorithm assumes that the best candidate solution at the moment is either the target prey or very near the optimum because the location of the ideal design in the search space is unknown beforehand. The other search agents will therefore attempt to adjust their positions in order to align with the best search agent once it has been determined. The following formulas represent this behavior:

- $\vec{D}= |\vec{C}. \overrightarrow{X*}(t) - \vec{X}(t)|$ (III.3)
- $\vec{X}(t+1) = \overrightarrow{X*}(t) - \vec{A}.\vec{D}$ (III.4)

Where t denotes the current iteration, $\vec{A}$ and $\vec{C}$ are coefficient vectors, $\overrightarrow{X*}$ is the position vector of the best solution found thus far, and $\vec{X}$ is the position vector. It is important to note that if a better solution is found, $\overrightarrow{X*}$ should be modified in each iteration.

- $\vec{A} = 2\vec{a} \cdot \vec{r} - \vec{a}$ (III.5)
- $\vec{C} = 2 \cdot \vec{r}$ (III.6)

The components of $\vec{a}$ are progressively decreased from 2 to 0 over iterations, whereas $\vec{r}$ is random vectors in [0, 1].

III.3.1.4. Techniques based on non-linear control

Non-linear control techniques enhance MPPT performance by using advanced mathematical models to predict and control the system's behavior. These include:

- **Sliding Mode Control (SMC):** A robust non-linear and high-speed nonlinear control technique that ensures fast convergence to the maximum power point (MPP) while effectively handling system uncertainties and disturbances. SMC operates by enforcing a sliding surface where the system trajectory is forced to move, leading to high tracking accuracy and robustness against rapid irradiance and temperature changes. However, a key challenge with SMC is the chattering effect, which can be mitigated using boundary layer control or higher-order SMC approaches [102].

- **Model Predictive Control (MPC)**: This advanced control strategy employs a dynamic optimization approach to predict the future states of the PV system and adjust the control variables in real time to maximize power extraction. MPC utilizes a system model to forecast the effects of different control actions over a finite prediction horizon and selects the optimal action that minimizes deviations from the maximum power point (MPP)[103]. This method ensures fast response times and high accuracy, making it particularly effective in rapidly changing environmental conditions. However, its implementation requires high computational power and precise system modeling.

- **Lyapunov-Based Control**: A stability-driven nonlinear control approach that ensures globally stable MPPT operation by leveraging Lyapunov functions to construct energy-based stability criteria. This method continuously evaluates a Lyapunov function to determine control actions that drive the system toward equilibrium while maintaining optimal power extraction. Lyapunov-based control is highly effective in ensuring global asymptotic stability and robustness against disturbances in PV systems [104]. Recent studies have demonstrated its efficiency in handling dynamic irradiance changes and load variations, making it a promising approach for real-time MPPT implementation [105]. However, its application requires precise modeling of the PV system and control tuning to achieve optimal results.

III.3.2. Maintaining Operation at Maximum Power Point (Tracking Loop)

The effectiveness of the tracking loop significantly impacts system efficiency, particularly during rapid changes in solar irradiance or temperature. A well-designed tracking loop prevents power loss and ensures smooth operation under varying environmental conditions. After the search loop detects the reference that is closest to the Maximum Power Point (MPP), the tracking loop is responsible for keeping the photovoltaic (PV) system operating at this point at all times. The process is achieved by dynamically adjusting the duty cycle of the DC-DC converter so as to move the system's output to align with the MPP. The two most popular control strategies employed in MPPT tracking loops are:

- Proportional–Integral (PI) Control: PI controllers decrease the reference-measured output difference by adjusting the control signal based on proportional and integral actions [106]. Simple to implement but they are often very sensitive to tuning parameters and are not able to learn in the event of fast changing conditions such as partial shading or rapid changes in irradiance.

- Sliding Mode Control (SMC): A strong and nonlinear control strategy known for its quick dynamic response rate and robustness to system perturbations [107]. SMC also results in chattering effects and may require advanced switching logic, thus being practically challenging to implement in PV systems.

III.4. Challenges in MPPT and Control Strategies

Traditional MPPT controllers used in the tracking loop, such as PI controllers, struggle with nonlinearity and varying operating conditions of PV systems. The transient response of the PV system differs depending on the operating region (current, voltage, or power) [108]. Standard controllers often fail to provide optimal performance across all regions, leading to increased oscillations and slower tracking speeds. Moreover, environmental disturbances such as partial shading introduce multiple local maxima in the P-V curve, making tracking even more complex.

III.5. Proposed LSTM-Based Control Approach

To address the inherent limitations of traditional tracking methods, a novel Long Short-Term Memory (LSTM) deep learning-based controller is proposed for the PV subsystem tracking loop. Unlike standard Artificial Neural Networks (ANNs), the LSTM architecture utilizes a specialized memory cell regulated by input, forget, and output gates, allowing it to process the sequential dependencies of PV voltage and irradiance fluctuations without suffering from vanishing gradients [109]. This controller is trained using a high-precision dataset generated by multiple controllers, which are individually optimized via Particle Swarm Optimization (PSO) for specific operating regions current, voltage, and power. By training on these multi-region datasets, the LSTM network learns region-specific dynamics, enabling it to dynamically adjust control parameters and adapt to rapidly changing environmental conditions more effectively than static PI or fuzzy logic algorithms. Consequently, the LSTM model masters complex nonlinear patterns, resulting in superior transient responses and a significant reduction in tracking error achieving a mean tracking error of only 0.2073 under partial shading compared to 0.7328 for optimized PI controllers.

III.5.1. Long Short-Term Memory

Over the past few years, neural network architectures have shown great success in many machine-learning applications [110]. In order to process sequential data, recurrent neural networks (RNNs) keep a hidden state that records data from earlier time steps. They frequently

struggle, though, when learning long-term dependencies, where knowledge from far-off time steps is essential for producing precise predictions for the present state [111]. This issue is referred to as the "exploding gradient" or "vanishing gradient" problem. An expansion of the RNN idea, the Long Short-Term Memory (LSTM) architecture presents one of the most effective answers to this gradient computation issue [112].

LSTM architectures involves the memory cell, which is controlled by three gates: the input gate, the forget gate and the output gate as shown in Figure III.2. These gates decide what information to add to, remove from and output from the memory cell.

The LSTM's forgetting gate's primary goal is to regulate the deletion of neuronal information. The hidden state h_{t-1} at time *t-1* and the input$x_t$at time *t* are what make up the forget gate's input. The output of the forget gate can therefore be represented as the activation function yields the output of the forget gate f_t [113]:

$$f_t = \alpha\left(w_{fx}x_t + w_{fh}h_{t-1} + b_f\right) \quad \text{(III.7)}$$

The weight matrices are denoted as w_{fx}, w_{fh}, while the bias vectors are represented by b_f, x_t represents the time-series data at the current time interval t and h_{t-1} represents the memory cell output at the previous interval (t-1).

The input gate is responsible for determining the selection of data that is to be incorporated into the cell state. The opening of this gate requires the completion of two sequential actions [114]. The initialization of the state is achieved via the *tanh* layer, which produces possible values C_t' for possible inclusion. A sigmoid layer based on the earlier time interval's memory cell result and the current input data x_t calculates the activation levels for the input gates. According to [115] , the equations for these two phases are as follows:

$$c_t^{'} = tanh(w_{cx}x_t + w_{ch}h_{t-1} + b_c) \quad \text{(III.8)}$$

$$I_t = \alpha(w_{ix}x_t + w_{ih}h_{t-1} + b_i) \quad \text{(III.9)}$$

The weight matrices are denoted as w_{ch}, w_{cx}, w_{ih}, and w_{ix}, while the bias vectors are represented by b_c and b_i.

Existing cellular changes C_t are then determined using the output of the forget and input gates. According to the novel cell, C_t is computed as follows:

$$C_t = C_{t-1} \odot f_t + i_t \odot C_t' \quad \text{(III.10)}$$

The symbol $\odot$ is used to represent the Hadamard product. According to Eq. (III.10), and for the present cellular conditions, contextual transformers (C_t) consist of a combination of the current memory (C_t') and the previous long-term memory (C_{t-1}). The forget gate f_t regulates

how much data from long term memory C_{t-1} is kept in the current cell states. Additionally, which the input gate determines how much data is kept in the current cell states by the current memory C'_t.

The output gate (o_t) determines specific details from the cell state to generate the output (h_t). The following equations are used to calculate the height of the memory cell [116]:

$$o_t = \alpha(w_{Gx}x_t + w_{Gh}h_{t-1} + b_G) \quad \text{(III.11)}$$

$$h_t = o_t \odot tanh(c_t) \quad \text{(III.12)}$$

The weight matrices w_{Gx} and w_{Gh}, the bias vectors b_G, and the output vector $h_t$of the LSTM layer are denoted as such.

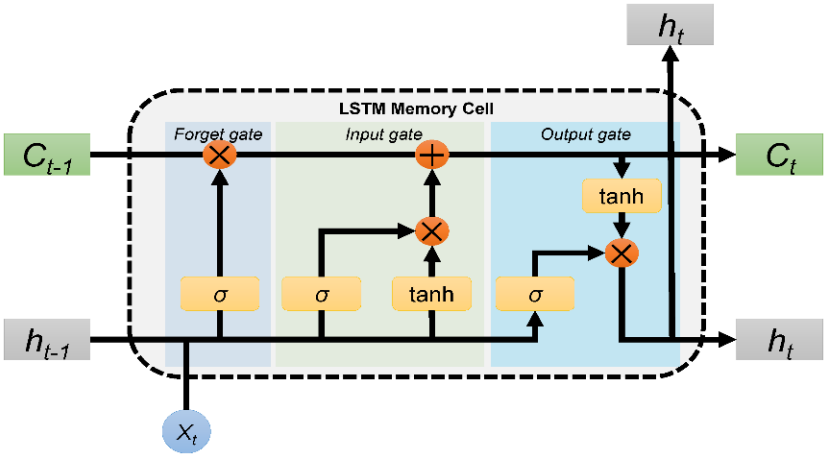

Figure III.2. The architecture of an LSTM cell.

III.6. Development of LSTM based controller

As illustrated in Figure III.3, the training data of the LSTM controller is formulated from input–output data collected over different operating areas of the PV system. In the current-source area, a PI controller is optimized through the Particle Swarm Optimization (PSO) method, according to a voltage reference V_{ref} representative of the given region. The respective tuned controller is referred to as PI*. The identical optimization process is applied to the power-source and voltage-source regions, leading to the creation of two additional region-specific PI controllers.

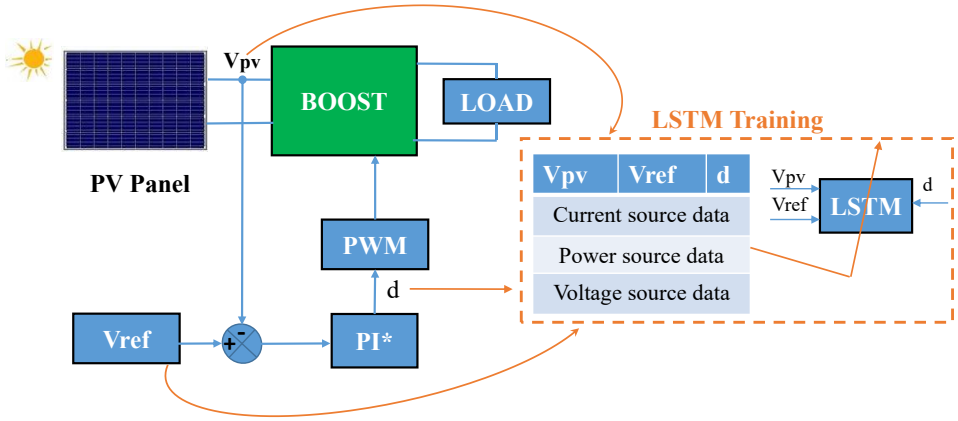

Figure III.3. LSTM training using optimal PI* input/output data.

The optimally tuned PI controllers (denoted PI*) corresponding to each operating region, as depicted in Figure III.4, are integrated into the PV system model to produce simulation data. These simulations generate input–output pairs in the format [V_{pv}, V_{ref} | d]. Where V_{pv} represents the time series of the PV array voltage, V_{ref} is the voltage reference specific to the active operating region, and d denotes the converter duty cycle. The complete LSTM training dataset is constructed by concatenating the simulation data from all defined operating regions, enabling the network to learn a generalized control behavior across varying system conditions.

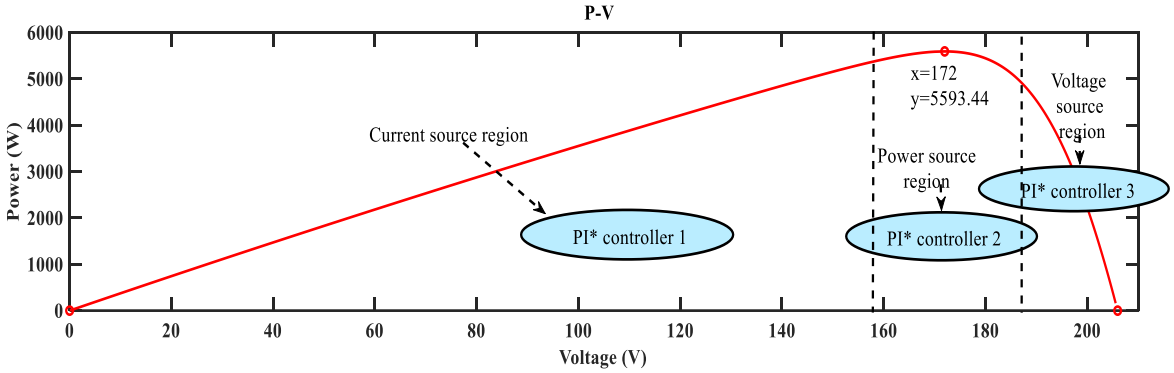

Figure III.4. Different regions of the P-V curve and derived optimal controllers for each region.

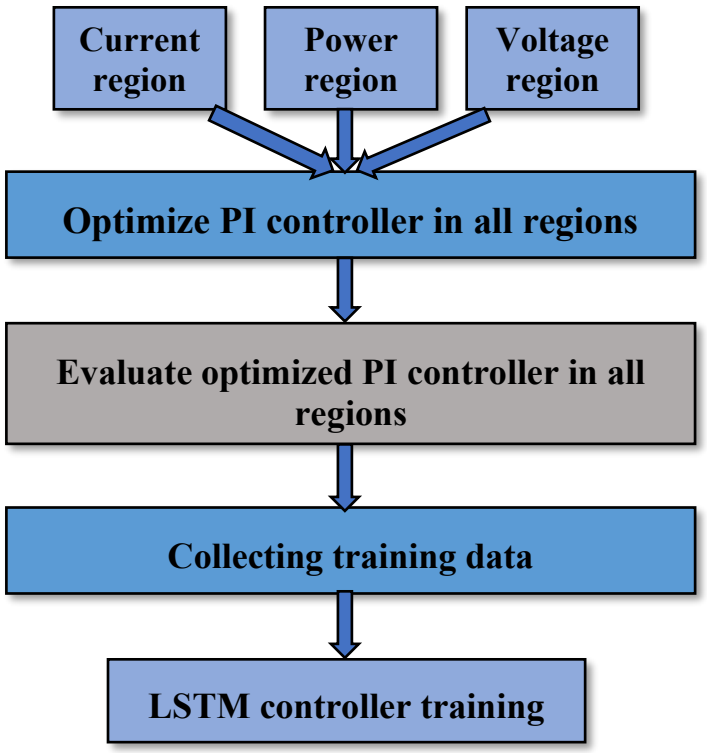

Figure III.5. Steps of the proposed LSTM controller training procedure.

Figure III.5 depicts the various steps involved in designing the proposed LSTM controller. The LSTM NNs are trained using the Adam optimization approach [117]. A fast and efficient stochastic optimization technique only requires first-order gradients and little memory. The Adam optimizer has excellent computing performance, is simple to implement, requires little memory, and is invariant to gradient diagonal rescaling.

III.7. Performance evaluation of LSTM controller

The proposed LSTM controller has been evaluated in various simulation scenarios, including:

- **Step changes in reference voltage:** The LSTM controller demonstrates reduced tracking errors and faster response times compared to PI controllers.
- **Stair-shaped reference voltage tracking:** A dynamic test covering different operating regions shows that the LSTM controller provides more stable and accurate reference tracking.
- **Partial shading conditions:** When tested under partial shading, the LSTM-based controller, integrated with a Particle Swarm Optimization (PSO)-based MPPT algorithm, efficiently tracks the global MPP, outperforming traditional methods in terms of precision and stability.

III.8. Training of the LSTM network-based controller

An input/output data collection has been conducted in order to train the LSTM network, which is used to replace the optimized PI controllers in the current, power, and voltage operating regions. Together with the reference voltage and controller output, the PV system's reaction to a variable reference voltage has been gathered as follows [V_{pv}, V_{ref}, d] (see Table III.1). Where d is the controller output (duty cycle), which is sent to the PWM module, V_{pv} is the measured voltage of the PV system, and V_{ref} is the reference voltage that stretches from open circuit voltage to short circuit.

The structure and training parameters selected have a significant impact on the trained LSTM network's performance. The two features utilized as inputs, PV voltage (V_{pv}) and reference voltage (V_{ref}), respectively, define the structure of the LSTM controller used in this work (see Table III.1). The control signal (d) is the structure's response. The number of hidden units, which must strike a balance between problem difficulty and speed of execution, is the primary indicator of the LSTM structure's complexity. The suggested LSTM controller structure uses 200 hidden units. The LSTM structure weights are learned and updated in each time step using the Adam optimizer, a stochastic gradient descent optimization algorithm.

Table III. 1. Collected training data description.

[V_{pv}, V_{ref}, d]	Size
Current source region	50000×3
Power source region	50000×3
Voltage source region	50000×3

A decreasing learning error (0.0404) and a total training duration of 186 minutes at the 50th training epoch are displayed in Figure III.6, which displays the training progress. Training time is mostly determined by the PC's processor, which in this case is an Intel(R) Core (TM) i5-11300U CPU running at 2.30GHz with 16 GB of RAM. Using GPU processors in high-performance PCs, which are frequently utilized these days for deep learning tasks, could significantly cut down on training time.

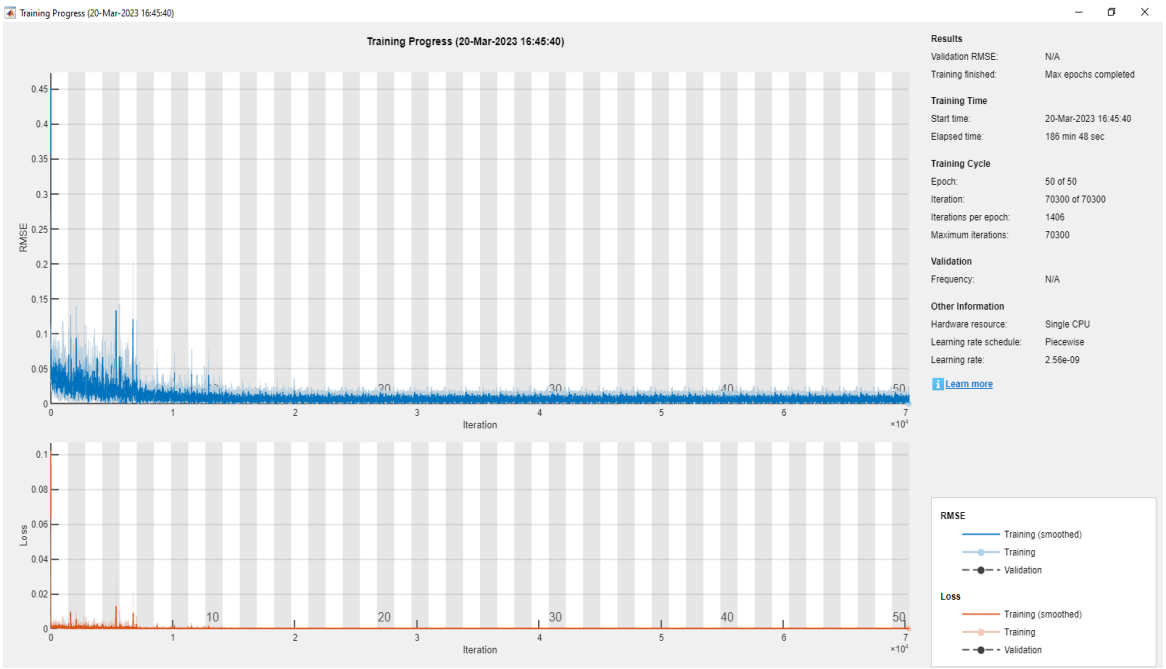

Figure III.6. Training progress of the proposed LSTM network using all regions data.

III.9. Dynamic performance evaluation of the LSTM based controller

The proposed LSTM network-based controller is evaluated using different voltage variation patterns and then compared with a PI controller optimized by PSO algorithm in different regions.

III.9.1. Step change in reference voltage Evaluation of LSTM in different operating regions

At STC operating conditions, an evaluation is carried out of the trained LSTM controller for a step change in the reference voltage in different operating regions and comparing the obtained response with that of the PI controller optimized for the same region.

As shown in Figure III.7, Figure III.8 and Figure III.9, it is noted that although the PI controller takes shorter time to converge, the LSTM response is better centered around the reference voltage in all regions. In addition, Table III.2 gives the Mean Absolute Error (MAE).

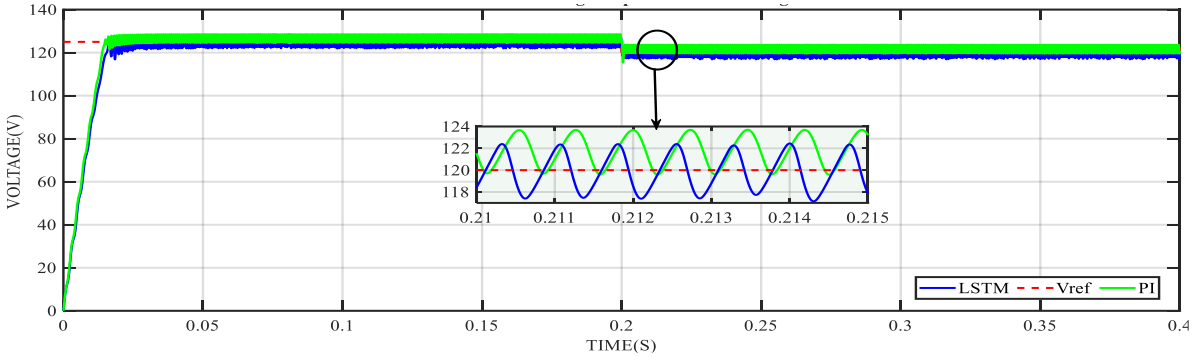

Figure III. 7. PV power response in current region.

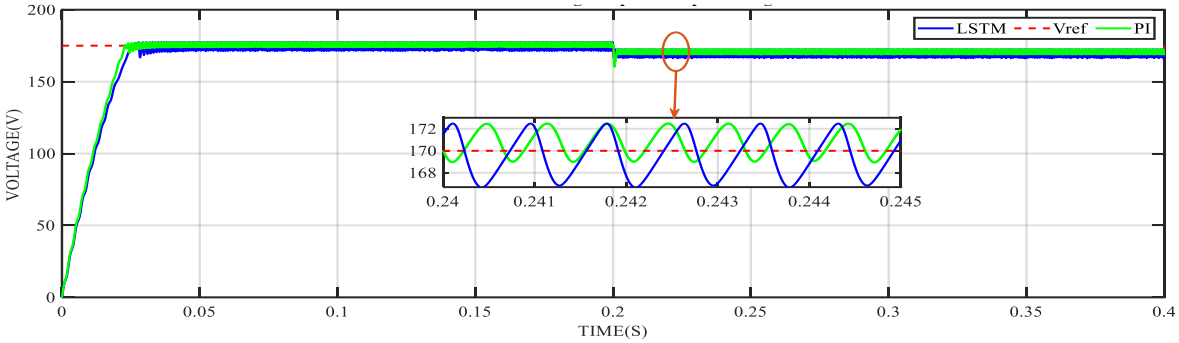

Figure III.8. PV power response in power region.

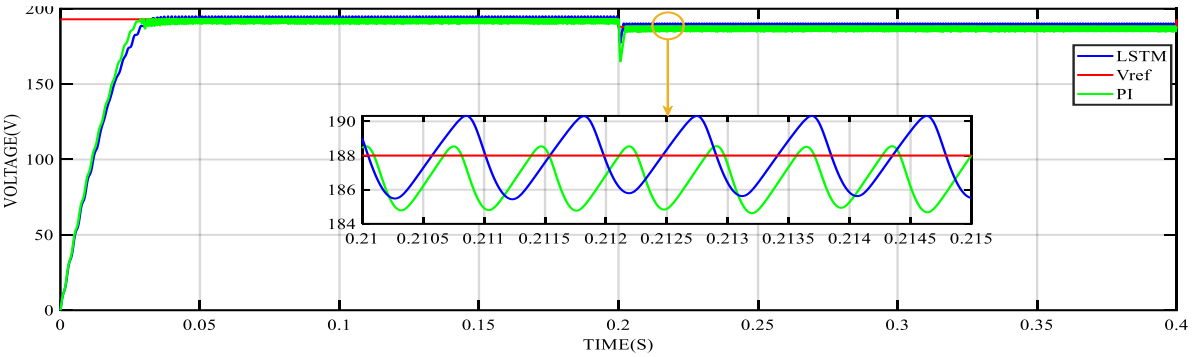

Figure III.9. PV voltage response in voltage region.

Table III. 2. Step change evaluation comparison results.

Tuned region	PI* controller parameters	MAE error		Min absolute error	
		LSTM	PI	LSTM	PI
Current source	[Kp, Ki] = [-0.35, -0.065]	1.3329	1.9448	7.9569e-06	1.6455e-05
Power source	[Kp, Ki] = [-0.259, -0.001]	0.9112	1.5970	7.5231e-06	8.7579e-06
Voltage source	[Kp, Ki] = [-0.205, -0.0001]	1.2896	1.8173	4.3455e-06	6.1351e-06

III.9.1. LSTM controller stair reference voltage evaluation

Both PI and LSTM controllers are used to evaluate the PV system for the entire operational regions. The reference voltage is lowered by a predetermined step change and after a predetermined amount of time to simulate a stair transition from open-circuit voltage to short-circuit voltage. Figure III.10 displays the PV system's response when both controllers are used. Comparing the LSTM-based controller to the power-region-tuned PI* controller, it is seen that the LSTM-based controller exhibits superior transient responsiveness throughout all operating regions. 2.1868 is the PI error and 0.6707 is the LSTM mean error.

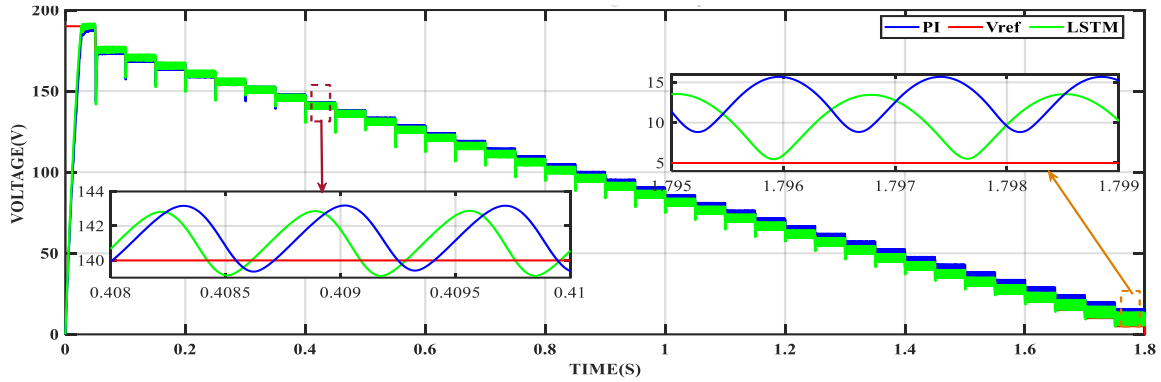

Figure III.10. PV system evaluation using the LSTM controller stair shaped reference voltage.

III.10. Partial shading evaluation of LSTM

The PV array has been partially shaded in this situation. Using PI and LSTM tracking controllers, the PSO MPPT starts the global MPP search. For comparison, the LSTM controller uses the voltage reference produced by the PSO MPPT algorithm for the PI controller, which has been previously stored. The resulting voltage and power responses are displayed in Figure III.11 and Figure III.12 , respectively. With an LSTM mean tracking error of 0.2073 and a PI controller mean error of 0.7328, the search converges after 40 iterations.

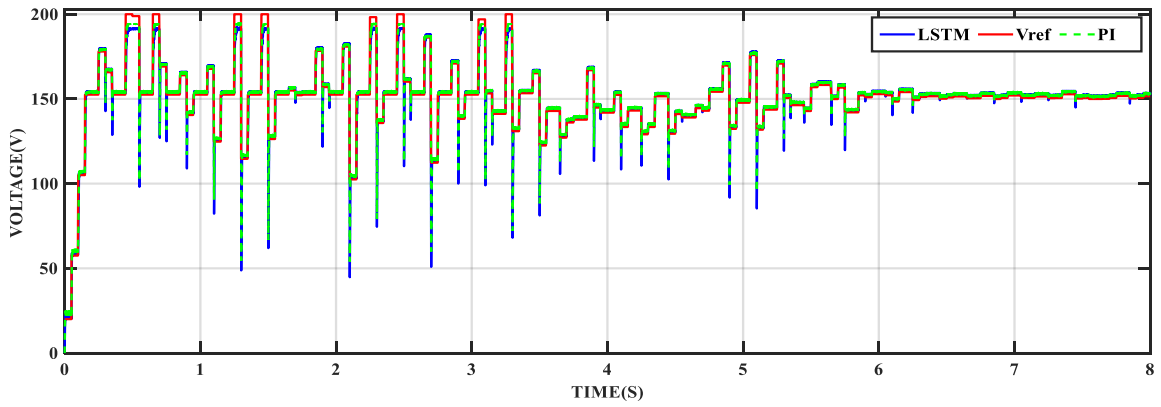

Figure III.11. PV voltage response using PI and LSTM controllers under PS.

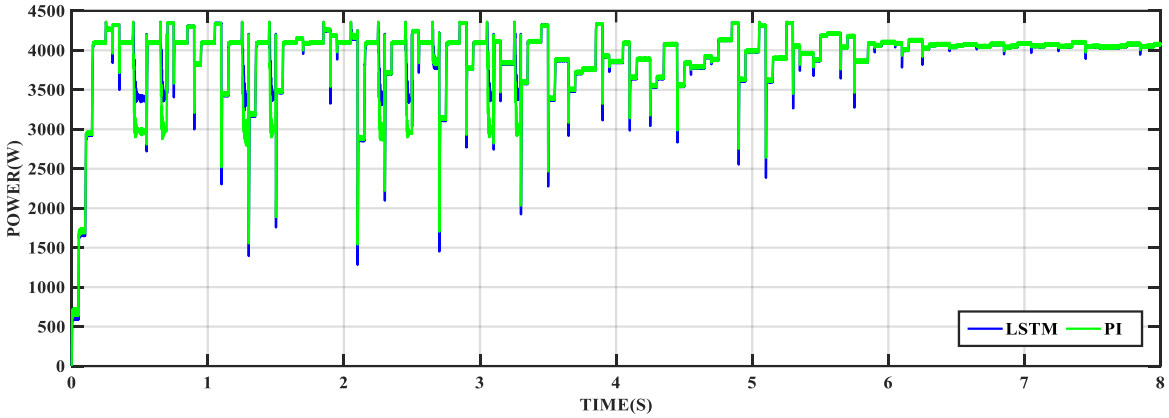

Figure III.12. PV power response using PI and LSTM controllers under PS.

III.11. Performance Comparison

To evaluate the effectiveness of the proposed LSTM-based MPPT controller, a comparative performance analysis is conducted against conventional and advanced algorithms reported in the literature. The assessment focuses on several key criteria.

- Tracking efficiency reflects the controller's ability to accurately reach and maintain operation at the maximum power point (MPP).
- Response time measures how quickly the controller adapts to changes in irradiance.
- Steady-state oscillations indicate the extent of power fluctuations around the MPP during stable operation.
- Robustness under partial shading conditions is also considered, as it determines the controller's ability to identify and track the global MPP in the presence of multiple local maxima.

These indicators collectively provide a comprehensive basis for validating the dynamic and steady-state performance of the proposed strategy under varying environmental conditions.

Table III. 3. Comparative analysis against conventional and advanced MPPT methods.

MPPT Technique	Tracking Efficiency	Response Time	Steady-State Oscillations	Performance in Partial Shading
P&O Algorithm	Moderate	Fast	High	Poor
INC Algorithm	High	Fast	Moderate	Moderate
Fuzzy Logic MPPT	High	Moderate	Low	Good
LSTM-Based MPPT (Proposed)	Very High	Very Fast	Very Low	Excellent

Table III.3 demonstrate that the proposed LSTM-based MPPT controller significantly outperforms conventional methods in all key performance metrics. Traditional techniques such as P&O and PI controllers exhibit higher oscillations and struggle under rapid irradiance changes. The fuzzy logic MPPT method improves performance but lacks adaptability compared to LSTM-based MPPT. The deep learning-based approach excels in maintaining efficiency across different PV operating regions, particularly under partial shading scenarios, making it a promising solution for future renewable energy applications.

III.12. Conclusion

This chapter discusses an MPPT control technique based on deep learning for PV systems with the use of an LSTM neural network. Various methods of MPPT like conventional, modified, and improved methods were presented and studied in terms of identifying their drawbacks under dynamic working conditions and partial shading conditions. To address these issues, an LSTM controller has been created and trained using input-output data from optimally tuned PI controllers in different PV operating zones. Simulation outcomes have validated the effectiveness of the proposed strategy, demonstrating improved convergence, reduced steady-state oscillations, and enhanced tracking accuracy compared to conventional PI controllers.

The LSTM-based controller performed best, particularly for non-uniform conditions of irradiance, confirming its potential as an effective and adaptive MPPT scheme. The results are indicative of the possible use of the proposed strategy in hybrid renewable energy systems and real-time embedded system.

Chapter IV

Optimization and management of energy flow in a multi-source hybrid system

IV.1. Introduction

A hybrid multi-source system must be optimally designed in order to guarantee a reliable, sustainable and economically viable energy supply, depending on the imposed load profile. The objective is to meet the requirements of continuity of service while minimizing the overall cost of the installation and its operation. For this, several optimization criteria are commonly used in the literature and in technical-economic modeling tools. Among the most relevant, we distinguish: the unit cost of the energy produced which makes it possible to evaluate the economic profitability of the system, the life cycle cost (LCC) which takes into account all the financial expenses associated with the project over its operating life and the probability of loss of power (LPSP), which measures the ability of the system to meet the load in all circumstances [118], [119]. However, achieving these goals requires more than just static sizing. It is crucial to adopt dynamic optimization strategies adapted to the complexity of hybrid systems. These strategies aim to intelligently control energy flows between sources, storages and loads, depending on weather conditions, consumption profiles and energy priorities.

In the remainder of this chapter, we will present the main optimization criteria chosen for our hybrid system, then the sizing methodology, before analyzing different energy management strategies adapted to our multi-source architecture.

IV.2. Hybrid system optimization criteria

A multi-source system must be optimally designed in order to guarantee a reliable, sustainable and economical energy supply, depending on the imposed load profile. The objective is to meet the requirements of continuity of service while minimizing the overall cost of the system. To this end, various optimization criteria are typically taken into account. The unit energy cost of the energy produced, which determines the economic profitability of the system, the life cycle cost (LCC) of the system, which covers all the costs related to the initial investment, maintenance, operation and replacement of system components and the probability of power loss (LPSP), which studies the system's ability to cover energy demand at any time. These indicators make it possible to orient the dimensioning and the management of the energy flows of the hybrid system, to ensure an optimal compromise between performance, reliability and cost, according to local technical and environmental constraints [120].

IV.2.1. Cost of energy

The unit cost of the energy produced constitutes a central economic indicator in the performance analysis of a hybrid energy system. It includes all the expenses associated with the

production, installation, operation, maintenance and replacement of components, related to the total amount of useful energy delivered over the operating period. This criterion thus makes it possible to compare different energy configurations in terms of profitability, while taking into account the technical and economic specificities of the installation site [121].

In a system combining intermittent sources a photovoltaic, a fuel cell as a backup source and hybrid storage devices (batteries and super capacitors), the cost of energy depends heavily on the sizing of the components, the energy management strategy adopted, and operating conditions. Tools such as HOMER or MATLAB/Simulink are usually used to simulate the operation of the system over a given period and accurately calculate the unit cost of energy.
The challenge of optimization is to reduce this cost while maintaining reliability and continuity of power supply, which implies a compromise between initial investment, management complexity, and energy security [122].

IV.2.2. Life Cycle Cost (LCC)

The life cycle costs (LCC) is the sum of all expenses incurred throughout the useful life of the hybrid system, including the original investment costs, operating and maintenance costs, and potential component replacements [123]. The concept makes it possible to reflect on the overall efficiency economy of an energy project, not only taking into account the initial costs but also the current future charges.

The LCC analysis is particularly interesting for comparing different configurations or operating strategies of a multi-source system (PV, fuel cell, battery, super capacitor) taking into account the possible evolution of maintenance costs, wear rates or replacement of equipment. As in the Net Present Value (NPV) analysis, which consists of comparing the discounted future revenues of a project with its initial costs to assess its long-term profitability, the choice of an appropriate discount rate in the LCC analysis is fundamental. A bad estimate at this level can distort the results and lead to suboptimal design decisions. If the NPV is often used in the private sector to maximize the financial value created, the LCC is generally preferred in public projects and autonomous systems where the main objective is to minimize the total cost of ownership in the long term. Thus, the LCC analysis remains a reference tool in the technical-economic evaluation of sustainable hybrid energy systems [124].

IV.2.3. Loss of Load Probability (LOLP)

In a hybrid multi-source system, the most critical criterion for ensuring the stability of the power supply is the probability of power loss, or LOLP. The criterion measures the frequency or duration during which the load cannot be met due to an energy deficiency in the system. It

makes it possible to evaluate to what extent the proposed architecture is capable of meeting energy needs in all circumstances, taking into account the variability of renewable sources.

The optimal calculation of the quantity of photovoltaic modules, fuel cells and the most significant storage devices (batteries and super capacitors) is partly fundamentally based on the analysis of this probability, to which economic criteria are added. The LOLP is therefore a fundamental indicator when sizing the system, because it avoids underestimating the production and storage capacities, which could lead to load decreases [125].

From a technical point of view, the LOLP is defined as the probability that the energy stock contained in the storage units (batteries and supercapacitors) is less than a minimum threshold necessary to satisfy the load in a given context. This relationship can be expressed in the following way:

$$LOLP = Pr\{ E_{Bt}(t) \leq E_{Bt_min} \ pour \ t \leq T \}$$

Where:

E_{Bt} (t) is the total energy available in the storage units at time t,

E_{Bt_min} is the minimum level of energy required to power the load,

T is the total duration of observation.

An LOLP that approaches zero means that a very safe system, capable of reacting to the load in almost all cases. On the other hand, a high LOLP value indicates that the system is poorly managed or undersized. The optimization is therefore such that the LOLP is minimized while maintaining an acceptable economic compromise, in this case in complex systems such as we are studying them here, by integrating intermittent renewable sources (PV), a backup fuel cell and hybrid storage units (supercapacitors + batteries).

IV.3. Proposed sizing procedure for a hybrid system

The optimal dimensioning of a multi-source hybrid system consists in defining the appropriate capacities of the sources (PV and fuel cell) and storage units (batteries, super capacitors) in order to guarantee the coverage of energy demand while operating with the lowest possible overall cost and losses. This process is based on a fine analysis of the load profile, on a detailed characterization of local resources (solar irradiation, temperature) and on a careful modeling of energy production. The simulation of the evolution of the state of charge of the storage devices is carried out to guarantee the stability of the system and the extension of the service life of the components. Advanced optimization techniques, such as evolutionary algorithms or artificial

intelligence, are used in environments such as MATLAB/Simulink to identify the optimal configuration [126].

IV.3.1. Load profile

The first step in the dimensioning of a hybrid system consists in analyzing in detail the profile of the electrical load to be satisfied. This analysis makes it possible to identify the average power, as well as the maximum and minimum values that the system will have to support. It also includes the study of the hourly and seasonal distribution of energy demand, in order to detect periods of high demand and adjust the capacity of sources and storage accordingly. In addition, it is essential to classify the loads according to their priority level, distinguishing between critical loads (to be supplied continuously), non-critical loads (which can be disconnected in the event of an energy deficit) and variable behavior loads. A detailed understanding of these parameters is essential to guarantee an adapted dimensioning of the system components, in particular of the production and storage units, while ensuring the reliability and stability of the power supply in the different operating scenarios [127].

IV.3.2. Radiation, temperature

The maximum size of a hybrid renewable energy system depends largely on a detailed description of local energy resources. To this end, it is necessary to study the solar radiation profile. These parameters have a direct influence on the efficiency of photovoltaic panels, and must therefore be taken into account in energy production models. The overall solar radiation, expressed in W/m^2, determines the amount of energy captured by the PV modules, while the ambient temperature affects their actual operating efficiency [128]. These data can be obtained from proven climatic databases, such as NASA-POWER [129], PVGIS [130], or from on-site measurement campaigns. Their integration into simulation tools makes it possible to predict the planned energy production, to detect its variability and to adjust the analysis of the sizing of renewable sources accordingly, allowing a better match between the available resources and energy needs.

IV.3.3. Energy produced by the hybrid system

Once the load profiles and the climatic resources have been established, it becomes possible to simulate the energy production of the hybrid system. This step is essential to evaluate the ability of each source (photovoltaic and fuel cell) to meet energy demand under realistic operating conditions. The photovoltaic production is determined from the incident solar radiation, the ambient temperature and the technical characteristics of the modules (efficiency,

surface, inclination, orientation). The fuel cell acts as a backup source, mobilized when renewable production becomes insufficient or when the state of charge of the storage units reaches a critical threshold. The total energy produced is therefore the weighted result of the contributions of the various sources, taking into account their availability, their conversion efficiency and any losses in the converters. This simulation makes it possible to validate the ability of the system to satisfy the load at all times, and constitutes an essential verification tool for the adjustment of the dimensioning [131].

IV.3.4. The state of charge of battery and supercapacitor

The precise management of the State of Charge (SOC) of the storage units constitutes a fundamental lever in the dimensioning and the optimal exploitation of hybrid multi–source systems. In an architecture combining batteries and supercapacitors, the functional complementarity between these two technologies makes it possible to ensure both the stability of the system and the resilience to rapid fluctuations in demand. Batteries, with a high energy density, are used for medium and long-term storage, while supercapacitors, with a high-power density, are mobilized to supply or absorb energy quickly, especially during peak loads or sudden variations in renewable production. The dynamic monitoring of the SOC makes it possible to avoid overloads and deep discharges, two major factors of premature degradation of the components [132]. To guarantee optimal operation, adaptive energy management algorithms are implemented, integrating safety thresholds, decoupling strategies, and load priority laws. The joint simulation of the SOC of batteries and supercapacitors, in interaction with the energy flows of the system, makes it possible to identify critical situations (energy deficits, storage saturation) and to refine the dimensioning of the storage units according to the real operating conditions.

IV.4. Overviews of optimal electrical energy management control strategies adapted to the hybrid system

In a multi-source hybrid system, intelligent energy management is a fundamental lever for ensuring the stability of the power supply, the durability of components and the technical-economic performance of the whole. Renewable source such as photovoltaic, although ecologically advantageous, are characterised by inherent temporal variability. If this variability is not rigorously controlled, it can lead to imbalances between production and consumption, transient overvoltages, or excessive overloading of storage devices, thereby compromising system reliability. To address this complexity, advanced control strategies are needed to ensure optimum coordination between primary sources, storage units (batteries and super-capacitors)

and electrical loads. These strategies are based on real-time integration of system status, weather forecasts and dynamic demand profiles, with the aim of optimally adjusting energy flows at each point in time [133]. The approaches most widely used in contemporary scientific literature include Model Predictive Control (MPC), Sliding Mode Control (SMC), Fuzzy Logic Control (FLC) and Artificial Neural Networks (ANN). Each of these methods offers specific advantages in terms of robustness, speed of response, adaptability and ease of implementation.The integration of these techniques makes it possible to improve the quality of service, reduce the LPSP (Loss of Power Supply Probability), and optimise the management of storage units, while extending the lifetime of sensitive components [134].

IV.4.1. Management strategy based on Predictive Control (MPC)

Model Predictive Control (MPC) is a sophisticated control approach for optimizing energy management in hybrid systems by anticipating changes in demand and generation conditions. Unlike conventional controls, MPC exploits a dynamic model of the system to predict its future behavior over a specified time horizon. At each sampling time, the controller solves a constrained optimization problem (for example, minimizing energy cost or battery wear) to calculate the optimal sequence of actions to take. Only the first action is applied, and the procedure is repeated at the next sampling time using the resampling principle (receding horizon) [135]. This method is particularly well suited to non-linear, multi-input and highly variable hybrid systems, notably due to the intermittency of renewable source (PV) and the complex dynamics of storage units. Because of its ability to integrate physical constraints (power limits, SOC operating range, etc.) and economic objectives, MPC is a promising solution for real-time control of intelligent hybrid systems. However, its implementation depends on accurate modelling of the system and sufficient computing capacity, particularly for embedded or real-time applications.

IV.4.2. Management strategy based on sliding mode control (SMC)

Sliding mode control (SMC) is a robust non-linear control strategy, particularly well-suited to hybrid systems subject to dynamic uncertainties, rapid disturbances, and unpredictable variations in renewable resources such as solar radiation. Its effectiveness lies in its ability to guarantee system stability, even in the presence of imprecise models or highly variable operating conditions. The fundamental principle of the SMC is illustrated in Figure IV.1. It consists of forcing the trajectories of the system to converge towards a specified sliding surface, then maintaining its evolution on this surface, independently of disturbances or parametric uncertainties. This approach is based on a discontinuous control law (often based on sign or

saturated functions), which corrects the deviation between the current state of the system and the desired dynamics, with greater speed and insensitivity than conventional methods [136]. However, to make SMC viable for real-world energy management, designers must implement additional chattering reduction algorithms or higher-order SMC approaches to limit energy losses and maintain overall system efficiency. In addition, its effectiveness still relies on the accurate definition of a sliding surface that forces the system trajectories to follow desired dynamic.

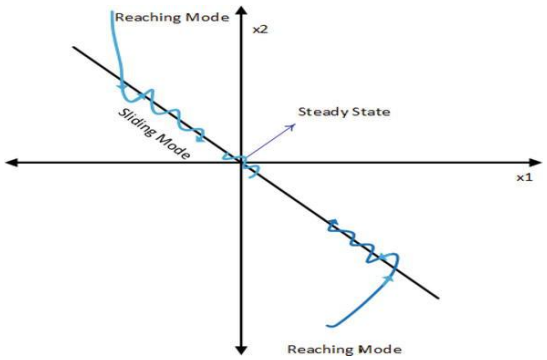

Figure IV.1. Illustration of the principle of control in sliding mode.

IV.4.3. Management strategy based on artificial neural network (ANN)

ANNs are dynamic and adaptive computer systems that can process inputs in parallel. These models are inspired by the information processing of biological neurons and their interconnections. They can learn complex non-linear relationships based on input and output models and do not require a physical understanding of the system [137].

In the context of energy management for the multi-source hybrid system, artificial neural networks (ANNs) are a particularly relevant approach. Their ability to model complex, non-linear and dynamically unstable relationships without the need for explicit analytical modelling makes them ideally suited to the operational requirements and optimisation constraints associated with this type of distributed energy architecture. ANNs are capable of automatically learning complex relationships between inputs (environmental parameters, load states, electrical demand, etc.) and outputs (control strategies, source activation, flow distribution, etc.), without the need for analytical modelling of the system. Network learning is generally supervised, based on historical data sets created by simulation or measured in real-life conditions. Optimisation algorithms such as error backpropagation or Levenberg-Marquardt are applied to adapt the synaptic weights of the network to minimise the error between the desired output and the actual output.

Various recent studies have shown that ANNs outperform conventional methods in highly non-linear or highly variable contexts, offering intelligent and adaptive energy management

[138],[139]. However, The effectiveness of an ANN management strategy hinges on the availability of large amounts of high-quality training data. These datasets must be collected from extensive simulations or real-life measurements under diverse environmental conditions to ensure the network can learn the system's behavior accurately and requires significant processing power and high-investment computing systems that introduce a highly complex structure compared to traditional linear controllers or rule-based logic.

IV.4.4. Management strategy based on fuzzy logic control (FLC)

Fuzzy logic control (FLC) is an intelligent regulation technique that is highly suitable for non-linear, uncertain and complex dynamic energy systems. The success of FLC is due to their ability to deal with the knowledge that is represented in a linguistic form instead of the conventional mathematical method. Unlike conventional methods that rely on a precise mathematical model, FLC is based on simulated human reasoning through fuzzy linguistic rules of the "IF-THEN" type, making it a preferred option for hybrid multi-source systems subject to rapid fluctuations. In the context of energy management, the FLC can take into account several critical variables at the same time, such as the time of day, the dynamic cost of energy, the state of charge (SOC) of the PV/battery pair and the power available from the grid. These real (or 'net') values are first fuzzified using membership functions-usually triangular-that convert these inputs into linguistic levels e.g. (low, medium, high), and then the inference engine uses a set of fuzzy rules to connect the input states to expected responses. The quality of the control is largely based on the relevance and coverage of the rules, which must cover all possible energy scenarios: day/night, high/low demand, peak/off-peak energy costs, etc. Finally, defuzzification translates the fuzzy results into concrete control values used to drive the system's actuators [140].

The diagram in Figure IV.2 describes the main stages of the fuzzy control process: input fuzzification, rule-based inference engine and output defuzzification. The architecture is one of great decision-making flexibility and improved robustness to uncertainty, making it an effective strategy for optimizing the distribution of energy between the different sources and loads of the hybrid system.

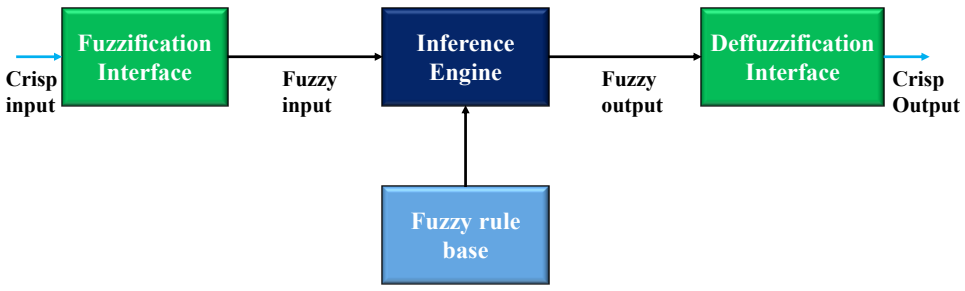

Figure IV.2. Operation of a fuzzy logic system.

In light of these capabilities, we have selected and implemented a fuzzy logic-based supervisor as the core of our energy management strategy (EMS) to coordinate the complex interactions between the photovoltaic array, fuel cell, and hybrid storage units. The primary motivation for choosing FLC lies in the limitations of classical controllers (such as PI), which are often too rigid to handle the highly intermittent nature of solar. While conventional controllers excel at local regulation, they lack the decision-making flexibility required to coordinate the interactions between dispatchable sources like the fuel cell and the intermittent PV subsystem. FLC provides a soft transition between various operational states, allowing the supervisor to prioritize system reliability and continuity of service without the instability associated with hard-threshold switching. In addition, our system utilizes a Hybrid Energy Storage System (HESS) where the battery manages medium-term energy and the supercapacitor handles high-frequency transients. FLC is uniquely capable of managing this dual-storage coordination, ensuring that each unit operates within its optimal range to extend hardware longevity and prevent premature aging as seen in Table IV. 1 .

Table IV. 1. Comparative Analysis of Energy Management Techniques.

Feature	Sliding Mode Control (SMC)	Artificial Neural Network	Model Predictive Control (MPC)	Fuzzy Logic (FLC)
Control Nature	Robust Non-linear	Data-driven "Black Box"	Optimization-based Predictive	Intelligent & Flexible
Model Requirement	Requires specified "sliding surface"	No analytical model; relies on data	Requires precise dynamic analytical model	No precise mathematical model needed
Handling Uncertainty	Excellent robustness to disturbances	Adaptive to unforeseen variations	Anticipatory relies on accurate forecasts	Superior handling of linguistic/stochastic uncertainty
Main Drawbacks	"Chattering" effect stresses hardware	Requires massive datasets and power	High computational expense sensitive to error	Performance depends on rule-base quality
Training/Design Effort	High switching logic complexity	Very High	High; complex problem formulation	Moderate; based on expert knowledge
Coordination of HESS	Fast but potentially unstable	Good at learning patterns	Excellent at solving constrained problems	Optimized for dual-storage (Battery/SC) coordination

IV.5. Analysis of classical energy management in the proposed system

In the literature and industrial applications, classical energy management in multi-source hybrid systems is generally based on fixed threshold logics, also called rule-based strategies [141]. This type of control in our system consists of defining static priority rules between the different sources (photovoltaic, fuel cell) and storage units (batteries, supercapacitors), without recourse to dynamic optimisation or demand or production prediction.

In the hybrid system studied, this strategy results in a simple hierarchy the energy produced by renewable sources is used as a priority, followed by the use of storage units, then finally the fuel cell in the event of a prolonged energy deficit. Batteries are called on as soon as production is insufficient, depending on a low SOC (State of Charge) threshold, while supercapacitors are used for rapid variations in load as illustrated in Figure IV. 3. This approach has the advantage of being simple to implement, low in computational cost, and widely used in isolated systems or microgrids [142]. In addition, conventional PI (Proportional-Integral) controllers can be used for local regulation of the voltage or current within the converters associated with the various units [143]. However, these controllers do not allow global coordination between the different sources and do not meet the requirements of energy optimisation in a dynamic environment.Although the traditional management strategy is appreciated for its simplicity of implementation, it nevertheless has several major structural limitations. Firstly, it cannot anticipate fluctuations in renewable resources or dynamic variations in demand, which considerably reduces its effectiveness in variable environments. Secondly, this approach can lead to excessive stress on storage devices, particularly batteries, accelerating their premature ageing and reducing their useful life [144]. In addition, conventional management does not explicitly incorporate economic considerations such as operating costs or optimisation of energy flows on a lifecycle scale. Finally, it is not very robust under complex operating conditions, particularly in the presence of non-linear behaviour, uncertainties or multiple constraints, which limits its applicability in advanced hybrid energy architectures.Thus, although effective in simple configurations, this strategy shows its limitations in the case of multi-source hybrid systems subject to high uncertainties. The above analysis will serve as a reference for comparison with the advanced management strategies, in particular those based on fuzzy logic, developed in the next section.

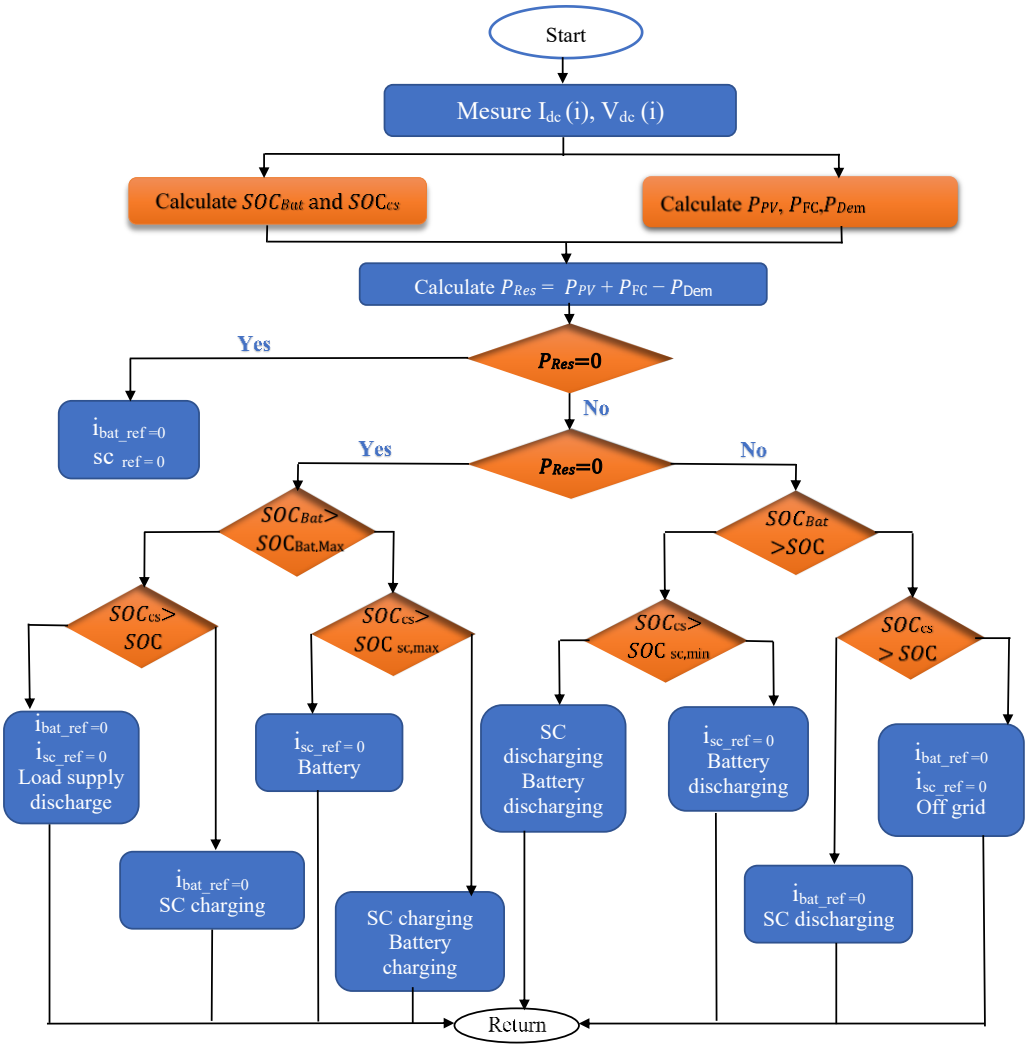

Figure IV. 3. Classical Supervisory Energy Management Algorithm.

IV.6. Development of fuzzy logic-based optimization strategy for power management of the proposed hybrid system

In multi-source renewable energy systems incorporating batteries, power control is relatively straightforward when the generated energy exceeds the load demand, the battery is charged. Conversely, if the load demand surpasses the generated energy, the battery discharges to compensate. However, in hybrid systems that integrate additional storage components, such as supercapacitors and are also connected to the utility grid, the control dynamics become increasingly complex. To address this complexity, we have developed an intelligent fuzzy logic-based algorithm, as illustrated in Figure IV.4. This strategy governs both control and energy management in a hybrid system composed of PV and fuel cell sources, supported by a dual storage system (battery and supercapacitor). Compared to the classical PI controller, the fuzzy logic controller demonstrates faster response time and enhanced dynamic performance.

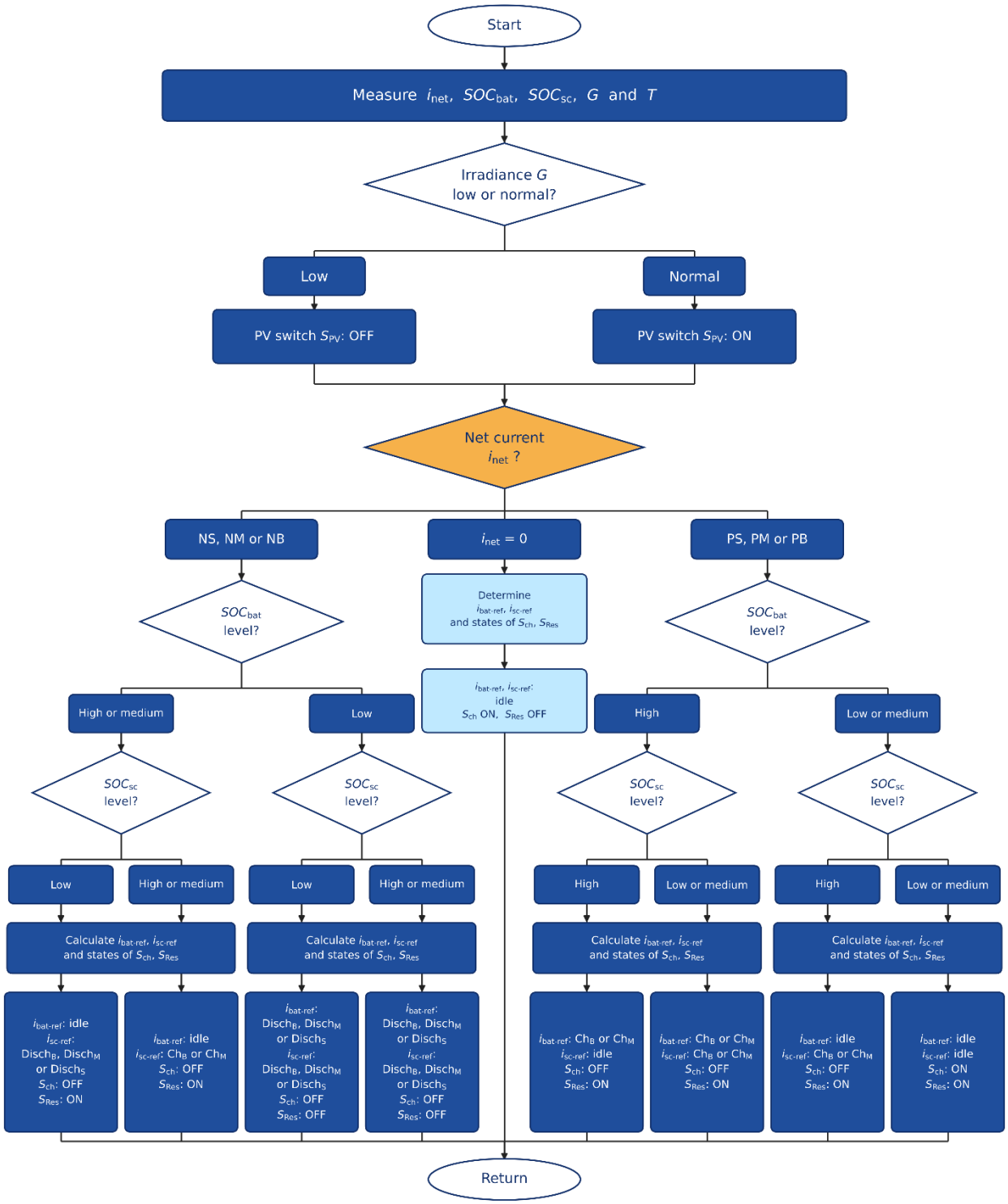

Figure IV.4. Proposed Supervisory Energy Management Algorithm.

In this work, the fuzzy logic energy management system maintains the same structural topology as the classical energy management system. However, the fuzzy logic controller, equipped with a comprehensive set of inference rules, replaces the conventional PI controller

block. This replacement enhances decision-making precision by offering a wider range of control possibilities, allowing the system to better adapt to varying operational scenarios.

IV.6.1. Identification of input and output variables with membership functions for the proposed CLF management unit

Trapezoidal membership functions have been selected to represent the fuzzy sets associated with each linguistic variable in the proposed energy management system. This choice is motivated by their simplicity, computational efficiency, and ability to approximate a wide range of nonlinearities. Each fuzzy set is characterized by its corresponding membership function, which defines the degree of belonging of a crisp input to the associated linguistic term over the universe of discourse.

The five input variables defined for the controller are as follows as shown in Figure IV.5, Figure IV.6, Figure IV. 7, Figure IV.8 and Figure IV.9:

- Net Current (i-net): Reflects the instantaneous power surplus or deficit within the system, guiding load-sharing decisions. The fuzzy linguistic terms used are: Negative Big (NB), Negative Medium (NM) and Negative Small (NS) to indicate different levels of power injection into the grid, and Positive Small (PS), Positive Medium (PM), and Positive Big (PB) to indicate power surplus. The Zero (Z) state represents a condition where there is no active energy exchange with the grid.

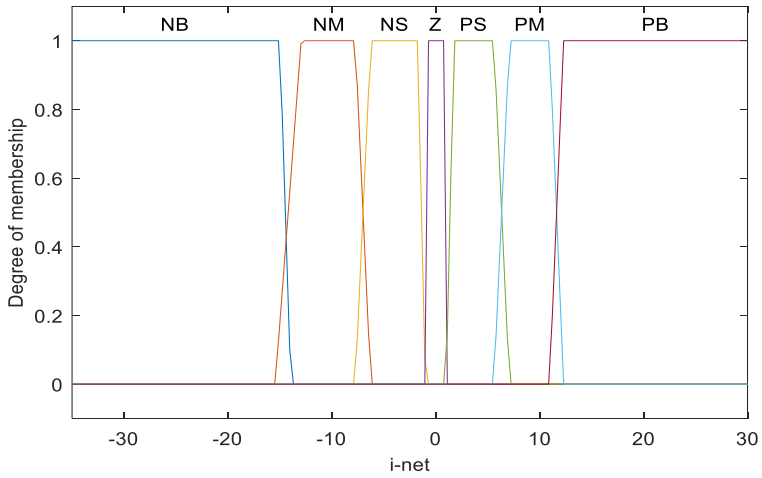

Figure IV.5. Membership function of net current.

- Battery State of Charge (SoC-bat): Indicates the energy level in the battery bank (Low, Medium or High) and determines its availability for charging or discharging.

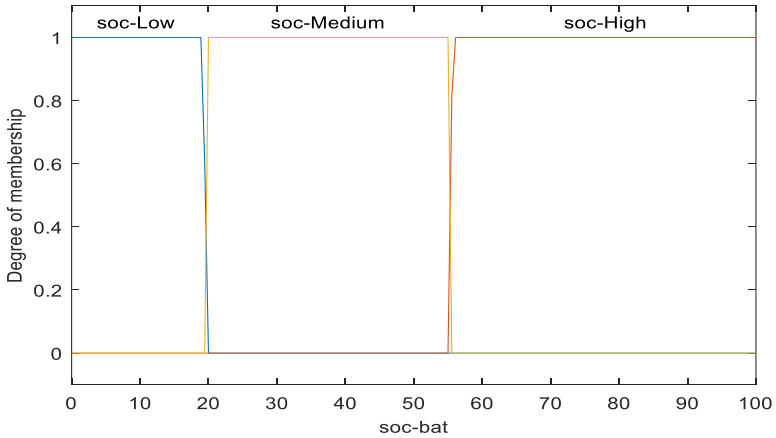

Figure IV.6. Membership function of battery state of charge.

- Supercapacitor State of Charge (SOC-sc): Represents the charge level in the supercapacitor. It can be Low, Medium or High, which serves as a fast-response energy buffer.

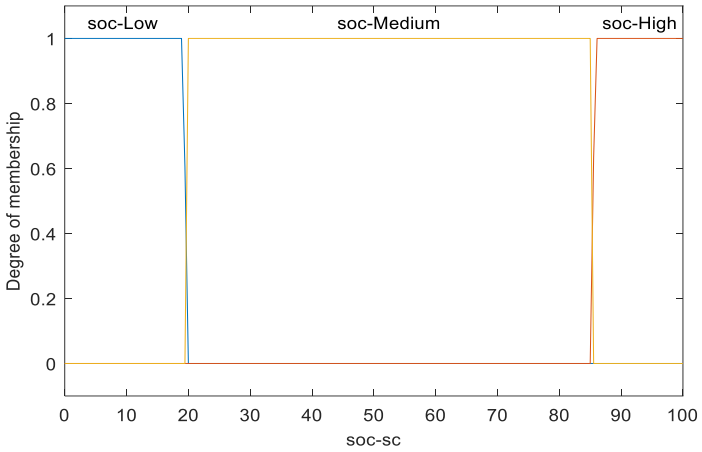

Figure IV. 7. Membership function of supercapacitor state of charge.

- Solar Irradiance (G): Affects the photovoltaic power generation and guides PV source engagement. The fuzzy linguistic terms used are: Low or Normal.

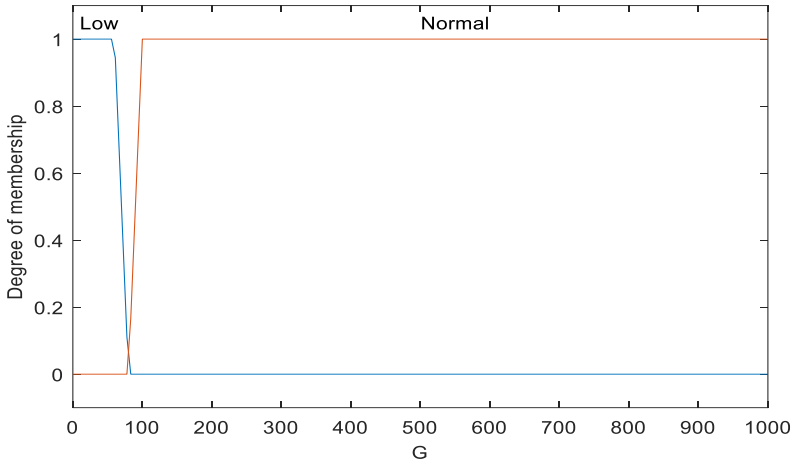

Figure IV.8. Membership function of solar irradiance.

- Ambient Temperature (T): Impacts the efficiency of both PV modules and power electronics, particularly under fluctuating environmental conditions. The fuzzy linguistic terms used are: Cold, Normal or Hot.

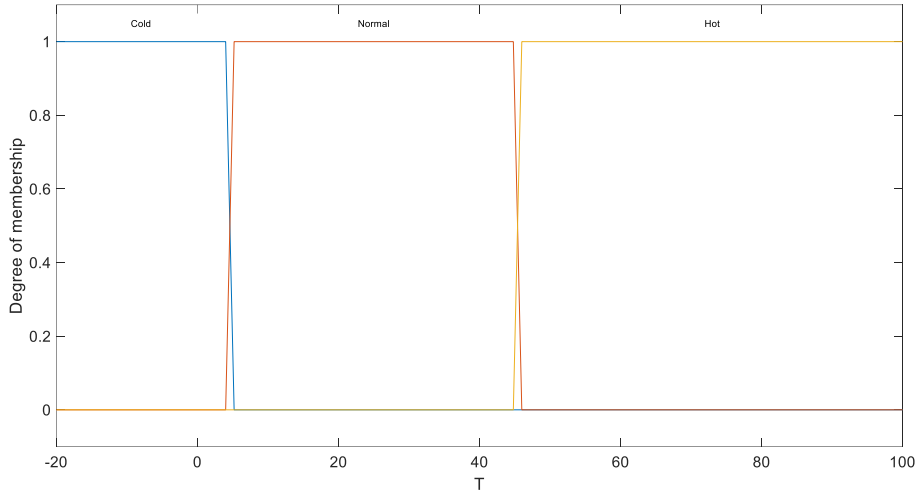

Figure IV.9. Membership function of ambient temperature.

The five output variables generated by the fuzzy inference process correspond to the system's coordinated control actions as shown in Figure IV.10, Figure IV. 11, Figure IV.12, Figure IV.13 and Figure IV.14:

- Battery Current Reference ($i_{bat-ref}$): Specifies the charging or discharging current set point for the battery. The fuzzy linguistic terms used are: Big Charged 'B.Ch', Moderately Charged 'M.Ch', Small Charged 'S.Ch', Small Discharged 'S.Dich', Moderately Discharged 'M.Dich', Big Discharged 'B.Dich'.

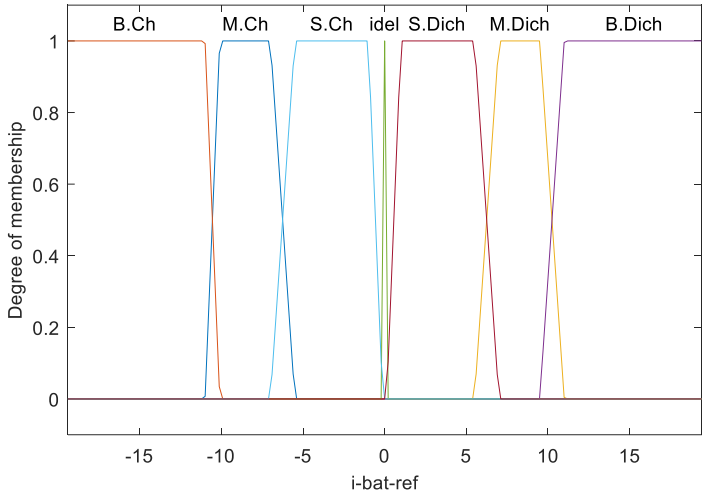

Figure IV.10. Membership function of battery current reference.

- Supercapacitor Current Reference ($i\text{-}_{sc\text{-}ref}$): Defines the operational mode of the SC, either absorbing or injecting current.

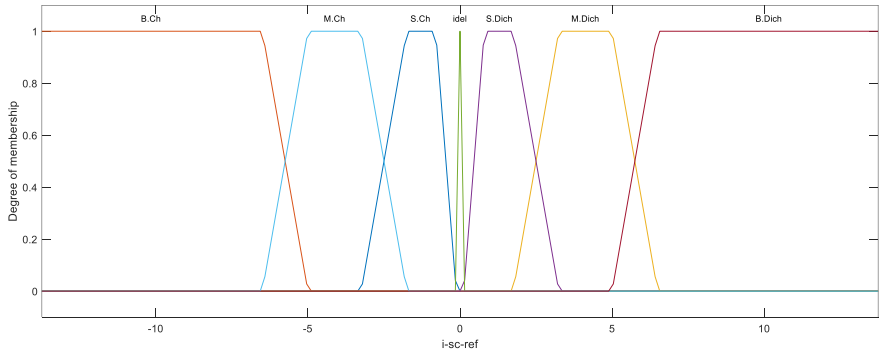

Figure IV. 11. Membership function of supercapacitor current reference.

- (K-grid): A binary signal (ON or OFF) that allows energy exchange with the external utility grid when appropriate.

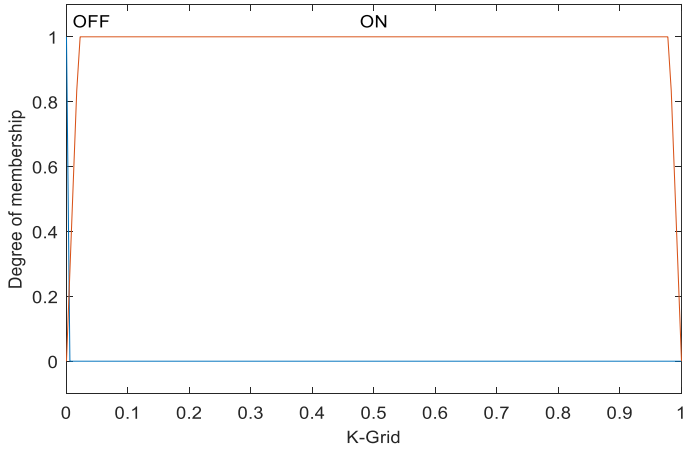

Figure IV.12. Membership function of grid enable signal.

- Dump Load Activation (K-dump): A binary signal (ON or OFF) used to activate the dump load for dissipating surplus energy, thereby preventing overcharging of storage components and maintaining system stability.

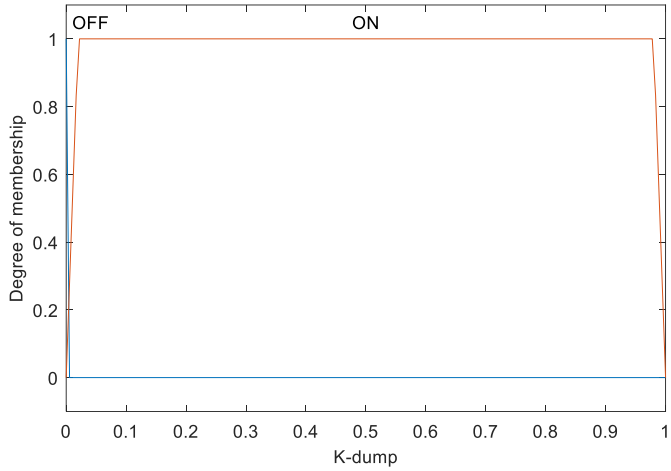

Figure IV.13. Membership function of dump load activation.

- PV Source Activation (K_{pv}): A binary control signal (ON or OFF) that determines whether the photovoltaic (PV) generator contributes to supplying power to the hybrid system load.

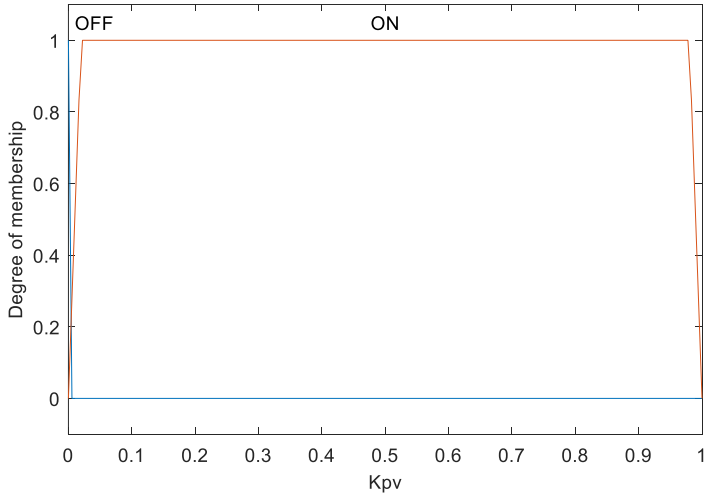

Figure IV.14. Membership function of PV source activation.

IV.6.2. Definition of fuzzy rules for decision making

A fuzzy logic–based energy management unit was developed to generate reference current signals for the battery and supercapacitor, as shown in Figure IV.15. The controller operates with five input variables and five output variables, and its decisions are governed by 252 fuzzy inference rules, ensuring adaptive power sharing according to the state of charge (SOC) levels and load requirements.

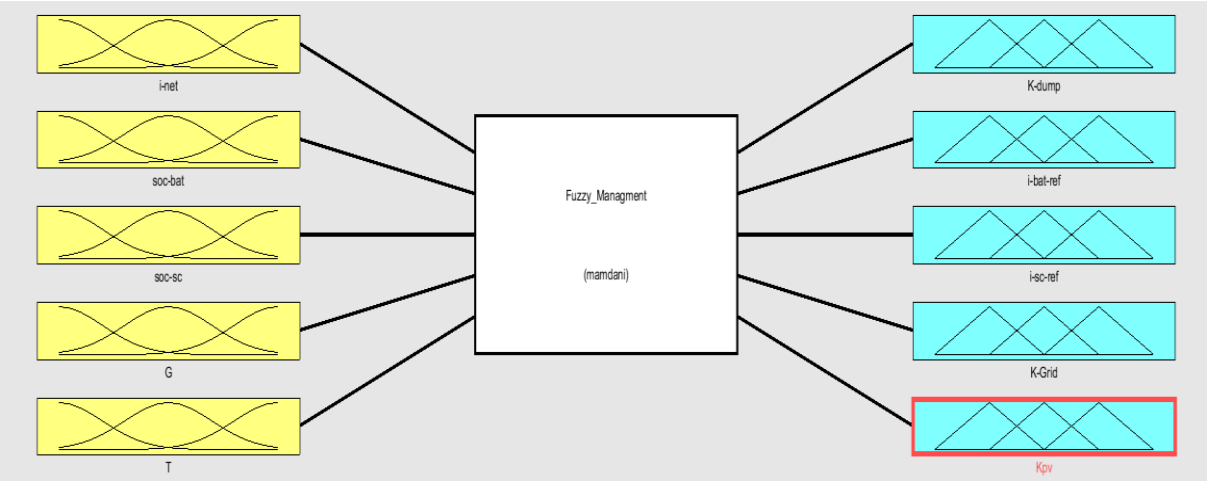

Figure IV.15. Energy management and control unit based on fuzzy logic.

Each fuzzy rule defines a conditional relationship between a specific combination of input membership functions and the corresponding output actions. For instance, a rule may state that if the net current is strongly positive, and both SOC-bat and SOC-sc are high, then the dump load should be activated, and the storage devices set to idle. This approach enables real-time, flexible decision-making that accommodates the system's nonlinear dynamics and the uncertainties of renewable generation.

The complete rule base was carefully constructed and validated through simulations to ensure reliable behavior under a wide range of scenarios, including fluctuating generation, partial storage, and varying loads. This structure provides a scalable and adaptive control logic suitable for autonomous energy management in hybrid renewable systems. The result of the fuzzy inference process is defuzzified into precise numeric outputs, which are then used to generate reference current signals for real-time control. This flexible, rule-based control strategy improves system stability, energy balance, and component longevity, especially under dynamic operating conditions.

A sample of the formulated rules is presented in (Table IV. 2, Table IV. 3). The inputs and outputs, along with their respective membership functions, have been implemented as follows:

Table IV. 2. Fuzzy input rules for the energy management unit.

Rules	Irradiance	Temperature	I_{net}	SOC_{bat}	SOC_{SC}	Operational State
R.1	Standard	Normal	Null	Medium	Medium	System Equilibrium
R.2	Standard	Normal	Negative Small	Medium	Medium	Power Deficit Mitigation
R.3	Standard	Normal	Negative Big	Medium	Medium	Power Deficit Mitigation
R.4	Standard	Normal	Negative Medium	Medium	Medium	Power Deficit Mitigation
R.5	Standard	Normal	Positif Medium	Medium	Medium	Energy Surplus Management
R.6	Standard	Normal	Positif Big	Medium	High	Energy Surplus Management
R.7	Standard	Normal	Positif Medium	High	High	Boundary Protection
R.8	Low	Normal	Positif small	High	High	Energy Surplus Management

The fuzzy output rule base translates the instantaneous power balance and storage state variables into coordinated control actions (Table IV. 2). Battery and supercapacitor current references are determined to ensure fast transient compensation and long-term energy balancing, while grid and renewable source switches are activated to maintain supply continuity and system reliability. An idle operating mode is enforced under balanced conditions to reduce unnecessary cycling and extend storage lifetime.

Table IV. 3. Fuzzy output rules for the energy management unit.

Rules	S_{ch}	S_{res}	S_{pv}	$i_{Bat-ref}$	i_{sc-ref}	Operational State
R.1	ON	OFF	OFF	Idle	Idle	System Equilibrium
R.2	ON	OFF	OFF	Moderately Discharged	Small Discharged	Power Deficit Mitigation
R.3	ON	OFF	OFF	Big Discharged	Moderately Discharged	Power Deficit Mitigation
R.4	ON	OFF	OFF	Small Discharged	Small Discharged	Power Deficit Mitigation
R.5	ON	OFF	OFF	Small Charged	Big Charged	Energy Surplus Management
R.6	ON	OFF	OFF	Big Charged	Idle	Energy Surplus Management
R.7	OFF	OFF	OFF	Big Inactif	Idle	Boundary Protection
R.8	ON	OFF	ON	Big charged	Moderately Discharged	Power Deficit Mitigation

IV.6.3. Performance Evaluation under Diverse Operating Scenarios

The operating behavior of the proposed fuzzy logic–based energy management system (EMS) is classified into four distinct operational states: Energy Surplus Management, System Equilibrium and Preservation, Power Deficit Mitigation, and Boundary Protection under Maximum Stress Conditions. The load demand must always be satisfied, serving as the fundamental constraint to ensure continuity of service and system reliability across all operating modes. This classification enables a structured interpretation of the controller's decision-making process under all possible operating scenarios.

IV.6.3.1. Energy Surplus Management (Scenarios 5 and 6)

These scenarios arise when renewable energy generation exceeds load demand, corresponding to a positive net current (i_{net}>0).

Scenario 5 occurs under a Positive Big surplus. In this case, the controller prioritizes the supercapacitor by assigning a Big Charge reference, allowing rapid absorption of high-power transients. The battery receives a Small Charge command, thereby mitigating peak current stress and reducing battery aging. The power balance for this specific operational state is governed by the following equation:

$$P_{\text{FC}}=\text{P}_{\text{Dem}}+\text{P}_{\text{Bat}}^{\text{ch}}+\text{P}_{\text{SC}}^{\text{ch}}$$

Scenario 6 addresses the condition in which the supercapacitor reaches a high state of charge under a Positive Big surplus. To preserve the supercapacitor's availability for future transient compensation, the controller sets its reference to Idle and redirects the surplus energy to the battery through a Big Charge command. This strategy ensures optimal utilization of the hybrid energy storage system (HESS). The power balance for this specific operational state is governed by the following equation:

$$P_{\text{PV}}+\text{P}_{\text{FC}}=\text{P}_{\text{Dem}}+\text{P}_{\text{Bat}}^{\text{ch(Big)}}$$

IV.6.3.2. System Equilibrium and Preservation (Scenario 1)

Scenario 1 represents the equilibrium operating point of the system, where the net current is Zero ($i_{net} = 0$), indicating a perfect balance between generation and load demand. Under this condition, no energy exchange with the storage units is required. Consequently, the fuzzy controller sets both battery and supercapacitor current references (i_{Bat_ref} and i_{SC_ref}) to Idle. This operating mode is essential for minimizing unnecessary charge–discharge micro-cycles, thereby extending the lifetime and improving the reliability of the HESS. The power balance for this specific operational state is governed by the following equation:

$$P_{\text{PV}}+\text{P}_{\text{FC}}=\text{P}_{\text{Dem}}$$

IV.6.3.3. Power Deficit Mitigation (Scenarios 2, 3 and 4)

Power deficit mitigation encompasses the coordinated control actions employed to compensate for periods of insufficient renewable generation, during which the net power balance becomes negative (i_{net}<0). In this regime, the HESS acts as the primary energy buffer, with grid support activated when required.

Scenario 2 corresponds to a Negative Small deficit, triggering a coordinated Small Discharge from both the battery and the supercapacitor to smoothly compensate for the power shortfall. The power balance for this specific operational state is governed by the following equation:

$$P_{PV}+P_{FC}+P_{Bat}^{Dich}+P_{SC}^{Dich}=P_{Dem}$$

Scenario 3 represents a Negative Big deficit, corresponding to a severe power shortage. The controller commands a Big Discharge from the battery and a Moderate Discharge from the supercapacitor. In this critical regime, the supercapacitor supplies the high-frequency current components associated with rapid load variations, thereby shielding the battery from steep current ramps and reducing electrochemical stress. The power balance for this specific operational state is governed by the following equation:

$$P_{PV}+P_{FC}+P_{Bat}^{Dich(big)}+P_{SC}^{Dich(mod)}=P_{Dem}$$

Scenario 4 reflects a Negative Medium deficit, in which the battery provides a Moderate Discharge to sustain the load while maintaining system stability. The power balance for this specific operational state is governed by the following equation:

$$P_{PV}+P_{FC}+P_{Bat}^{Dich(mod)}+P_{SC}^{Dich}=P_{Dem}$$

IV.6.3.4. Boundary Protection and Maximum Stress Response (Scenarios 7 and 8)

Scenarios 7 and 8 validate the robustness of the proposed EMS under extreme operating conditions and boundary constraints.

Scenario 7 corresponds to an overload protection mode, occurring under a Positive Big surplus when both storage units are at High SOC. In this case, further charging is inhibited, and the dump load switching signal (S_{ch}) is activated to dissipate excess energy. This prevents DC bus overvoltage and ensures compliance with system safety limits. The power balance for this specific operational state is governed by the following equation:

$$\boldsymbol{P_{FC}=P_{Dem}+P_{Dump}}$$

Scenario 8 represents the maximum stress operating point, characterized by a Negative Big deficit combined with Low solar irradiance. This scenario constitutes the most demanding condition in terms of system reliability. The fuzzy logic controller responds by activating all available backup resources, including fuel cell operation and grid support (S_{res}), while

commanding a Big Discharge from the battery and a Moderate Discharge from the supercapacitor. This coordinated response ensures continuity of power supply and prevents total load loss despite extreme operating stress. The power balance for this specific operational state is governed by the following equation:

$$P_{PV(low)} + P_{FC} + P_{Bat}^{Dich(big)} + P_{SC}^{Dich(mod)} = P_{Dem(big)}$$

By associating each operating scenario with explicit mathematical conditions on the net current and storage state variables, the proposed fuzzy energy management strategy ensures transparent decision-making, strict compliance with system boundary conditions, and effective mitigation of maximum stress levels across all operating regimes.

IV.6.4. Adaptation of the proposed control under variable operating conditions

In the hybrid energy system under design in this work, photovoltaic power has a critical role in providing the electrical load. To achieve efficient energy extraction by the PV subsystem, an LSTM-based MPPT controller previously designed and tested in Chapter 3 has been incorporated into the system. This controller, featured in [119] takes advantage of data-driven learning to track the maximum power point (MPP) under varying environmental and operating conditions. Unlike conventional MPPT methods using fixed algorithms or sensors, the LSTM controller is dynamically adjustable for nonlinear and region-based behavior in the PV system. Such adaptability enhances tracking precision and increases the robustness of the system, especially in partial shading conditions or when the irradiance changes sharply. In the fuzzy logic-based energy management system of this chapter, the reference voltage to the PV converter is provided by the output of the LSTM controller. This is then also synchronized with the other control signals (for example, K_{pv}, K_{grid}, and the storage commands) generated by the fuzzy logic decision unit as illustrated in Figure IV. 16. This integration ensures that while the LSTM module provides optimal PV performance, the fuzzy logic controller regulates global energy balance across all subsystems (fuel cell, battery, SC, grid, and dump load).

Simulation outcomes confirm that the hybrid solution combining AI-based MPPT with fuzzy logic energy management causes improved power stability, reduced switching transients, and increased overall system efficiency. Each of the eight scenarios represents a specific operating condition derived from the fuzzy rule base of the controller, considering the system's net power (P_{net}), the state of charge of storage devices (SOC_bat and SOC_sc), and the availability of renewable sources (PV), under varying temperature and irradiation conditions.

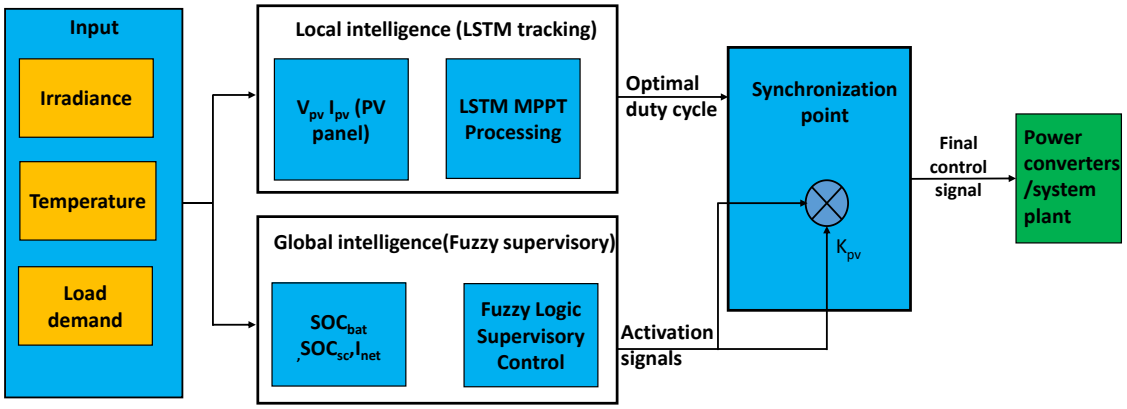

Figure IV. 16. diagram of the dual-layer intelligent architecture.

IV.7. Implementation optimization algorithm of the in a MATLAB

This section evaluates the performance of the proposed hybrid LSTM-fuzzy supervisory controller through comprehensive simulations in MATLAB/Simulink under dynamic operating conditions. The assessment framework employs eight operational scenarios (1–8) encompassing diverse load profiles and environmental variations to rigorously examine the controller's transient and steady-state behavior.

The simulation protocol incorporates realistic meteorological data including temporal variations in ambient temperature (T) and solar irradiance (G), as illustrated in Figure IV.17 and Figure IV. 18. This representative climatic profile enables systematic evaluation of the control strategy's tracking performance, power regulation capabilities and adaptability to fluctuating renewable energy availability. Performance metrics include transient response characteristics (settling time, overshoot, tracking accuracy) and steady-state indicators (efficiency, power quality, SOC regulation). The results provide quantitative validation of the proposed dual-layer intelligent architecture and demonstrate its superiority over conventional energy management strategies.

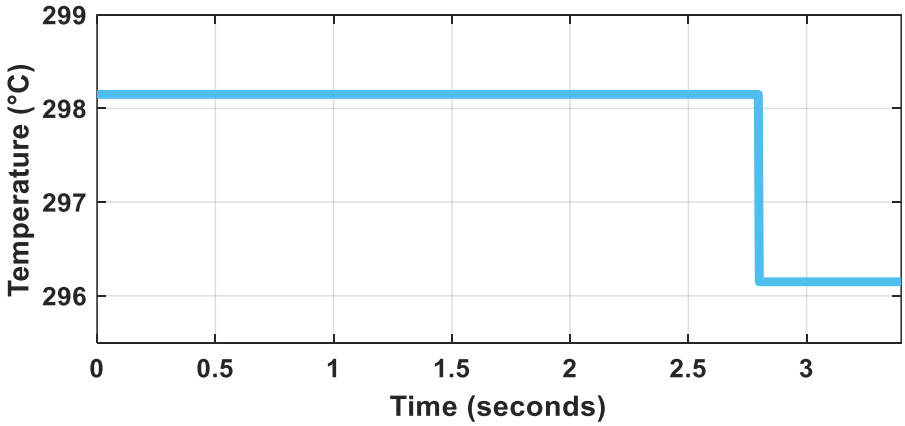

Figure IV.17. Evolution of the temperature.

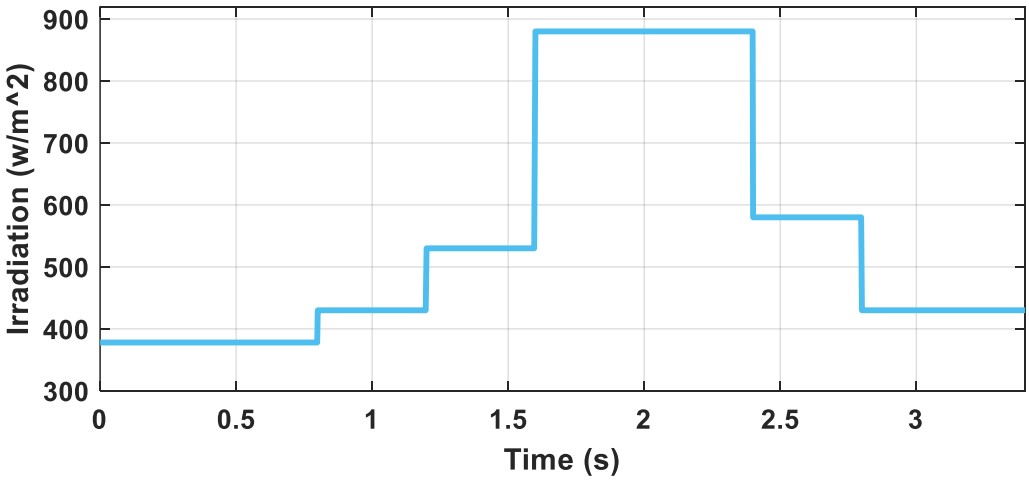

Figure IV. 18. Evolution of the irradiation.

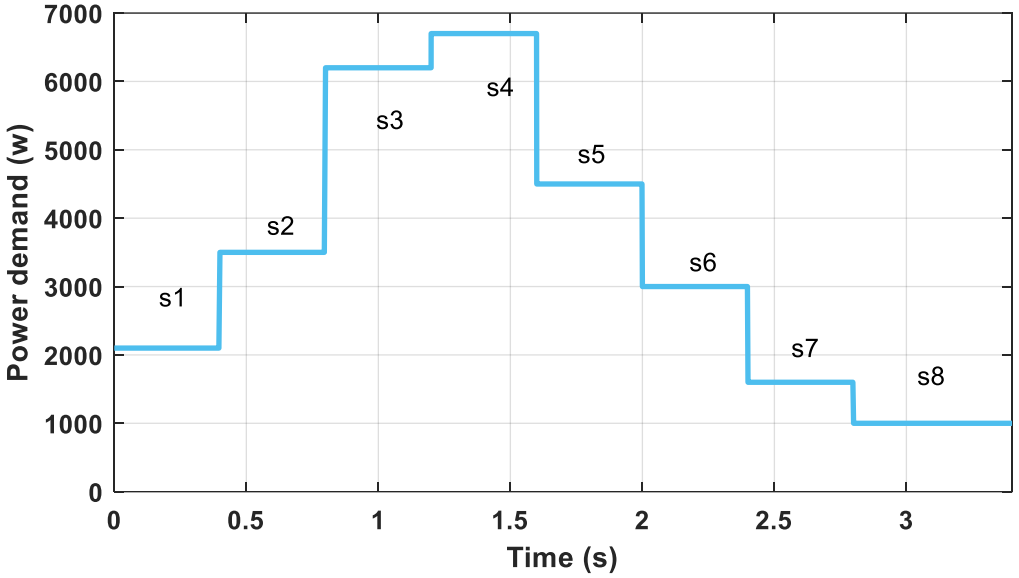

Figure IV.19. Change in power demand.

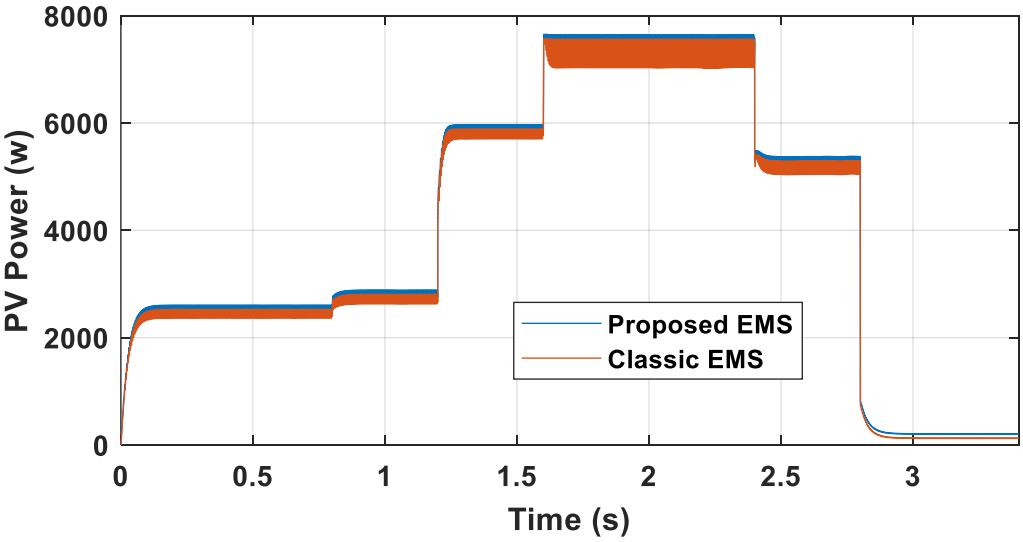

Figure IV. 20. Evolution of PV power.

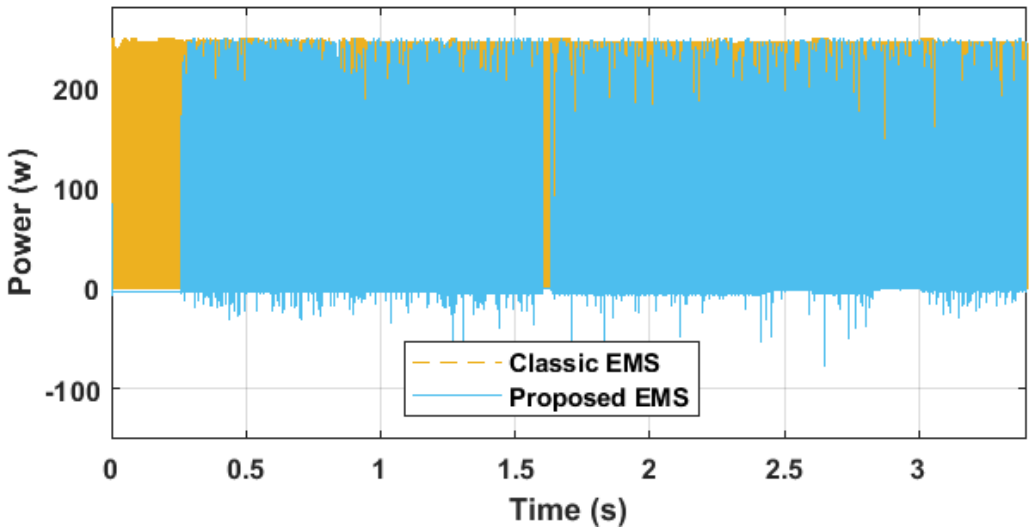

Figure IV. 21. Evolution of the power of the fuel cell.

Figure IV.19 shows the variation of the power demand, structured according to the eight operating scenarios defined for the energy management strategy of the proposed system. The profile starts at approximately 2.1 kW in S1 and increases stepwise to about 3.2 kW (S2), 4.7 kW (S3), 4.8 kW (S4) and a peak of 5 kW in S5 before decreasing successively to around 3 kW (S6), 1.6 kW (S7) and finally 1 kW in S8. Each plateau corresponds to a quasi-steady operating condition, while the abrupt transitions between steps emulate sudden load variations that challenge the hybrid system and its supervisory controller in terms of power sharing, storage utilization and grid support. This demand profile cannot be fully supplied by the active renewable sources (PV and fuel cell) alone, which makes it necessary for the hybrid energy storage system to compensate the resulting power deficit. Figure IV. 20 and Figure IV. 21 present the evolution of the power generated by the hybrid energy system, namely the photovoltaic arrayP_{PV} and the fuel cell P_{FC} respectively.

The corresponding states of charge of charge of the battery and supercapacitor are depicted in Figure IV. 22 and Figure IV. 23 respectively, highlighting the key role of the hybrid storage units in maintaining the supply demand balance and improving the reliability of the overall hybrid energy system.

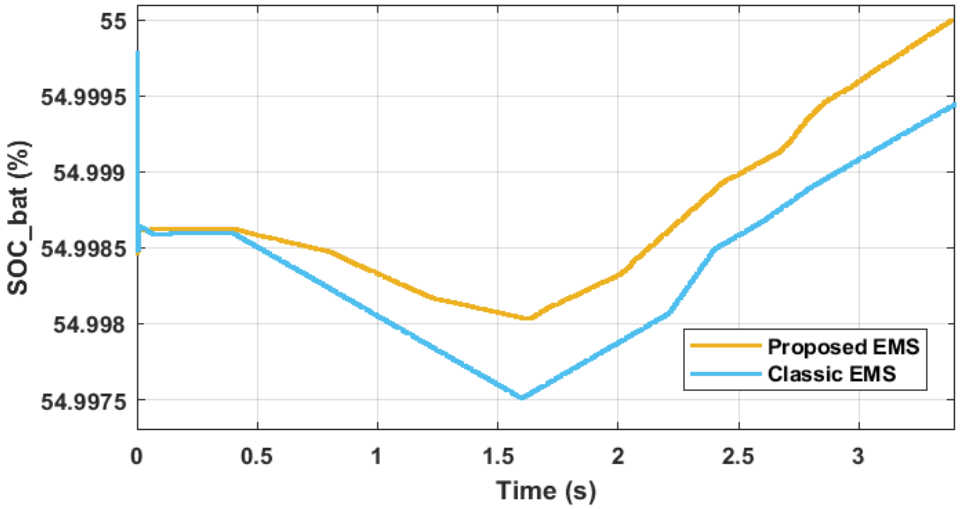

Figure IV. 22. Evolution state of charge of battery.

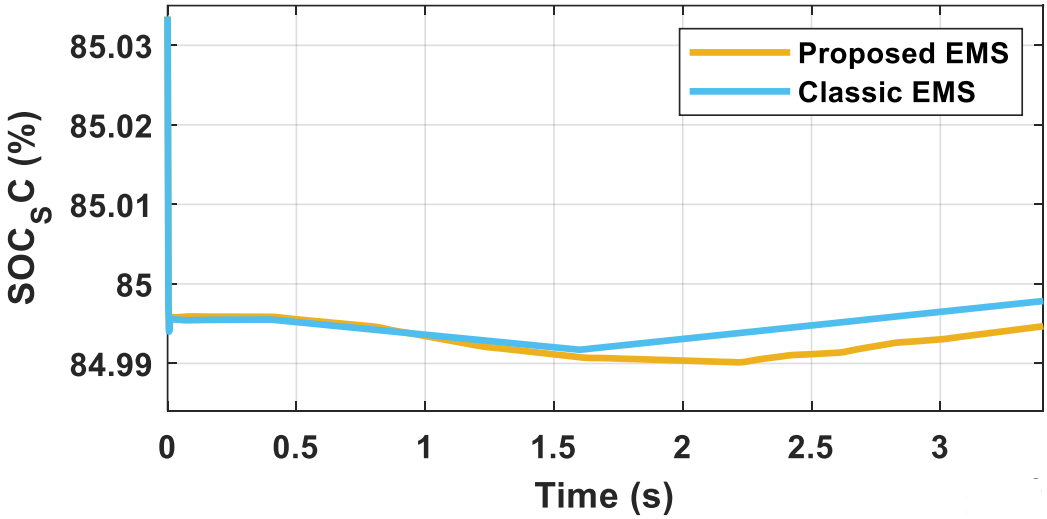

Figure IV. 23. Evolution the state of charge supercapacitor.

In Figure IV. 22 ,the battery SOC demonstrates a smoother trajectory under fuzzy control. Unlike the traditional approach, which often leads to ineffective use of storage devices and premature battery aging due to rigid thresholds, the fuzzy logic controller provides a soft transition between various operational states. This enables the battery to manage medium-term energy needs while avoiding the steep current ramps that characterize classical linear controllers.

In Figure IV. 23, the supercapacitor's rapid response is evident. While the classical controller exhibits a significantly slower response time reaching up to 0.23 s in some scenarios the proposed fuzzy supervisor reduces this response time to as low as 0.003 s. This high-speed coordination ensures that the supercapacitor effectively shaves high-frequency power transients, shielding the battery from electrochemical stress.

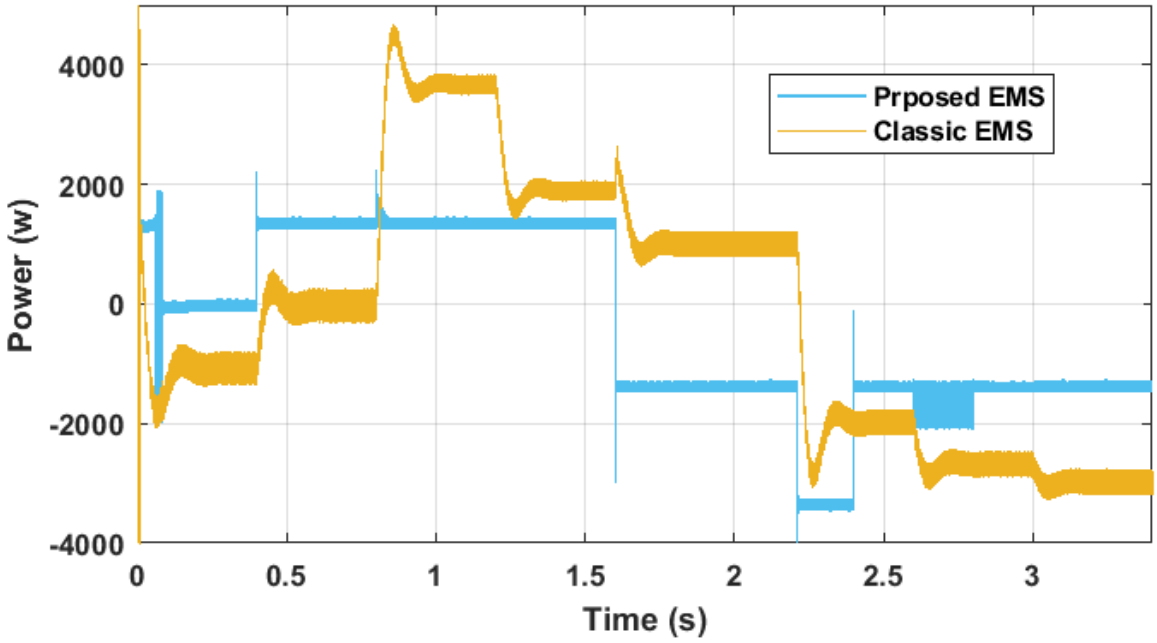

Figure IV. 24. Evolution of the battery power.

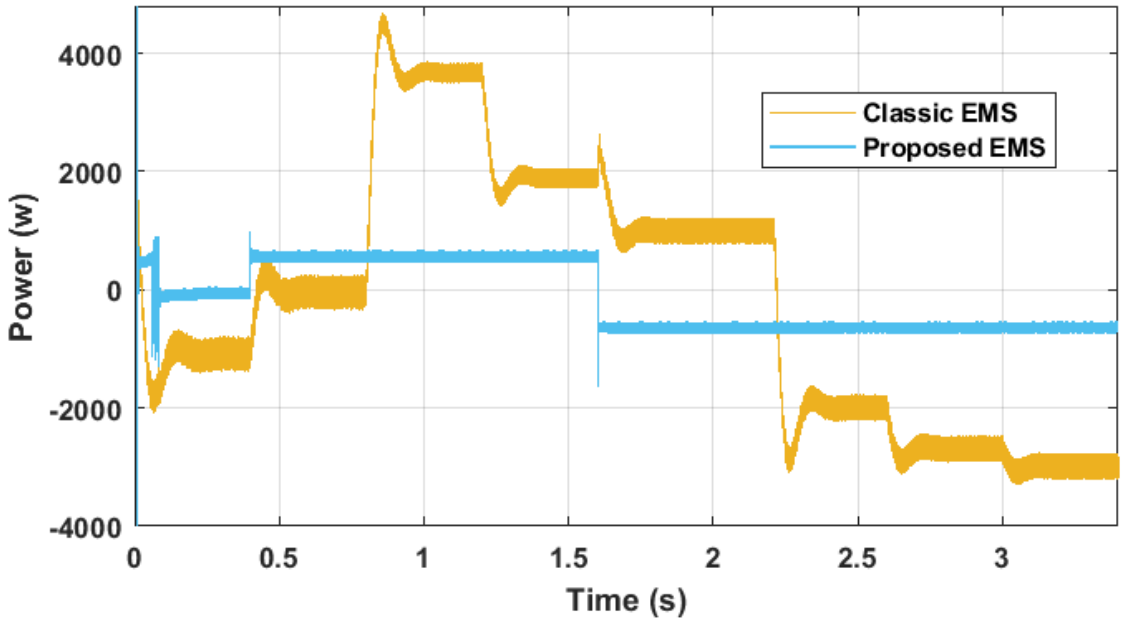

Figure IV. 25. Evolution of the supercapacitor power.

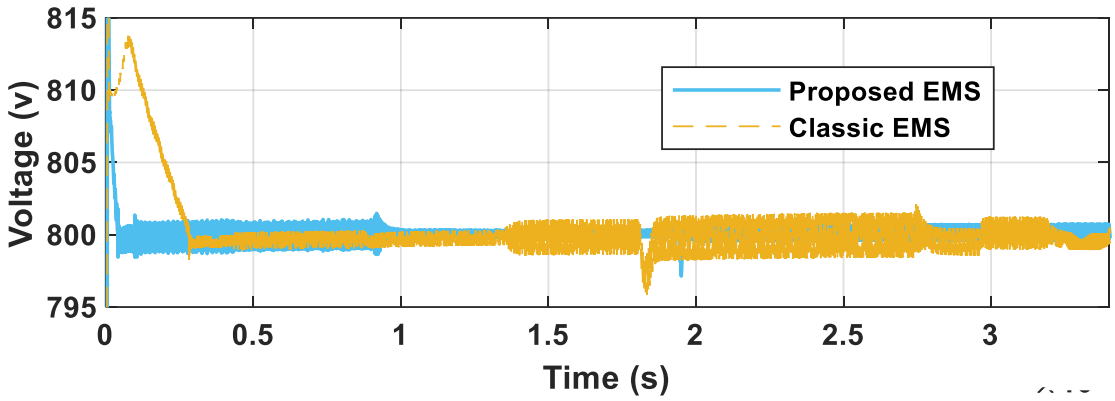

Figure IV. 26. Evolution of the DC bus voltage.

These scenarios are grouped into three main operating regions: low demand (S1–S2), increasing demand (S3–S5), and decreasing demand (S6–S8).

- ✓ During the initial low-demand scenarios (S1–S2), the system operates under moderate loading conditions, where both controllers maintain acceptable stability. However, the proposed energy management strategy demonstrates faster convergence and reduced oscillatory behavior during startup.
- ✓ In the increasing demand region (S3–S5), where the load reaches its peak, the superiority of the proposed controller becomes more evident. The classical approach exhibits noticeable voltage fluctuations and slower dynamic response, whereas the proposed strategy ensures smoother transitions and improved DC bus voltage regulation under high loading conditions.
- ✓ Finally, during the decreasing demand phase (S6–S8), the system experiences sudden load reductions. In this case, the proposed controller effectively manages the excess energy and maintains system stability with minimal voltage deviation. Conversely, the classical controller shows increased oscillations and reduced damping capability.

In all scenarios, the primary load demand is fully satisfied by the PV system. Under the supervision of the Fuzzy Logic controller, the Fuel Cell (FC) is not merely idling; it is commanded to provide a steady 1.26 kW to ensure the Hybrid Storage System (Battery/Supercapacitor) is charged and maintained at an optimal State of Charge (SoC). This proactive charging strategy managed more precisely by Fuzzy Logic than by rigid PI thresholds ensures the system is prepared for sudden irradiance drops or peak demand spikes.

Table IV.4 shown the performance evaluation under equilibrium and surplus conditions (S4–S6), where photovoltaic (PV) generation exceeds load demand due to high irradiance, the proposed fuzzy logic-based energy management strategy enables a rapid transition toward energy storage operation. In these scenarios, the battery response time is significantly reduced to approximately 0.03–0.07 s, compared to about 0.14–0.19 s for the classical controller, highlighting the improved dynamic performance of the proposed approach.

During power deficit conditions (S1–S3), resulting from reduced solar input or increased load demand, the proposed system ensures efficient power compensation through coordinated utilization of hybrid storage elements. In particular, the supercapacitor effectively handles high-frequency transients with response times on the order of 0.01–0.02 s, thereby enhancing system stability.

Under boundary operating conditions (S7–S8), the fuzzy supervisory control provides improved system adaptability and protection by ensuring smooth power redistribution and mitigating excessive voltage deviations. Overall, these results demonstrate that the integration of intelligent control strategies, including advanced MPPT and fuzzy-based energy management, significantly enhances system responsiveness, reduces transient oscillations, and improves the reliability of hybrid energy system operation under varying conditions.

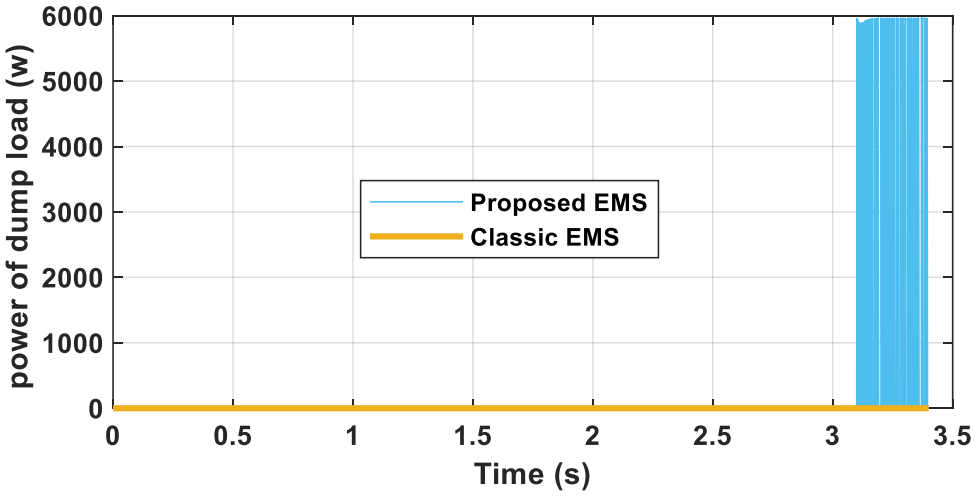

Figure IV. 27. Evolution the power of dump load.

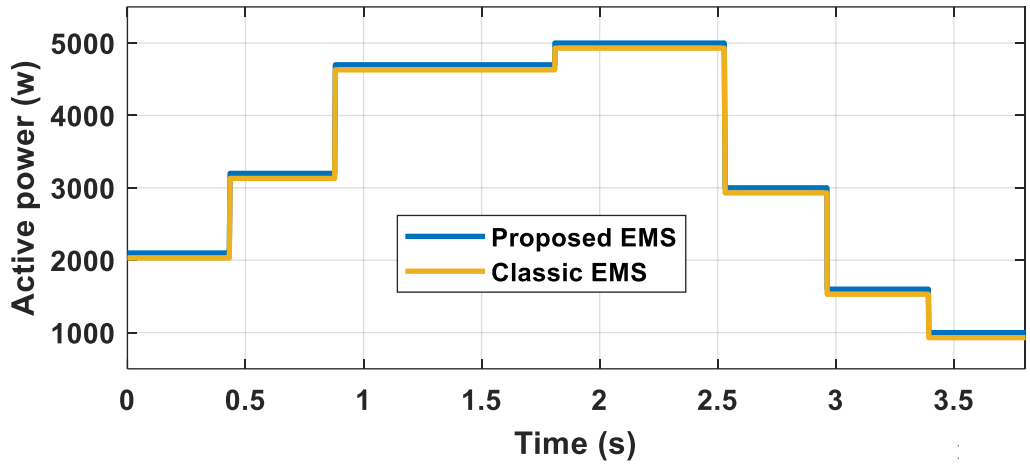

Figure IV.28. Evolution of active power.

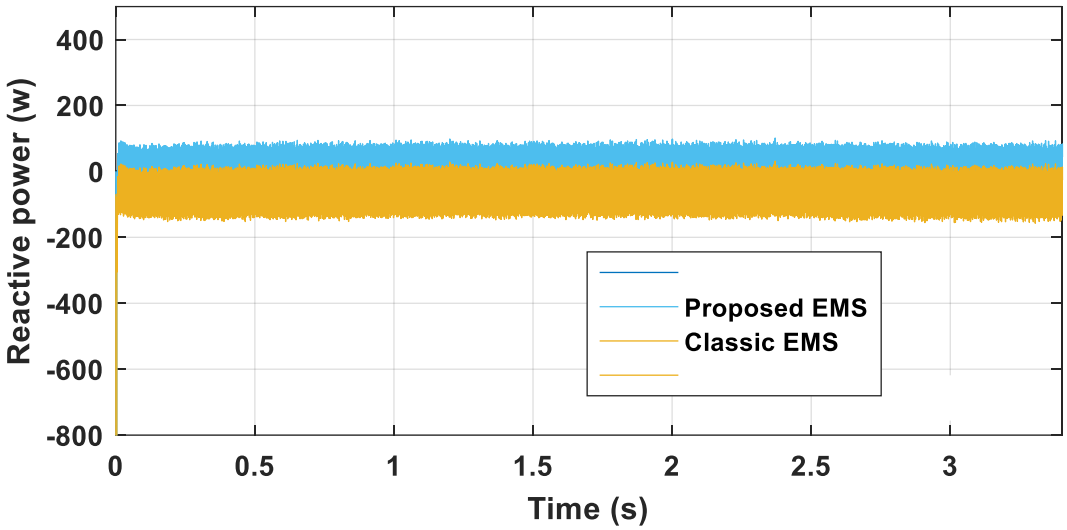

Figure IV. 29. Evaluation the reactive power.

Figure IV. 26 presents a comparative analysis of DC bus voltage regulation performance between the classical threshold-based energy management strategy and the proposed intelligent dual-layer control architecture. During the initial startup phase, both strategies exhibit a transient voltage overshoot before converging toward the nominal operating value of approximately 800 V. The classical control approach shows a more pronounced overshoot (reaching about 813–815 V) followed by damped oscillations before stabilization. In contrast, the proposed control strategy significantly reduces both the amplitude and duration of these transient oscillations, resulting in a smoother and faster convergence toward the steady-state operating point. Overall, the proposed method demonstrates enhanced voltage regulation performance, characterized by improved damping capability and reduced sensitivity to transient disturbances during system initialization.

Thus, to protect the storage system from overcharging and potential damage, the dump load is activated to dissipate the excess power, as illustrated by the dump-load power evolution in Figure IV. 27, which shows the increase in dissipated power whenever surplus energy appears on the DC bus.

Figure IV.28 and Figure IV. 29 shows the electrical power injected into the network, which can follow the desired value with accuracy. But a clear difference appears at the level of the quality (flexibility) of the active and reactive power, the simulation results showed the superiority of the proposed energy management which guarantees regular monitoring of the desired trajectory without phenomena of clicking or oscillations which appear exclusively in the classic energy management. The results reported in the eight scenarios confirm that the proposed hybrid LSTM-fuzzy supervisor significantly reduces the dynamic response time of the hybrid storage system compared with the classical management scheme, which is essential for fast protection and safe power sharing in all operating scenarios. In particular, the activation of the dump load in Scenario 7 corresponds to a state of pronounced power surplus, where the net current is classified as “Positive Big” (PB) and both the battery and supercapacitor operate in the “High” state-of-charge region according to the fuzzy membership functions. Under these conditions, the global fuzzy controller sets the dump-load control signal K_{dump} to “ON”, since further charging of the storage units would increase the risk of overcharge and accelerate their ageing.

The dump load operates as a protective mechanism within the DC microgrid by dissipating excess renewable energy through a resistive element, thereby preventing overvoltage on the DC bus and safeguarding power electronic converters and storage components from harmful transients. Under such operating conditions, the proposed fuzzy supervisory controller ensures a rapid adjustment of both battery and supercapacitor power to their new operating points. Specifically, the response times are reduced to approximately 0.03–0.07 s for the battery and 0.01–0.02 s for the supercapacitor, enabling effective mitigation of transient disturbances and contributing to enhanced system stability.

Table IV.4. Performance Evaluation under Diverse Operational Scenarios.

Scenario	Classic EMS		Proposed EMS	
	$T_{res,bat}$ (s)	$T_{res,sc}$ (s)	$T_{res,bat}$ (s)	$T_{res,sc}$ (s)
S1	0.23	0.23	0.04	0.01
S2	0.17	0.17	0.03	0.01
S3	0.23	0.23	0.04	0.01
S4	0.19	0.19	0.03	0.01
S5	0.14	0.14	0.07	0.02
S6	0.185	0.185	0.04	0.01
S7	0.14	0.14	0.03	0.01
S8	0.14	0.14	0.03	0.01

IV.9. Conclusion

In this chapter, a novel hybrid power system architecture was investigated, integrating renewable generation units (photovoltaic array, and fuel cell) with a dual-storage system composed of a battery and a supercapacitor. To ensure efficient and reliable operation, an energy management strategy based on fuzzy deterministic rules was developed and applied to multiple operating scenarios, including charging, standby, and discharging modes. The results demonstrated that the proposed strategy successfully balances generated and consumed power across all cases, while maintaining stable operation of the hybrid system. Furthermore, the incorporation of an LSTM-based controller within the PV subsystem enabled more accurate and adaptive tracking of the maximum power point under dynamic environmental conditions, thereby enhancing the overall efficiency and stability of the system. Collectively, these findings confirm that the hybrid system can operate close to its maximum potential under diverse conditions, while ensuring robustness through the combined contributions of intelligent control and hybrid energy storage.

Future developments of this hybrid architecture could focus on hardware-in-the-loop validation and experimental prototyping, in order to capture non-ideal converter dynamics, sensor noise, and communication delays that care not represented in pure simulation. In addition, extending the proposed control framework to real-time embedded platforms would allow a detailed assessment of computational cost, memory requirements, and implementation constraints associated with LSTM-based MPPT and fuzzy energy management in practical controllers. Finally, integrating the hybrid system into a grid-connected environment with

demand response and dynamic pricing would open the way to smart micro-grid applications, where the supervisory strategy simultaneously optimizes technical performance and economic benefits for different categories of loads.

General conclusion

General Conclusion

This thesis has addressed the optimization and performance analysis of a hybrid multi-source and multi-load energy system, designed to provide reliable, efficient, and sustainable power supply in the context of renewable integration. The studied system combines photovoltaic generation and a fuel cell with complementary storage units composed of a battery and a supercapacitor. This architecture was selected for its capacity to ensure supply–demand balance, improve operational flexibility, and enhance the reliability of energy delivery, particularly in isolated or rural applications.

A first contribution of this work lies in the detailed modeling and simulation of the proposed hybrid system under MATLAB/Simulink, which enabled the evaluation of various operating scenarios and the identification of critical factors influencing performance. Classical energy management strategies were first implemented and assessed, highlighting their strengths and inherent limitations. Building on this foundation, an intelligent fuzzy-rule–based control strategy was developed, demonstrating superior adaptability and robustness in managing the dynamic interactions between generation and storage units. Beyond rule-based methods, this research further explored advanced optimization approaches. In particular, the use of deep learning through Long Short-Term Memory (LSTM) networks was introduced within the photovoltaic subsystem. The LSTM-based controller enhanced the accuracy of maximum power point tracking under rapidly varying irradiance, thereby improving energy harvesting efficiency and system stability. The integration of such intelligent models illustrates the potential of machine learning techniques to complement and surpass conventional control strategies in renewable energy systems. The findings of this thesis confirm that the hybrid system is capable of operating at or near its maximum potential under diverse conditions while ensuring the continuity of supply and prolonging the lifetime of storage components. Moreover, the methodological framework developed here provides a basis for future research on hybrid renewable systems incorporating additional sources, demand-side management, and real-time optimization.

Nevertheless, Future work on this hybrid architecture should move beyond simulation by incorporating hardware-in-the-loop testing and experimental prototyping. Such validation would make it possible to account for practical effects that are difficult to model accurately, including non-ideal power converter behavior, sensor inaccuracies, and communication delays. Moreover, implementing the proposed control strategy on real-time embedded platforms would

enable a realistic evaluation of computational burden, memory usage, and hardware constraints related to the deployment of LSTM-based MPPT algorithms and fuzzy energy management in actual controllers. In a broader perspective, coupling the hybrid system with a grid-connected environment that includes demand response mechanisms and dynamic electricity pricing could pave the way for smart microgrid applications, where the supervisory control not only enhances technical performance but also maximizes economic benefits across different types of loads.

In conclusion, this thesis contributes to the advancement of hybrid renewable energy systems by combining rigorous system modeling, intelligent energy management, and deep learning–based optimization. It opens new pathways for the design of resilient, sustainable, and intelligent energy infrastructures, capable of addressing the growing challenges of the global energy transition.

Appendices

1. PV panel

Parameters of KC200GT solar array (panel)	
• Maximum power (P_{max})	200.143 W
• Current MPP (I_{mp})	7.61 A
• Voltage MPP (V_{mp})	26.3 V
• light-generated current (I_{pv})	8.214 A
• Short-circuit current (I_{sc})	8.21 A
• Open-circuit current (V_{oc})	32.9 V
• Parallel resistance (R_p)	415.405 Ω
• Series resistance (R_s)	0.221 Ω
• Number of series cells (N_s)	54

2. Supercapacitor

Parameter	Value
Rated capacitance (F)	99.5
Equivalent DC series resistance (Ohms)	8.9e-3
Rated voltage (V)	463.59
Number of series capacitors	18
Number of parallel capacitors	1
Initial voltage (V)	400
Operating temperature (Celsius)	45
Current prior open-circuit (A)	10

3. Fell cell

Parameter	Value
Fuel cell type	PEMFC
Rated power (P_{FC})	1.26 kW
Nominal DC voltage (V_{dc})	24 V
Stack voltage at 0 A (V_0)	42 V
Stack voltage at 1 A (V_1)	35 V
Nominal current (I)	52 A
Nominal voltage (V)	24.23 V
Maximum current (I_{max})	100 A
Minimum voltage at max current	20
Number of cells (N_{cell})	42
Nominal stack efficiency	46 %
Operating temperature (T_{FC})	70 °C
Nominal air flow rate (I_{pm})	2400
Fuel supply pressure (P_{H2})	1.5 bar
Air supply pressure (P_{air})	1.0 bar
Hydrogen concentration (H_2)	99.95 %
Oxygen concentration (O_2)	21 %
Water vapor (air)	1%

4. Battery

Parameter	Value
Type	Lead-acid
Nominal voltage (V)	400
Rated capacity (Ah)	100
Initial state-of-charge (%)	54.9998
Battery response time (s)	100

References

[1] J. C. León Gómez, S. E. De León Aldaco, and J. Aguayo Alquicira, “A review of hybrid renewable energy systems: architectures, battery systems, and optimization techniques,” Eng, vol. 4, no. 2, pp. 1446–1467, 2023, doi: 10.3390/eng4020084.

[2] K. S. Krishna and K. S. Kumar, “A review on hybrid renewable energy systems,” Renew. Sustain. Energy Rev, vol. 52, pp. 907–916, 2015, doi: 10.1016/j.rser.2015.07.187.

[3] Q. Hassan, S. Algburi, A. Z. Sameen, H. M. Salman, and M. Jaszczur, “A review of hybrid renewable energy systems: Solar and wind-powered solutions: Challenges, opportunities, and policy implications,” Results Eng., vol. 20, p. 101621, 2023, doi : 10.1016/j.rineng.2023.101621.

[4] S. Peláez-Peláez, A. Colmenar-Santos, C. Pérez-Molina, A. E. Rosales, and E. Rosales-Asensio, “Techno-economic analysis of a heat and power combination system based on hybrid photovoltaic-fuel cell systems using hydrogen as an energy vector,” Energy, vol. 224, 2021, doi: 10.1016/j.energy.2021.120110.

[5] A. Maheri, I. Unsal, and O. Mahian, “Multiobjective optimisation of hybrid wind-PV-battery-fuel cell-electrolyser-diesel systems: An integrated configuration-size formulation approach,” Energy, vol.241, p.122825, 2022, doi:10.1016/j.energy.2021.122825.

[6] E. Graham, N. Fulghum, and K. Altieri, "Global Electricity Review 2024," Ember, London, UK, May 2024. [Online]. Available: https://ember-energy.org/latest-insights/global-electricity-review-2024/

[7] S. Vighetti, “Systèmes photovoltaïques raccordés au réseau: Choix et dimensionnement des étages de conversion,” Ph.D. dissertation, Univ. Grenoble, France, 2010, p. 185.

[8] https://www.powerelectronictips.com/solar-cells-power-part-1-basic-operation/.

[9] C.-T. Chen, R. A. Islam, and S. Priya, “Electric energy generator,” IEEE Transactions on Ultrasonics, Ferroelectrics, and Frequency Control, vol. 53, no. 3, pp. 656–661, Mar. 2006.

[10] https://www.britannica.com/technology/wind-turbine.

[11] V. Das, S. Padmanaban, K. Venkitusamy, R. Selvamuthukumaran, F. Blaabjerg, and P.Siano, “Recent advances and challenges of fuel cell based power system architectures and control–A review,” Renew. Sustain. Energy Rev., vol. 73, pp. 10–18, 2017, doi: 10.1016/j.rser.2017.01.148.

[12] D. Canever, G. J. W. Dudgeon, S. Massucco, J. R. McDonald, and F. Silvestro, “Model validation and coordinated operation of a photovoltaic array and a diesel power plant for distributed generation,” in Proc. IEEE Power Eng. Soc. Summer Meet., vol. 1, pp. 626–631, 2001.

[13] https://www.toromontpowersystems.com/electric-power/products/diesel-generators.

[14] W. Tutak and A. Jamrozik, "Generator gas as a fuel to power a diesel engine," Thermal Science, vol. 18, no. 1, pp. 205-216, 2014, doi: 10.2298/TSCI120719003T.

[15] D. Kundu, E. Talaie, V. Duffort, and L. F. Nazar, “The emerging chemistry of sodium ion batteries for electrochemical energy storage,” Angew. Chem. Int. Ed., vol. 54, no. 11, pp. 3431–3448, Mar. 2015.doi: 10.1002/anie.201410376.

[16] Z. Qi and G. M. Koenig, “Flow battery systems with solid electroactive materials,” J. Vac. Sci. Technol. B, vol. 35, no. 4, 2017.

[17] https://boattest.com/article/what-you-need-know-about-lead-acid-batteries.

[18] M. Yaseen et al., “A review of supercapacitors: materials design, modification, and applications,” Energies, vol. 14, no. 22, p. 7779, 2021.

[19] Y. Shao et al., “Design and mechanisms of asymmetric supercapacitors,” Chem. Rev., vol. 118, no. 18, pp. 9233–9280, 2018.

[20] Z. Qi and G. M. Koenig, “Flow battery systems with solid electroactive materials,” J.Vac. Sci. Technol. B, vol. 35, no. 4, 2017.

[21] M. Chennaif, M. Maaouane, H. Zahboune, M. Elhafyani, and S. Zouggar, “Tri-objective techno-economic sizing optimization of off-grid and on-grid renewable energy systems using electric system cascade extended analysis and system advisor model,” Appl. Energy, vol. 305, p. 117844, Jan. 2022.

[22] B. F. Silinto, C. Van der Laag Yamu, C. Zuidema, and A. P. C. Faaij, “Hybrid renewable energy systems for rural electrification in developing countries: A review on energy system models and spatial explicit modelling tools,” Renew. Sustain. energy Rev., vol. 207, p. 114916, 2025, doi: 10.1016/j.rser.2024.114916.

[23] B. A. Bhayo, H. H. Al-Kayiem, S. I. U. Gilani, and F. B. Ismail, “Power management optimization of hybrid solar photovoltaic-battery integrated with pumped-hydro-storage system for standalone electricity generation,” Energy Convers. Manag., vol. 215, no. February, p. 112942, 2020, doi: 10.1016/j.enconman.2020.112942.

[24] M. El-Sayed M. Essa et al., “Improving micro-grid management: A review of integration of supercapacitor across different operating modes,” Heliyon, vol. 11, no. 3, p. e42178, 2025, doi: 10.1016/j.heliyon.2025.e42178.

[25] M. Z. Kreishan and A. F. Zobaa, “Optimal allocation and operation of droop-controlled islanded micro-grids: A review,” Energies, vol. 14, no.15, 2021, doi: 10.3390/en14154653.

[26] M.U. Emezirinwune, I. A. Adejumobi, O. I. Adebisi, and F. G. Akinboro, “Synergizing hybrid renewable energy systems and sustainable agriculture for rural development in Nigeria,” e-Prime - Adv. Electr. Eng. Electron. Energy, vol. 7, no. March, p. 100492, 2024, doi: 10.1016/j.prime.2024.100492.

[27] M. Jaszczur, Q. Hassan, P. Palej, and J. Abdulateef, “Multi-objective optimisation of a micro-grid hybrid power system for household application,” Energy, vol. 202, p. 117738, July 2020.

[28] S. Chandak and P. K. Rout, “The implementation framework of a micro-grid: A review,” Int. J. Energy Res., vol. 45, no. 3, pp. 3523–3547, Mar. 2021.

[29] Q. Hassan, M. Jaszczur, and J. Abdulateef, “Optimization of PV/wind/diesel hybrid power system in HOMER for rural electrification,” in J. Phys.: Conf. Ser., vol. 745, no. 3, p. 032006, Sept. 2016.

[30] Q. Hassan, “Optimisation of solar-hydrogen power system for household applications,” Int. J. Hydrogen Energy, vol. 45, no. 58, pp. 33111–33127, Nov. 2020.

[31] B. Ceran, Q. Hassan, M. Jaszczur, and K. Sroka, “An analysis of hybrid power generation systems for a residential load,” in E3S Web Conf., vol. 14, p. 01020, 2017.

[32] A. Khan, M. Bressel, A. Davigny, D. Abbes, and B. Ould Bouamama, “Comprehensive Review of Hybrid Energy Systems: Challenges, Applications, and Optimization Strategies,” Energies, vol. 18, no. 10, pp. 1–34, 2025, doi: 10.3390/en18102612.

[33] R. Goebel, R. G. Sanfelice, and A. R. Teel, “Hybrid dynamical systems,” IEEE Control Syst. Mag., vol. 29, no. 2, pp. 28–93, Apr. 2009.

[34] M. Hasan, N. A. Zarin, M. R. Ahmed, and O. Farrok, “Global pathways for hybrid renewable energy systems: challenges, solutions, policy, and regulatory frameworks,” Energy Convers. Manag. X, vol. 29, no. August 2025, p. 101534, 2026, doi: 10.1016/j.ecmx.2026.101534.

[35] T. Nakken, L. R. Strand, E. Frantzen, R. Rohden, and P. O. Eide, “The Utsira wind-hydrogen system—Operational experience,” in Proc. Eur. Wind Energy Conf., Athens, Greece, Feb. 2006.

[36] M. Virji et al., “Analyses of hydrogen energy system as a grid management tool for the Hawaiian Isles,” Int. J. Hydrogen Energy, vol. 45, no. 15, pp. 8052–8066, Mar. 2020.

[37] M. Landau and H. Deubler, “10 years PV hybrid system as an energy supply for a

remote alpine lodge," in Proc. 4th Eur. PV-Hybrid and Mini-Grid Conf., Glyfada, Greece, 2008.

[38] H. Aki et al., "Fuel cells and energy networks of electricity, heat, and hydrogen in residential areas," Int. J. Hydrogen Energy, vol. 31, no. 8, pp. 967–980, 2006.

[39] H. Aki, Y. Taniguchi, J. Kondoh, I. Tamura, A. Kegasa, Y. Ishikawa, S. Yamamoto, and I. Sugimoto, "The operation result of the demonstration of energy networks of electricity, heat, and hydrogen at an apartment building in 2007," in Proc. ACEEE Summer Study Energy Efficiency Buildings, 2008.

[40] H. Aki et al., "Fuel cells and energy networks of electricity, heat, and hydrogen: A demonstration in hydrogen-fueled apartments," Int. J. Hydrogen Energy, vol. 37, no. 2, pp. 1204–1213, 2012, doi: 10.1016/j.ijhydene.2011.10.021.

[41] N. Hatziargyriou, H. Asano, R. Iravani, and C. Marnay, "Micro-grids: An overview of ongoing research, development, and demonstration projects," IEEE Power Energy Mag., vol. 5, no. 4, pp. 78–94, Jul./Aug. 2007.

[42] Y. Kojima, "Operation Result of the Hachinohe Microgrid Demonstration Project," presented at the 5th Microgrid Symposium, San Diego, USA, Mitsubishi Electric, pp. 1–18.

[43] K. W. Harrison, G. D. Martin, T. G. Ramsden, W. E. Kramer, and F. J. Novachek, "The wind-to-hydrogen project: operational experience, performance testing, and systems integration," 2011.

[44] Erdiwansyah, R. Mamat, S. M. Rosdi, M. F. Ghazali, M. I. M. Rashid, A. Z. Syahir, A. F. Yusop, and A. Tamimi, "A review on AI-enhanced circular energy storage systems for renewable integration," Energy 360, vol. 5, no. October 2025, p. 100051, 2026, doi: 10.1016/j.energ.2025.100051.

[45] A. C. Andrew, C. W. Higgins, M. A. Smallman, M. Graham, and S. Ates,''Herbage yield,Lamb growth and foraging behavior in agrivoltaic production system,'' Frontiers Sustain. Food Syst., vol. 5, pp. 1–12,Apr. 2021, doi: 10.3389/fsufs.2021.659175.

[46] R. Nobre, S. Boulêtreau, F. Colas, F. Azemar, L. Tudesque, N. Parthuisot,P. Favriou, and J. Cucherousset, ''Potential ecological impacts of floating photovoltaics on lake biodiversity and ecosystem functioning,''Renew. Sustain. Energy Rev., vol. 188, Dec. 2023, Art. no. 113852, doi:10.1016/j.rser.2023.113852.

[47] A. M. Adeyinka, O. C. Esan, A. O. Ijaola, and P. K. Farayibi, "Advancements in hybrid energy storage systems for enhancing renewable energy-to-grid integration," Sustain. Energy Res., vol. 11, no. 1, 2024, doi: 10.1186/s40807-024-00120-4.

[48] D. S. Pillai, V. Shabunko, and A. Krishna, ''A comprehensive review on building

integrated photovoltaic systems: Emphasis to technological advancements, outdoor testing, and predictive maintenance,''Renew. Sustain. Energy Rev., vol. 156, Mar. 2022, Art. no. 111946, doi:10.1016/j.rser.2021.111946.

[49] N. Ullah et al., "Blockchain-powered grids: Paving the way for a sustainable and efficient future," Heliyon, vol. 10, no. 10, p. e31592, 2024, doi: 10.1016/j.heliyon.2024.e31592.

[50] Electricity and Gas Regulatory Commission (CREG), "National energy strategy 2011–2030," Mar. 2011, p. 9.

[51] Bouzeroura Lynda, G. S. (2019). Program for the Development of Renewable Energies and Energy Efficiency in Algeria in the Period Between 2015-2030. Dafater Economics Magazine, 11(2), 155.

[52] A. B. Stambouli, Z. Khiat, S. Flazi, and Y. Kitamura, "A review on the renewable energy development in Algeria: Current perspective, energy scenario and sustainability issues," Renew. Sustain. energy Rev., vol. 16, no. 7, pp. 4445–4460, 2012.

[53] T. Makhlouf, "The legal system for the promotion of renewable energies in Algerian l egislation," Algerian J. Secur. Dev., no. 160, p. 9, Jan. 2020.

[54] Abd Erzzag Fawzi, L. R. (2014, décembre). The Reality of Exploiting Renewable Energies in Algeria and ItsRole in Achieving Sustainable Development: A Case Study of Algeria. Economic Studies and Research in Renewable Energies(1).

[55] Nassima, S. (2019). The Legal and Institutional Framework for the Renewable Energy Sector in Algeria. Academic Studies, 6(1), 536.

[56] I. Hannache and S. B., "Investment in renewable energies in Algeria as an alternative to the post-oil phase," Econ. Stud. Res. Renew. Energy, no. 7, Dec. 2017.

[57] A. Layachi, E. Cheikh Larbi, and A. Mokhtar, "Algeria and the transition to renewable energy: the path to achieving energy security," J. Financ. Invest. Sustain. Dev. , vol. 8, no. 1, pp. 58–77, 2023.

[58] People's Democratic Republic of Algeria, "Executive Decree No. 20-322 of November 22, 2020, outlining the authority of the Minister of Renewable Energies and Energy Transition," Algerian Official Gazette, no. 69, p. 5, Nov. 2020.

[59] N. Hatziargyriou, Microgrids and Active Distribution Networks, London, U.K.: The Institution of Engineering and Technology (IET), 2009.

[60] Tian, Hongmei, et al. "A cell-to-module-to-array detailed model for photovoltaic panels." Solar energy 86.9 (2012): 2695-2706.

[61] M. G. Villalva, J. R. Gazoli, and E. Ruppert Filho, “Modeling and circuit-based simulation of photovoltaic arrays,” 2009 Brazilian Power Electron. Conf. COBEP2009, no. November, pp. 1244–1254, 2009, doi: 10.1109/COBEP.2009.5347680.

[62] J. Benziger, “Reactor dynamics of PEM fuel cells,” in Device and Materials Modeling in PEM Fuel Cells, Springer, 2009, pp. 91–122.

[63] Bahri, Hamza, Abdelghani Harrag, and Hegazy Rezk. "Optimal configuration and technoeconomic analysis of hybrid photovoltaic/PEM fuel cell power system." Journal of New Materials for Electrochemical Systems 25.2 (2022).

[64] T. Wilberforce, A.G. Olabi, D. Monopoli, M. Dassisti, E.T. Sayed, M. A. Abdelkareem, Design optimization of proton exchange membrane fuel cell bipolar plate, Energ. Conver. Manage. 277 (2023) 116586.

[65] M. T. Gencoglu and Z. Ural, “Design of a PEM fuel cell system for residential application,” Int. J. Hydrogen Energy, vol. 34, no. 12, pp. 5242–5248, 2009.

[66] D. Lemian and F. Bode, “Battery-supercapacitor energy storage systems for electrical vehicles: a review,” Energies, vol. 15, no. 15, p. 5683, 2022.

[67] M. García-Plaza, D. Serrano-Jiménez, J. E.-G. Carrasco, and J. Alonso-Martínez, “A Ni–Cd battery model considering state of charge and hysteresis effects,” J. Power Sources, vol. 275, pp. 595–604, 2015.

[68] N. A. Ahmed, M. Miyatake, and A. K. Al-Othman, “Power fluctuations suppression of stand-alone hybrid generation combining solar photovoltaic/wind t urbine and fuel cell systems,” Energy Convers. Manag., vol. 49, no. 10, pp. 2711–2719, 2008.

[69] F. Belhachemi, S. Rael, and B. Davat, “A physical based model of power electric doublelayer supercapacitors,” in Conference Record of the 2000 IEEE Industry Applications Conference. ThirtyFifth IAS Annual Meeting and World Conference on Industrial Applications of Electrical Energy (Cat. No. 00CH37129), 2000, vol. 5, pp. 3069–3076.

[70] W. S. Ebhota and T.-C. Jen, “Fossil fuels environmental challenges and the role of solar photovoltaic technology advances in fast tracking hybrid renewable energy system,” *Int. J. Precis. Eng. Manuf. Technol.*, vol. 7, no. 1, pp. 97–117, 2020.

[71] S. Dubey, J. N. Sarvaiya, and B. Seshadri, “Temperature dependent photovoltaic (PV) efficiency and its effect on PV production in the world–a review,” *Energy procedia*, vol. 33, pp. 311–321, 2013.

[72] K. Y. Yap, C. R. Sarimuthu, and J. M.-Y. Lim, “Artificial intelligence based MPPT techniques for solar power system: A review,” *J. Mod. Power Syst. Clean Energy*, vol. 8, no. 6, pp. 1043–1059, 2020.

[73] L. Meegahapola, A. Sguarezi, J. S. Bryant, M. Gu, E. R. Conde D, and R. B. A. Cunha, "Power system stability with power-electronic converter interfaced renewable power generation: Present issues and future trends," Energies, vol. 13, no. 13, p. 3441, 2020.

[74] M. R. AlRashidi, M. F. AlHajri, K. M. El-Naggar, and A. K. Al-Othman, "A new estimation approach for determining the I–V characteristics of solar cells," Sol. Energy, vol. 85, no. 7, pp. 1543–1550, 2011.

[75] B. Madaci, R. Chenni, E. Kurt, and K. E. Hemsas, "Design and control of a stand-alone hybrid power system," Int. J. Hydrogen Energy, vol. 41, no. 29, pp. 12485–12496, 2016.

[76] A. El Aroudi, R. Haroun, M. Al-Numay, and M. Huang, "Multiple-loop control design for a single-stage PV-fed grid-tied differential boost inverter," Appl. Sci., vol. 10, no. 14, p. 4808, 2020.

[77] O. Singh and S. K. Gupta, "A review on recent Mppt techniques for photovoltaic system," 2018 IEEMA Eng. Infin. Conf. eTechNxT 2018, pp. 1–6, 2018, doi: 10.1109/ETECHNXT.2018.8385315.

[78] S. A. Sarang et al., "Maximizing solar power generation through conventional and digital MPPT techniques: a comparative analysis," Sci. Rep., vol. 14, no. 1, p. 8944, 2024, doi: 10.1038/s41598-024-59776-z.

[79] K. L. Lian, J. H. Jhang, and I. S. Tian, "A maximum power point tracking method based on perturb-and-observe combined with particle swarm optimization," IEEE J.photovoltaics, vol. 4, no. 2, pp. 626–633, 2014.

[80] D. Pilakkat and S. Kanthalakshmi, "An improved P&O algorithm integrated with artificial bee colony for photovoltaic systems under partial shading conditions," Sol. Energy, vol. 178, pp. 37–47, 2019.

[81] D. Sera, L. Mathe, T. Kerekes, S. V. Spataru, and R. Teodorescu, "On the perturb-and-observe and incremental conductance MPPT methods for PV systems," IEEE J. photovoltaics, vol. 3, no. 3, pp. 1070–1078, 2013.

[82] D. Baimel, S. Tapuchi, Y. Levron, and J. Belikov, "Improved fractional open circuit voltage MPPT methods for PV systems," Electronics, vol. 8, no. 3, p. 321, 2019.

[83] B. Ankaiah and J. Nageswararao, "Enhancement of solar photovoltaic cell by using short-circuit current MPPT method," Int. J. Eng. Sci. Invent., vol. 2, no. 2, pp.45–50, 2013.

[84] F. El Aamri, H. Maker, D. Sera, S. V. Spataru, J. M. Guerrero, and A. Mouhsen, "A direct maximum power point tracking method for single-phase grid-connected PV inverters," IEEE Trans. Power Electron., vol. 33, no. 10, pp. 8961–8971, 2017.

[85] M. Killi and S. Samanta, “Modified perturb and observe MPPT algorithm for drift avoidance in photovoltaic systems,” IEEE Trans. Ind. Electron., vol. 62, no. 9, pp. 5549–5559, 2015.

[96] K. S. Tey and S. Mekhilef, “Modified incremental conductance MPPT algorithm to mitigate inaccurate responses under fast-changing solar irradiation level,”Sol.energy, vol. 101, pp. 333–342, 2014.

[87] M. H. Ibrahim, S. P. Ang, M. N. Dani, M. I. Rahman, R. Petra, and S. M. Sulthan, “Optimizing Step-Size of Perturb & Observe and Incremental Conductance MPPT Techniques Using PSO for Grid-Tied PV System,” IEEE Access, vol. 11, no. January, pp. 13079–13090, 2023, doi: 10.1109/ACCESS.2023.3242979.

[88] W. Xiao, W. G. Dunford, P. R. Palmer, and A. Capel, “Application of centered differentiation and steepest descent to maximum power point tracking,” IEEE Trans. Ind. Electron., vol. 54, no. 5, pp. 2539–2549, 2007, doi: 10.1109/TIE.2007.899922.

[89] M. A. Abo-Sennah, M. A. El-Dabah, and A. E. B. Mansour, “Maximum power point tracking techniques for photovoltaic systems: A comparative study,” Int. J. Electr. Comput. Eng., vol. 11, no. 1, pp. 57–73, 2021, doi: 10.11591/ijece.v11i1.pp57-73.

[90] M. H. Zafar et al., “A novel meta-heuristic optimization algorithm based MPPT control technique for PV systems under complex partial shading condition,” Sustain.Energy Technol. Assessments, vol. 47, p. 101367, 2021.

[91] H. Gohar Ali, R. Vilanova Arbos, J. Herrera, A. Tobón, and J. Peláez-Restrepo, “Non-linear sliding mode controller for photovoltaic panels with maximum power point tracking,” Processes, vol. 8, no. 1, p. 108, 2020.

[92] K. Y. Yap, C. R. Sarimuthu, and J. M. Y. Lim, “Artificial Intelligence Based MPPT Techniques for Solar Power System: A review,” J. Mod. Power Syst. Clean Energy, vol. 8, no. 6, pp. 1043–1059, 2020, doi: 10.35833/MPCE.2020.000159.

[93] M. A. Sasi, “Fuzzy Logic Control of MPPT Controller for PV Systems,” no. May, pp. 1–17, 2017.

[94] G. Li, S. Xie, B. Wang, J. Xin, Y. Li, and S. Du, “Photovoltaic Power Forecasting with a Hybrid Deep Learning Approach,” IEEE Access, vol. 8, pp. 175871–175880, 2020, doi: 10.1109/ACCESS.2020.3025860.

[95] C. Jiang, “African vulture optimized RNN algorithm maximum power point tracking (MPPT) controller for photovoltaic (PV) system,” Meas. Sensors, vol. 36, no. May 2023, p. 101392, 2024, doi: 10.1016/j.measen.2024.101392.

[97] J. H. Holland, Adaptation in natural and artificial systems: an introductory analysis with applications to biology, control, and artificial intelligence. MIT press, 1992.

[96] N. Boutasseta, M. Ramdani, and S. Mekhilef, "Fault-tolerant power extraction strategy for photovoltaic energy systems," Sol. Energy, vol. 169, no. February, pp. 594–606, 2018, doi: 10.1016/j.solener.2018.05.031.

[98] M. Seyedmahmoudian et al., "State of the art artificial intelligence-based MPPT techniques for mitigating partial shading effects on PV systems – A review," Renew. Sustain. Energy Rev., vol. 64, pp. 435–455, 2016, doi: 10.1016/j.rser.2016.06.053.

[99] A. Boussafa, R. Rabeh, M. Ferfra, and K. Chennoufi, "Experimental test of optimizing maximum power point tracking performance in solar photovoltaic arrays based on backstepping control and optimized by genetic algorithm," Results Eng., vol. 23, no. August, p. 102746, 2024, doi: 10.1016/j.rineng.2024.102746.

[100] S. Titri, C. Larbes, K. Y. Toumi, and K. Benatchba, "A new MPPT controller based on the Ant colony optimization algorithm for Photovoltaic systems under partial shading conditions," Appl. Soft Comput. J., vol. 58, pp. 465–479, 2017, doi: 10.1016/j.asoc.2017.05.017.

[101] S. Mohanty, B. Subudhi, and P. K. Ray, "A new MPPT design using grey Wolf optimization technique for photovoltaic system under partial shading conditions," IEEE Trans. Sustain. Energy, vol. 7, no. 1, pp. 181–188, 2016, doi: 10.1109/TSTE.2015.2482120.

[102] H. G. Ali and R. V. Arbos, "Chattering free adaptive sliding mode controller for photovoltaic panels with maximum power point tracking," Energies, vol. 13, no. 21, pp. 1– 14, 2020, doi: 10.3390/en13215678.

[103] Z. Lin and D. Rong, "Integrating PQTCN-MPC with innovation: A new strategy for accurate PV power prediction," Comput. Electr. Eng., vol. 123, no. PC, p. 110188, 2025, doi: 10.1016/j.compeleceng.2025.110188.

[104] A. Hussain, M. M. Garg, M. P. Korukonda, S. Hasan, and L. Behera, "A parameter estimation based MPPT method for a PV system using Lyapunov control scheme," IEEE Trans. Sustain. Energy, vol. 10, no. 4, pp. 2123–2132, 2018.

[105] S. Manna, A. K. Akella, and D. K. Singh, "Novel Lyapunov-based rapid and ripple-free MPPT using a robust model reference adaptive controller for solar PV system," Prot. Control Mod. Power Syst., vol. 8, no. 1, pp. 1–25, 2023.

[106] R. D. Bhagiya and R. M. Patel, “PWM based double loop PI control of a bidirectional DC-DC converter in a standalone PV/battery DC power system,” in 2019 IEEE 16th India council international conference (INDICON), 2019, pp. 1–4.

[107] M. R. Mojallizadeh, M. Badamchizadeh, S. Khanmohammadi, and M. Sabahi, “Designing a new robust sliding mode controller for maximum power point tracking of photovoltaic cells,” Sol. Energy, vol. 132, pp. 538–546, 2016.

[108] W. Xiao, W. G. Dunford, P. R. Palmer, and A. Capel, “Regulation of photovoltaic voltage,” IEEE Trans. Ind. Electron., vol. 54, no. 3, pp. 1365–1374, 2007, doi: 10.1109/TIE.2007.893059.

[109] A. Rehail, B. Meghni, N. Boutasseta, and M. Benghanem, “Design and Dynamic Performance Evaluation of an LSTM Based Deep Learning Controller for PV Systems Operating in Different Voltage Regions,” Appl. Sol. Energy, vol. 60, no. 6, pp. 785–7 99, 2024.

[110] A. Bashar, “Survey on evolving deep learning neural network architectures,” J. Artif. Intell., vol. 1, no. 02, pp. 73–82, 2019.

[111] S. Li, W. Li, C. Cook, C. Zhu, and Y. Gao, “Independently recurrent neural network (indrnn): Building a longer and deeper rnn,” in Proceedings of the IEEE conference on computer vision and pattern recognition, 2018, pp. 5457–5466.

[112] A. Graves and A. Graves, “Long short-term memory,” Supervised Seq. Label. with Recurr. neural networks, pp. 37–45, 2012.

[113] Z. Z. Zhao et al., “Bioactive polyketides and 8,14-seco-ergosterol from fruiting bodies of the ascomycete Daldinia childiae,” Phytochemistry, vol. 142, pp. 68–75, 2017, doi: 10.1016/j.phytochem.2017.06.020.

[114] C. Xu, J. Ji, and P. Liu, “The station-free sharing bike demand forecasting with a deep learning approach and large-scale datasets,” Transp. Res. Part C Emerg. Technol., vol. 95, no. September 2017, pp. 47–60, 2018, doi: 10.1016/j.trc.2018.07.013.

[115] J. Ke, H. Zheng, H. Yang, and X. (Michael) Chen, “Short-term forecasting of passenger demand under on-demand ride services: A spatio-temporal deep learning approach,” Transp. Res. Part C Emerg. Technol., vol. 85, no. June, pp. 591–608, 2017, doi: 10.1016/j.trc.2017.10.016.

[116] T. Fischer and C. Krauss, “Deep learning with long short-term memory networks for financial market predictions,” Eur. J. Oper. Res., vol. 270, no. 2, pp. 654–669, 2018, doi: 10.1016/j.ejor.2017.11.054.

[117] D. P. Kingma and J. L. Ba, "Adam: A method for stochastic optimization," 3rd Int. Conf. Learn. Represent. ICLR 2015 - Conf. Track Proc., pp. 1–15, 2015.

[118] J. C. León Gómez, S. E. De León Aldaco, and J. Aguayo Alquicira, "A Review of Hybrid Renewable Energy Systems: Architectures, Battery Systems, and Optimization Techniques," *Eng.*, vol. 4, no. 2, pp. 1446–1467, 2023, doi: 10.3390/eng4020084.

[119] D. Rekioua and E. Matagne, *Optimization of Photovoltaic Power Systems: Modelization,Simulation and Control*. Springer, 2012. doi:10.1007/978-1-4471-23463.

[120] T. Ma, H. Yang, and L. Lu, "A feasibility study of a stand-alone hybrid solar–wind–battery system for a remote island," *Applied Energy*, vol. 121, pp. 149–158, 2014, doi: 10.1016/j.apenergy.2014.01.090.

[121] S. S. Chandel, A. Agarwal, and M. N. Agarwal, "Review of HOMER software for sizing standalone and grid connected hybrid renewable energy systems," Renewable and Sustainable Energy Reviews, vol. 62, pp. 609–620, Sep. 2016, doi: 10.1016/j.rser.2016.04.050.

[122] N. Bizon, "Hybrid renewable power sources: Optimization of energy management," Renewable and Sustainable Energy Reviews, vol. 49, pp. 421–431, 2015.

[123] B. Poudel, M. B. Trabia, and N. T. Ndeh, "Optimization of Hybrid Energy Systems Using LCC and System Reliability," *IEEE Trans. on Sustainable Energy*, vol. 10, no. 3, pp. 1291–1300, 2019.

[124] H. Rezzouk and A. Mellit, "Feasibility study and sensitivity analysis of a stand-alone photovoltaic–diesel–battery hybrid energy system in the north of Algeria," Renewable and Sustainable Energy Reviews, vol. 43, pp. 1134–1150, 2015.

[125] T. Khatib and A. Mohamed, "A review on sizing methodologies of photovoltaic array and storage battery in a standalone photovoltaic system," *Energy Conversion and Management*, vol. 120, pp. 430–448, 2016.

[126] J. C. León Gómez, S. E. De León Aldaco, and J. Aguayo Alquicira, "A review of hybrid renewable energy systems: Architectures, battery systems, and optimization techniques," Engineering, vol. 4, no. 2, pp. 1446–1467, 2023, doi: 10.3390/eng4020084.

[127] M. Z. Jacobson, M. A. Delucchi, Z. A. F. Bauer, S. C. Goodman, W. E. Chapman, M. A. Cameron *et al.*, "100% Clean and Renewable Wind, Water, and Sunlight All-Sector Energy Roadmaps for 139 Countries of the World," *Joule*, vol. 1, no. 1, pp. 108–121, 2017, doi: 10.1016/j.joule.2017.07.005.

[128] T. Ma, H. Yang, and L. Lu, "A review of the modeling and control strategies of hybrid renewable energy systems," *Renewable and Sustainable Energy Reviews*, vol. 41, pp. 848–859, 2015, doi: 10.1016/j.rser.2014.08.039.

[129] NASA Prediction Of Worldwide Energy Resources (POWER), "NASA-POWER Data Access Viewer," [Online]. Available: https://power.larc.nasa.gov.

[130] European Commission Joint Research Centre,"Photovoltaic GeographicalInformation System (PVGIS)," [Online]. Available: https://joint-research-centre.ec.europa.eu/photovoltaic-geographical-information-system-pvgis_en.

[131] T. Ma, H. Yang, and L. Lu, "A review of the modeling and control strategies of hybrid renewable energy systems," *Renewable and Sustainable Energy Reviews*, vol. 41, pp. 848–859, 2015, doi: 10.1016/j.rser.2014.08.039.

[132] M. A. Zdiri, S. Kermadi, and M. H. Bouanane, "Design and analysis of sliding-mode artificial neural network control strategy for hybrid PV-battery-supercapacitor system," *Energies*, vol. 15, no. 11, p. 4099, 2022, doi: 10.3390/en15114099.

[133] M. S. Hossain Lipu, A. Arefi, M. A. Mahmud, and A. H. Etemadi, "Review of voltage and frequency control strategies for islanded microgrids," *IEEE Access*, vol. 7, pp. 1 44051–144069, 2019, doi: 10.1109/ACCESS.2019.2944312.

[134] M. Koulali, L. Khriji, and M. Zellouma, "Sliding fuzzy controller for hybrid PV/wind/battery system," *J. Electr. Syst. Autom.*, vol. 53, no. 3, pp. 273–280, 2020, doi: 10.18280/jesa.530301.

[135] M. S. Mahmoud and F. M. Al-Sunni, *Control and Optimization of Distributed Generation Systems*, Springer, 2015.

[136] M. A. Zdiri, S. Kermadi, and M. H. Bouanane, "Design and analysis of sliding-mode artificial neural network control strategy for hybrid PV-battery-supercapacitor system," *Energies*, vol. 15, no. 11, p. 4099, 2022, doi: 10.3390/en15114099.

[137] J. Faria, J. Pombo, M. do Rosário Calado, and S. Mariano, "Power management control strategy based on artificial neural networks for standalone PV applications with a hybrid energy storage system," *Energies*, vol. 12, no. 5, 2019, doi: 10.3390/en12050902.

[138] A. Ghaemi, M. J. Sanjari, H. Mokhtari, and A. Yazdani, "Optimal energy management of renewable micro-grid with hybrid storage using neural network and dynamic programming," *IEEE Transactions on Smart Grid*, vol. 10, no. 2, pp. 2004–2013, 2019, doi: 10.1109/TSG.2017.2782747.

[139] K. Chandrasekaran, J. Selvaraj, C. R. Amaladoss, and L. Veerapand, "Hybrid renewable energy based smart grid system for reactive power management and voltage profile enhancement using artificial neural network," *Energy Sources, Part A: Recovery, Utilization, and Environmental Effects*, vol. 43, no. 19, pp. 2419–2442, 2021, doi: 10.1080/15567036.2021.1902430.

[140] S. Mekhilef, R. Saidur, and A. Safari, "Comparative study of different control strategies for standalone PV system," *Energy Conversion and Management*, vol. 69, pp. 17–26, 2013, doi: 10.1016/j.enconman.2013.01.022.

[141] S. Mekhilef, R. Saidur, and A. Safari, "Comparative study of different control strategies for standalone PV systems," Energy Conversion and Management, vol. 69, pp. 17–26, 2013, doi: 10.1016/j.enconman.2013.01.022.

[142] M. Kamel, M. E. El-Shimy, and M. A. H. Ali, "Feasibility analysis and techno-economic design of stand-alone PV/wind/battery hybrid energy system using HOMER," Energy Conversion and Management, vol. 124, pp. 289–300,2016,doi: 10.1016/j.enconman.2016.07.061.

[143] M. A. Eltawil and Z. Zhao, "Grid-connected photovoltaic power systems: Technical and potential problems—A review," Renewable and Sustainable Energy Reviews, vol. 14, no. 1, pp. 112–129, 2010, doi: 10.1016/j.rser.2009.07.015.

[144] H. Rezzouk and A. Mellit, "Feasibility study and sensitivity analysis of a stand-alone photovoltaic–diesel–battery hybrid energy system in the north of Algeria," Renewable and Sustainable Energy Reviews, vol. 43, pp. 1134–1150, 2015, doi: 10.1016/j.rser.2014.11.093.